# INTEGRATED VOLT/VAR OPTIMIZATION IN DISTRIBUTION SYSTEMS IN PRESENCE OF DISTRIBUTED GENERATION

**Ph. D. Thesis**

*by*

**SARAN SATSANGI**



**DEPARTMENT OF ELECTRICAL ENGINEERING
INDIAN INSTITUTE OF TECHNOLOGY ROORKEE
ROORKEE – 247667 (INDIA)
JULY, 2019**

# INTEGRATED VOLT/VAR OPTIMIZATION IN DISTRIBUTION SYSTEMS IN PRESENCE OF DISTRIBUTED GENERATION

A THESIS

*Submitted in partial fulfilment of the requirements for the award of the degree*
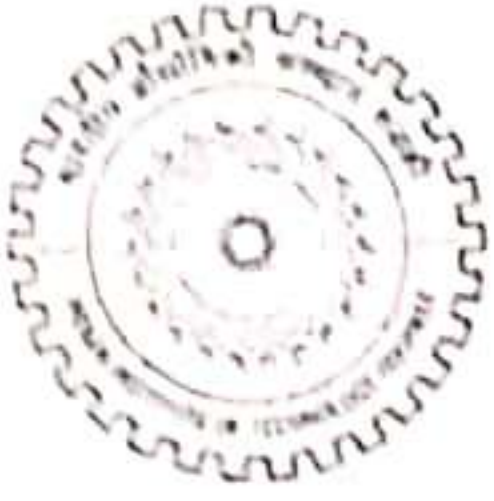
of

DOCTOR OF PHILOSOPHY

in

ELECTRICAL ENGINEERING

by

SARAN SATSANGI



DEPARTMENT OF ELECTRICAL ENGINEERING
INDIAN INSTITUTE OF TECHNOLOGY ROORKEE
ROORKEE – 247667 (INDIA)
JULY, 2019

# INDIAN INSTITUTE OF TECHNOLOGY ROORKEE

## STUDENT'S DECLARATION

I hereby certify that the work presented in the thesis entitled "INTEGRATED VOLT/VAR OPTIMIZATION IN DISTRIBUTION SYSTEMS IN PRESENCE OF DISTRIBUTED GENERATION" is my own work carried out during a period from July, 2014 to July, 2019 under the supervision of Dr. Ganesh Balu Kumbhar, Associate Professor, Department of Electrical Engineering, Indian Institute of Technology Roorkee, Roorkee.
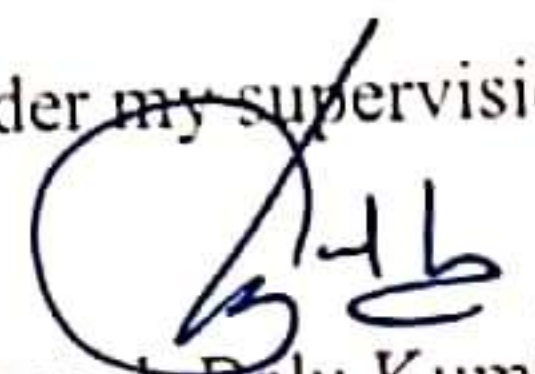
The matter presented in the thesis has not been submitted for the award of any other degree of this or any other Institute.

(SARAN SATSANGI)

Dated: September 24, 2019
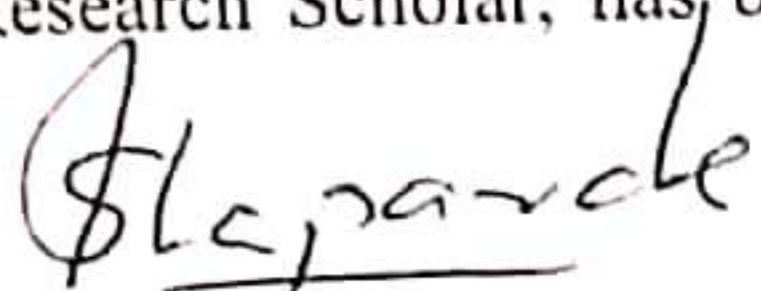
## SUPERVISOR'S DECLARATION

This is to certify that the above mentioned work is carried out under my supervision.

(Ganesh Balu Kumbhar)
Supervisor

Dated: September 24, 2019

The Ph. D. Viva-Voce Examination of Saran Satsangi, Research Scholar, has been held on September 24, 2019.

Chairperson, SRC

S. A. Khapande
External Examiner

This is to certify that the student has made all the corrections in the thesis.

Supervisor

Head of the Department

Dated: September 24, 2019

# ABSTRACT

In recent years, smart grid initiatives, such as improvement in energy efficiency, demand reduction, better utilization of equipment, have created growing interest in Volt/VAr Optimization (VVO). The VVO can be effectively utilized to enhance the efficiency of a distribution network by means of coordinating Volt/VAr Control (VVC) devices. This research aims to study the effect of smart-grid technologies on the performance of traditional VVC devices and developing VVO frameworks in the presence of new technologies. With motivation to tackle new challenges, the research work presented in this thesis is divided into three parts, viz., identifying a suitable load model for volt/VAr optimization, VVO framework considering distributed generation in presence of harmonics, and development of VVO strategies for future distribution network. Each one of this is briefly discussed below.

In a distribution network, the proper load modeling is necessary in order to accurately schedule the VVC devices. Previously, most of the research has been carried out to evaluate the energy losses of the distribution network by considering the constant power type of loads. A few researchers have considered different types of load models, such as constant power ($PQ$), constant current ($I$) and constant impedance ($Z$). However, there is no research on the effect of load models on the scheduling of VVC devices. The purpose of this research is to show the impact of load models on various operating parameters in the VVC. In this thesis, the impact of different load models on the scheduling of VVC devices is analyzed. Time-series simulations are carried on a modified IEEE-123 node unbalanced radial distribution network, where industrial, commercial, and residential loads are connected at various locations. A comparative study is performed under VVO framework to analyze energy consumption, losses, and peak load demand. It has also been observed that the load models make considerable effects on the settings of VVC devices. Therefore, the first objective of this thesis is to find the best settings of VVC devices with various load models while minimizing apparent energy losses of the network.

Loads of a practical distribution network are voltage-dependent. Both real and reactive power components of a load will be affected by the variation in the terminal voltage. Consequently, rather than minimizing the active energy demand of the distribution network, the focus of this thesis to reduce the daily apparent energy demand of the network utilizing VVO.

In this, On-Load Tap Changers (OLTC) and Voltage Regulators (VRs) are used for voltage optimization, whereas Capacitor Banks (CBs) have been utilized as a local reactive power (VAr) generators (in the distribution system) provided operational and system constraints satisfied. This research also focuses on the minimization of daily apparent energy demand of the substation by means of optimal scheduling of OLTC, VRs, and CBs. The Solar Photovoltaic (SPV) systems and wind turbine generators are also assumed to be connected in the distribution system. Moreover, this study is extended to consider the effect of harmonics in the load currents. All the simulations are performed on the modified IEEE 33-bus (single-phase balanced) and IEEE 123-bus (three-phase unbalanced) radial distribution systems. More savings in terms of substation apparent energy are accomplished when DGs are connected into the system. Reductions up to 20% in substation's apparent energy and 37% in network energy losses have been achieved.

In the present scenario, many SPV systems have been installed in the distribution network, most of them are operating at the unity power factor, which do not provide any reactive power support. In the future distribution grid, there will be significant advances in operating strategies of SPV systems with the introduction of smart inverter functions. The new IEEE Std. 1547-2018 incorporates dynamic VVC for smart inverters. These smart inverters can inject or absorb reactive power and maintain the voltages at points of common coupling (PCCs) based on local voltage measurements. With multiple inverter-interfaced SPV systems connected to the grid, it become necessary task to develop local, distributed or hybrid VVC algorithms for maximization of energy saving. This research aims to estimate the substation energy savings by means of centralized and decentralized control of inverters of SPV system along with various VVC devices. The control strategies of each SPV inverter have been accomplished in compliance with IEEE Std. 1547-2018. The time series simulations are carried out on the modified IEEE-123 node test system. The results show that considerable energy savings can be obtained by considering smart inverter functions. The saving can be further increased by incorporating optimal intelligent VVC characteristics.

All the proposed case studies are verified using simulation performed on standard test systems. The results and important findings obtained through simulation studies are presented in this thesis.

# ACKNOWLEDGMENTS

It is my desire and a great pleasure to offer my sincere thanks to all those who have contributed, in whatever way, to the completion of my work.

First, I take this opportunity to express my sincere gratitude to my supervisor Dr. G. B. Kumbhar, Associate Professor, Department of Electrical Engineering, Indian Institute of Technology (IIT) Roorkee, Roorkee, India for his constant encouragement and motivation throughout the duration of this research work. I also express my sincere gratitude to Dr. B. Das, Professor and Head, Department of Electrical Engineering, IIT Roorkee, India who constantly encouraged me during my Ph.D programme.

I am also thankful to my research committee members, Prof. P. Jena and Prof. B. Anand, for their constructive suggestions during several meetings held for this research work. I would also like to thank other faculty members of Electrical Engineering Department, IIT Roorkee for their moral support and providing the excellent laboratory facilities during this research work at IIT Roorkee. I would thank the Ministry of Human Resources Development (MHRD), Government of India for providing the fellowship for carrying out this research work. I would like to thank the anonymous reviewers of my research work, who gave me the suggestions to improve the quality of the research work and the direction for the additional work.

My journey in IIT Roorkee has been blessed with many friends who played a major role in maintaining a constantly high level of motivation, and thus help me in the progress of my work. I would give special acknowledgment to my fellow researchers, Mr. Kanhaiya Kumar, Mr. Sukhlal Sisodiya, Dr. Ankit Kumar Singh, Dr. Santosh Kumar Singh, Mr. Praveen Kumar, Dr. Mithun Mondal, Mr. K. A. Chinmaya, Mr. V. Sidhartha, Mr. Naveen Yella, Dr. P. Sanjeev, Mr. Jose Thankachan, and Mr. Ajay Kumar Maurya.

I wish to express my hearty gratitude to my wife Shalu, daughters Shabda and Shreyanshi, parents, in-laws and all my family members, for their endless moral support and encouragement. Finally, I am very thankful to all-merciful God who gave me blessing and wisdom to carry out this Ph.D. research work.

(Saran Satsangi)

iii

iv

# CONTENTS

# LIST OF FIGURES

# LIST OF TABLES

xvi

# LIST OF ABBREVIATIONS

| | |
|---|---|
| **AA** | All Aluminium |
| **ACSR** | Aluminium Conductor Steel Reinforced |
| **ACO** | Ant Colony Optimization |
| **BFA** | Bacterial Foraging Algorithm |
| **BSO** | Bee Swarm Optimization |
| **CO** | Commercial |
| **CN** | Concentric Neutral |
| **RE** | Residential |
| **IN** | Industrial |
| **VVO** | Volt/VAr Optimization |
| **VVC** | Volt/VAr Control |
| **DG** | Distributed Generation |
| **DSO** | Distribution System Operator |
| **PSO** | Particle Swarm Optimization |
| **GDP** | Gross Domestic Product |
| **GA** | Genetic Algorithm |
| **NSGA** | Non Sorting Genetic Algorithm |
| **LP** | Linear Programming |
| **NLP** | Non Linear Programming |
| **MILP** | Mixed Integer Linear Programming |
| **MINLP** | Mixed Integer Non Linear Programming |
| **PF** | Power Factor |
| **MIQCP** | Mixed Integer Quadratic Constrained Programming |
| **DP** | Dynamic Programming |
| **DER** | Distributed Energy Resources |
| **OO** | Ordinal Optimization |
| **OLTC** | On Load Tap Changer |
| **PV** | Photovoltaic |

| | |
|---|---|
| **VR** | Voltage Regulator |
| **RMS** | Root Mean Square |
| **WT** | Wind Turbine |
| **PDIPM** | Prime Dual Interior Point Method |
| **CVR** | Conservation Voltage Reduction |
| **THD** | Total Harmonic Distortion |
| **AMI** | Advanced Metering Infrasturcture |
| **UPF** | Unity Power Factor |
| **EV** | Electric Vehicle |
| **ELM** | Exponetial Load Model |
| **TLA** | Teaching Learning Algorithm |
| **SA** | Simulated Annealing |
| **PS** | Pattern Search |
| **TS** | Tabu Search |
| **SFLA** | Shuffled Frog Leaping Algorithm |
| **MA** | Memetic Algorithm |
| **HBMO** | Honey Bee Mating Optimization |
| **GSA** | Gravitational Search Algorithm |
| **NN** | Neural Network |
| **ANFIS** | Adaptive Neuro Fuzzy Inference System |
| **MAS** | Multi Agent System |
| **SVC** | Static VAr Compensator |
| **RES** | Renewable Energy Sources |
| **DCDA** | Discrete Coordinate Descent Algorithm |
| **SPEA** | Strength Pareto Evolutionary Algorithm |
| **SPV** | Solar Photovoltaic |
| **OpenDSS** | Open Distribution System Simulator |
| **IVVC** | Intelligent Volt/VAr Control |
| **IVVCC** | Intelligent Volt/VAr Control Characteristics |
| **USD** | United States Dollar |

# LIST OF SYMBOLS

$S_i$      Complex power defined for $i^{th}$ node

$\delta_i$      Voltage angle at $i^{th}$ node

$\theta_i$      Angle of complex power load $(S_i)$

$P_{i,t}^r$      Nominal real power of $i^{th}$ node at time $t$

$Q_{i,t}^r$      Nominal reactive power of $i^{th}$ node at time $t$

$P_{i,t}^l$      Real power consumption of $i^{th}$ node at time $t$

$Q_{i,t}^l$      Reactive power consumption of $i^{th}$ node at time $t$

$V_{i,t}$      Actual complex voltage of $i^{th}$ node at time $t$

$k_i^p$      Voltage exponents of real power for $m^{th}$ node

$G^{std}$      Standard solar irradiance, i.e., $1000 w/m^2$

$k_i^q$      Voltage exponents of reactive power for $i^{th}$ node

$k_n^{Temp}$      Temperature coefficient of PV-plate connected at $n$ th node

$r_{ij}$      Resistance of branch between $i$ and $j$ node

$T_{n,t}^c$      Cell Temperature of $n$ th SPV generator over time $t$

$x_{ij}$      Reactance of branch between $i$ and $j$ node

$T$      Reference cell temperature, i.e., $25 \deg C$

$z_{ij}$      Complex impedance of branch between $i$ and $j$ node

$N_b$      Total nodes in the distribution system

$P_{n,t}^{wt}$      Real power output of WT generator connected at node $n$ over time $t$

$P_{n,max}^{wt}$      Maximum power capacity of WT generator connected at node $n$

$V_i^{min}$    Minimum allowable voltage at $i^{th}$ node

$V_i^{max}$    Maximum allowable voltage at $i^{th}$ node

$v_{ci}/v_{co}/v_r$   cut-in/cut-off/rated speed of wind turbine

$V_{j,t}^{vr}$    Regulation ratio of $j^{th}$ regulator at time $t$

$w_t$    Actual speed of wind turbine over time $t$

$N_{pv}/N_{wt}$   Total number of SPV/WT generators

$Tap_{j,t}^{vr}$   Tap position of $j^{th}$ regulator at time $t$

$\triangle V_j$    Voltage change per step of $j^{th}$ regulator

$cos\phi_m^{pv}$   Power factor of $m$ th SPV generator

$MT_j^{vr}$   Daily maximum allowable tap operations of $j^{th}$ regulator

$cos\phi_n^{wt}$   Power factor of $n$ th WT generator

$MS_k^{cb}$   Daily maximum allowable switching operations of $k^{th}$ capacitor unit

$r_{ij}$    Resistance of line between node $i$ and $j$

$N_{vr}$    Total number of voltage regulators in the distribution system

$Sw_{k,t}^{cap}$   Switch position of $k^{th}$ capacitor at time $t$

$x_{ij}$    Reactance of line between node $i$ and $j$

$N_{cap}$    Total number of capacitor units in the distribution system

$q_k^{cap}$    Rated kVAr of $k^{th}$ capacitor

$z_{ij}$    Complex impedance of line between node $i$ and $j$

$V_i^{min}/V_i^{max}$   Minimum/Maximum allowable voltage at $i^{th}$ node

$\Delta q_k^{cap}$   kVAr change per capacitor tap step at $k^{th}$ node

$Tap_{k,t}^{cap}$ Tap position of $k^{th}$ capacitor at time $t$

$Q_{k,t}^{r}$ Rated kVAr of $k^{th}$ capacitor at time $t$

$P_{m,t}^{pv}$ Real power output of SPV generator connected at node $n$ over time $t$

$P_{m}^{rated}$ Rated power capacity of SPV connected at node $n$

$G_{t}$ Solar irradiance over time $t$

$I^{r}$ RMS fundamental current under rated frequency and rated load conditions

$N_{h}$ Highest harmonic order

$P_{cu-loss}$ Transformer Cu loss considering harmonics

$P_{cu-loss}^{r}$ Transformer Cu loss at rated condition

$P_{ec-loss}$ Transformer winding eddy current loss considering harmonics

$P_{ec-loss}^{r}$ Transformer winding eddy current loss at rated condition

$P_{LL}^{r}$ Total load loss at rated condition

$P_{NLL}$ No-load loss of transformer

$P_{os-loss}$ Other stray current loss considering harmonics

$P_{os-loss}^{r}$ Other tray current loss at rated condition

$Q_{m}^{max}$ Maximum allowed reactive power capability of $m^{th}$ inverter unit

$Q_{m,t}^{pv}$ Reactive power output of a SPV generator connected at node $m$ over time $t$

$S_{m}^{rated}$ The inverter's kVA rating of $m^{th}$ photovoltaic generator

$V^{r}$ RMS fundamental voltage under rated frequency and rated load conditions

$V_{i,t}(f_{h})$ Actual complex voltage of $i^{th}$ node at time $t$ and harmonic frequency $f_{h}$

$V_{ref}$ The reference voltage for the inverter

# CHAPTER 1

# INTRODUCTION

## 1.1 Background

In the present scenario, one can not imagine a life without electricity. The electrical energy is the core of advancement. Without electricity, communities live in darkness, essential services such as hospitals and schools suffer, and other organizations operate under crippling constraints. The innovations, investments, and setup of new industries are possible through electrical energy. Per capita energy consumption is one of the important indicators of the country's development. In India, the per capita GDP (in USD) and electricity consumption (in kWh) for the year of 2005 was 707 USD and 631.4 kWh, respectively. However, this crossed 1606 USD and 1075 kWh in 2015 [1, 2]. This clearly demonstrates that there is a significant correlation between per capita energy consumption and GDP.

Thirst for energy is expanding altogether with the increase in the economy around the globe which burdens the grid due to energy deficit, peak demand, and $CO_2$ emission. Both energy and peak demand deficit over a span of 10 years are shown in Fig. 1.1. Due to technological advancement, the shortfall in the demand is somehow decreasing but still a long way to accomplish proper balance. Moreover, a great portion of generated energy is wasting in-terms of Transmission and Distribution (T & D) losses. In India, the average T & D losses are still 21.3% (for 2016-17). The bar chart shown in Fig. 1.2 demonstrates that considerable research and advancement required to bring these losses to the average T& D losses of the world, i.e., 8.25% (approx.) [6]. This gives motivation to the distribution utilities and Distribution Network Operators (DNOs) to focus on energy efficient techniques for decreasing peak demand and energy deficits.

In a distribution system, energy efficiency is an important objective of any DNO. In the recent years, smart grid initiatives have created a growing interest in Volt/VAr Optimization (VVO) for improvement in energy efficiency, demand reduction, better utilization of overall equipment. The VVO functionality can be defined as "the optimal control of various Volt/VAr Control (VVC) devices such as on-load tap changers, voltage regulators, capacitor
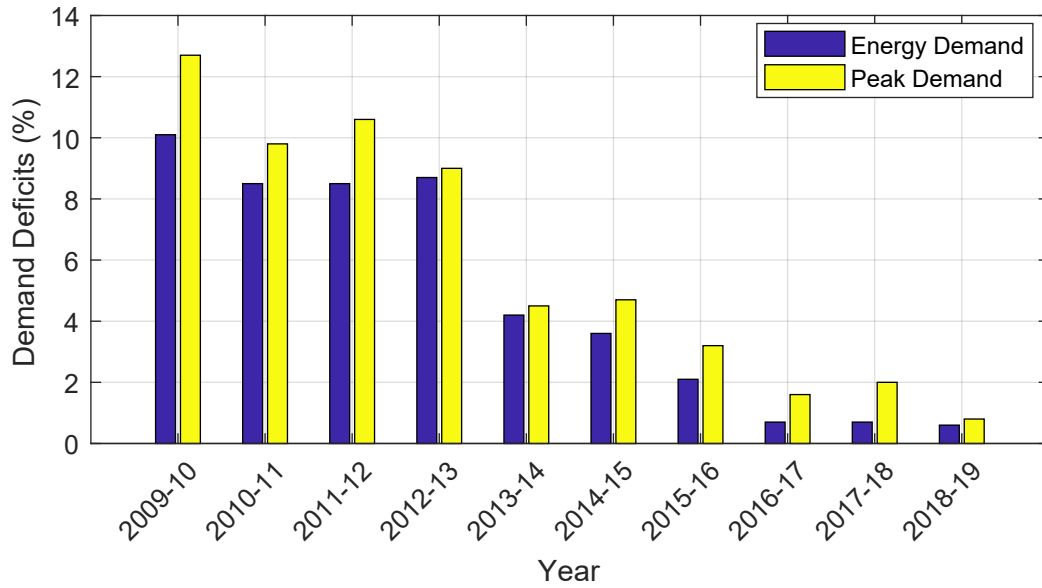
Fig. 1.1. All India energy and peak demand deficits over a period of 10 years [3]
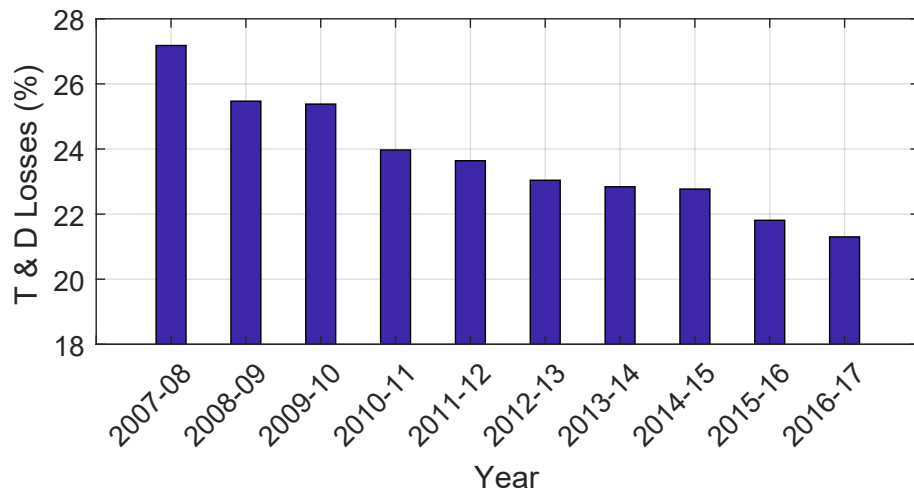


Fig. 1.2. All India average T& D losses over a period of 10 years [1, 4, 5]

2

banks so as to fulfill the different objectives". The objective functions considered by various researchers are minimizing the system losses, minimizing the energy consumption, minimizing the voltage deviation, minimizing the peak-load demands, etc. The important benefits of VVO can be summarized as:

(a) It decreases the peak demand and total energy intake of a distribution utility.

(b) It decreases the losses in overhead lines, underground cables, and distribution transformers.

(c) It improves environment and social welfare by reducing $CO_2$ emission and fuel consumption.

(d) It reduces energy bills of consumers.

## 1.2 Motivation

In the recent years, VVO is gaining attention among the other energy-efficient techniques to reduce the energy consumption and losses in a distribution network. In VVO, both voltage and reactive power (VAr) of the distribution system are optimized in order to minimize the peak demand, minimize the energy consumption, minimize the losses, etc. [7]. Worldwide, many utilities, such as American Electric Power [8], BC Hydro [9, 10], Avista [11], Siemens [12], Taiwan Power Company [13] have utilized VVO to decrease energy consumption and energy losses. In a practical distribution system, major portion of loads are of three types, viz., Industrial (IN), Commercial (CO), and Residential (RE) with aggregate load demand changing over the time. This change is dependent on voltage exponents of active and reactive powers. For these loads, voltage exponents of reactive power are higher than real power [14]. Therefore, the reactive power is more sensitive to voltage than that of active power. Thus, active and reactive components of connected load respond differently with optimized voltages over the time. The proper load modeling is necessary in order to accurately schedule the VVC devices. In the past, most of the research has been carried out to evaluate the energy losses of the distribution network by considering constant power type of loads. Some research also has considered different types of load, such as constant power ($PQ$), constant current ($I$) and

3

constant impedance ($Z$). However, there is no research on the effect of load models on the scheduling of VVC devices.

On the other hand, due to distinct characteristics of active and reactive loads and variation in the terminal voltage, each class of customer having different voltage sensitivities [14]. Therefore, voltage control and VAr flow in the distribution system affects both real and reactive powers in a distinct way. Moreover, the presence of a shunt capacitor provides a leading current, and hence, both active and reactive power losses will also be affected. This gives the motivation to focus on minimization of apparent energy demand or apparent energy losses instead of active energy demand and losses. There is no literature on minimization of apparent energy demand. Apart from energy demand, the impact of Distributed Generation (DG) and Conservation Voltage Reduction (CVR) has been studied [15] for the perspective of voltage profile on peak-loading condition. However, its impacts on energy savings under the VVO framework needs to be studied. Moreover, the harmonics have received less attention in VVO problem formulation because of complexity. Ref. [16–19] deals with the harmonics considering of non-linear loads. However, the voltage reliance on the real and reactive components of the load has been neglected

In the present scenario, many Solar Photovoltaic (SPV) systems have been installed in the distribution network. Many SPV systems are still operated with conventional inverters at unity power factor. These inverters can only supply active power to the grid. However, nowadays, SPV systems are increasingly paired with smart inverters, which can inject as well as absorb reactive power and control the voltages at the point of common coupling. These smart inverters have the capabilities to take self decisions based on local or distributed measurements (in terms of voltage, currents, power factor etc.). Earlier, Distributed Energy Resources (DERs) were not allowed to participate in the voltage regulation. Thereafter, in 2014 an amendment was made in IEEE Std.1547-2003 to allow the smart inverter-based generation to participate in the voltage regulation [20]. Recently (2018), Std.1547-2003 is revised and certain operational constraints have been introduced for smart inverter based PV generators [21].

In future, there can be obligations for distribution utilities and DER operators to follow IEEE Std.1547-2018 to control the voltages over the distribution systems. The traditional

4

VVO formulation will significantly change with these additional sources and constraints. In this case, the VVO also needs to incorporate various smart inverter functions [22]. The smart inverter based VVC can be included in the VVO formulation into two ways, i.e., based on local measurements, and based on distributed coordinated measurement. In local measurement based control, the DERs (through the smart inverter) can supply or absorb reactive power (Q) power based on local feedback signal, e.g. voltage, power factor, etc. On the other hand, the reactive power can be supplied or absorbed based on the feedback signal received from the centralized control system. In the method based on centralized control, utility perform optimization in order to achieve a set of objectives to issue a control command to the smart inverters.

## 1.3 Background Survey

This section gives a brief survey of the important works related to the issues considered in this thesis. It also legitimately justifies the pertinence and need of the fundamental contributions of this work.

The investigation of switched capacitors with different load models ($PQ$ and $Z$) is carried out in [23]. It is shown that switching 'ON' a capacitor can correct power factor ($pf$) and decrease the losses. However, in the case of constant impedance load, an improvement in the voltage profile increases the load and losses. In [24, 25], the effect of load models on real and reactive power losses is studied for planning DGs. It is highlighted that load models can significantly affect the size and location of DG. In [26], an investigation of energy losses with various load models is carried for DG planning and it is reported that the reactive power drawn by DGs gets significantly affected with type of load model. The effect of load models on feeder reconfiguration has been studied in [27], where minimization of power losses has been considered. Here, power-in-take, reconfiguration, and losses of the distribution network has been studied with various models. In the literature, research have been carried to study the impact of load models on capacitor switching [23], DG planning [24–26], feeder reconfiguration [27], etc. However, to the best of the author's knowledge, scheduling of VVC devices considering various load models has not been studied so far.

The vast majority of the research performed in the domain of VVC has considered min-

imization of real power (*kW*) and energy losses (*kWh*) for optimal coordination of VVC devices. However, minimization of apparent energy losses (*kVAh*) has received little attention and considered in few studies [28, 29]. But as reported in [8], 5% energy losses have occurred in the distribution system. This has been focused in many studies [11, 12, 30–35], where the prime objective was the minimization of active energy demand. Aside from the consideration of the apparent energy demand of a distribution network, the harmonics have also been considered in this research. Because of complexity, the harmonics have received less attention in VVO problem formulation. Ref. [16–19] deals with the harmonics considering non-linear loads. However, the voltage reliance on the real and reactive components of the load has been neglected.

In the past, a few researchers have worked on the VVO by considering Renewable Energy Sources (RES) in the distribution grid. In [36, 37], real and reactive power of wind farms are considered as control variables with real power of other RES. Whereas, only real power has been taken as a control variable in [38–40]. A few studies, [18, 19, 41], have also utilized converter capability to control reactive power. The dispatchable DGs are considered in [42], where both power factor and active power have been taken as control variables. Thereafter, power factor based reactive power control of PV and/or WT generators has been studied in [43–46]. In the literature, a very few studies have considered SPV systems operating with smart inverters [47–50].

## 1.4 Objectives and Scope

With motivation to tackle above challenges, this research intends to target the following objectives.

1. To study the effect of load model on scheduling of VVC devices in a distribution network and to identify the suitable load model for the purpose of volt/VAr control and optimization.

2. To minimize apparent energy losses of the distribution network along-with the effect of various load models on scheduling of VVC devices and to obtain the optimal schedule of these devices.

3. To develop an integrated VVO formulation in the presence of distributed generation

alongside harmonics in the load current while maintaining the load-to-voltage dependency.

4. To minimize apparent energy demand of the distribution network in presence of distributed generation and harmonics on the load-side and to obtain the best schedule of VVC devices.

5. To propose CVR/VVO formulation to maximize energy savings in a distribution network in presence of distributed SPV systems with intelligent volt/VAr control based on IEEE Std. 1547-2018.

## 1.5 Research Contributions

In this research work, an attempt has been made to accomplish the above objectives. The various contributions, which have been made through this thesis, are summarized as follows:

1. The effect of load models on the scheduling of VVC devices has been studied under VVO framework. Considering impact of various load models on scheduling of VVC devices in presence of VVO formulation, the best settings of VVC devices has been evaluated with various load models while minimizing apparent energy losses of the network. It is very important to select a suitable load model for proper scheduling of VVC devices. It is observed that the exponential load models with a proper choice of exponents accurately emulate the practical loads.

2. Due to distinct voltage dependence of active-reactive powers of the loads and losses, minimization of apparent energy of the distribution system is considered instead of minimization of active energy or losses. Alongside the objective function, DGs are considered to increase the savings in-terms reduction of substation apparent energy demand.

3. The harmonics are considered on the load-side while maintaining the voltage-dependence of different practical loads. The impact of harmonics with and without local generation has been studied in order to minimize substation apparent energy demand.

4. The VVO formulation of a future distribution system has been proposed as per the DER interconnection guidelines of IEEE Std. 1547-2018. The limited reactive power

capability of a smart inverter has been taken into account while dealing with the reactive power dispatch. Smart inverters have been considered to operate on a unique and optimal Intelligent Volt/VAr Control Characteristic (IVVCC). Therefore, the determination of an optimal IVVCC has also been taken into account while achieving the VVO objectives.

## 1.6 Organization of the Thesis

The research presented in this thesis has been organized into six chapters and the work included in each chapter has been presented in the following sequence:

1. This chapter gives an overview of VVC and optimization in distribution system. It highlights its need, status, and challenges. It also presents the motivations, objectives and scope of the research work.

2. Chapter 2 presents a brief literature review on the load models, VVO, and solution techniques utilized by the researchers worldwide.

3. Chapter 3 presents an overview of different load models that are broadly acknowledged in VVO. The purpose of this chapter is to identify a suitable load model for VVO. Different loads in the distribution network influence losses as well as effect voltage profile, energy intake, power factor, and so forth. Therefore, an investigation of the impacts of load models on planning or scheduling of VVC devices is necessary under VVO. In this chapter, the impact of load models on the day-ahead scheduling of VVC devices in order to achieve minimal apparent power and energy losses have been considered.

4. Chapter 4 focuses on the VVO model with and without DGs in order to minimize substation's daily apparent energy demand. Apart from the consideration of the apparent energy demand of a distribution substation, the harmonics have also been considered in this chapter. The study presented in this chapter is conducted into two scenarios, i.e., with and without DGs.

5. Chapter 5 deals with the VVO strategies of a distribution network considering smart inverter based SPV systems. The focus of this chapter is to consider the participation of the DERs in the voltage and reactive power management. Thus, a VVO formulation has been developed in accordance with IEEE Std. 1547-2018.

6. Chapter 6 concludes the work with a summary of the research in the thesis, contributions and directions for the future research.

Appendix A describes about the system data used in this thesis. Publications during the research work are provided in Appendix B.

# CHAPTER 2

# LITERATURE REVIEW

## 2.1 Introduction

A distribution system is different than the transmission system due to distinct features, such as high $\frac{R}{X}$ ratio, minimum automation, radial network, less system monitoring, etc. Traditional distribution systems were considered passive network due to the absence of local generation. But in a smart grid environment, operating conditions will be very different due to various technologies such as Distributed Generations (DGs) [51], Electric Vehicles (EVs), Advanced Metering Infrastructure (AMI), Distribution Management System (DMS), etc.

Energy efficiency is one of the main aim of Distribution System Operator (DSO) in the vision of the smart grid. This can be achieved simply by reducing ohmic losses $(I^2R)$, which are the major part of system losses. Supply quality is also important for the distribution network, because mostly feeders are radial in nature. In a radial system, the customer near to the substation have good enough voltage, while it may be worse for the customer at the last node. The losses can be reduced by installing capacitors near to the load centre, which will simply minimize the reactive power flow from the substation. Whereas the voltage is managed by simply lowering or raising the taps of On Load Tap Changers (OLTCs) of substation transformer and/or Voltage Regulators (VRs). The voltage on a distribution feeder can also be optimized using Conservation Voltage Reduction (CVR) techniques whereas capacitors are used to optimize the VAr flow. The Volt/VAR Optimization (VVO) is the capability to optimize the objectives such as VAr flow or power loss minimization, load reduction, etc. using optimization algorithms and control variables, subject to various operating and system constraints through decentralized or centralized decision makings [7, 52].

This chapter has reviewed the VVO methods and available practical experiences along with VVO formulation.

## 2.2 Problem Formulation

### 2.2.1 Distribution Test Systems

The VVO has been performed on various test and practical distribution networks (IEEE benchmark and other test systems). Summary of all the test cases along with VVO references is displayed in Table 2.1.

### 2.2.2 VVO Technology

VVO can be decoupled into two sub-problems, i.e., voltage optimization, and VAr optimization. The CVR can also be used as one of the voltage optimization technique for the distribution system having mainly Residential (RE) and Commercial (CO) loads. These two are discussed here:

#### 2.2.2.1 Conservation Voltage Reduction (CVR)

This concept works on the fact that the majority of electrical loads in the distribution system are of constant impedance ($Z$) type, which consumes less energy when the voltage is reduced to its allowable lower limits [94]. By reducing the terminal voltage in a controlled manner, the load consumption gets reduced without affecting the equipment performance and quality of supply. The effect of CVR can be evaluated by CVR factor ($CVR_f$), which can be defined as [95] :

$$CVR_f = \frac{\Delta E\%}{\Delta V\%} \tag{2.1}$$

where $\Delta E\%$ is the percentage of energy savings caused by $\Delta V\%$ voltage reduction. The percentage of energy savings depends on the possibilities of percentage voltage reduction, and load characteristics. Energy savings can be significant for the $Z$-types of load. There is also considerable energy savings for the constant current ($I$) types of load. It is found that household devices consist of a great fraction of load which is $Z$-type and $I$-type [96]. Thus, reduction in the operating voltage of these devices would result in significant energy savings.

The RE and CO customers have a great portion of their loads as $Z$ and $I$-type [97], therefore CVR concept can be effectively applied to these classes of customers. The distribution utilities intentionally reduce the system voltage in order to minimize the end-use en-

Table 2.1. Distribution test systems used for VVO applications

| Test System | VVO Reference(s) |
| --- | --- |
| IEEE 13-Bus | [32, 53] |
| IEEE 34-Bus | [31, 32, 35, 54–57] |
| IEEE 37-Bus | [41] |
| IEEE 123-Bus | [32, 39, 42, 58] |
| 13-Bus | [59] |
| 14-Bus | [60, 61] |
| 17-Bus | [62, 63] |
| 29-Bus (Thailand System) | [64, 65] |
| 30-Bus (Carolina Distribution System) | [16, 17, 53, 66–70] |
| 33-Bus | [29, 71–75] |
| 69-Bus (PG&E Distribution System) | [31, 33, 34, 39, 40, 53, 61, 73, 76–81] |
| 70-Bus | [36–38, 82, 83] |
| 80-Bus | [56] |
| 85-Bus | [73] |
| 94-Bus (Portuguese System ) | [84] |
| 95-Bus (U.K. Generic Distribution System) | [35, 85] |
| 119-Bus | [80] |
| 120-Bus | [86] |
| 135-Bus (Brazil Distribution Network) | [87] |
| 136-Bus | [78] |
| 138-Bus | [31] |
| 141-Bus | [73] |
| Taiwan Distribution System | [30, 88–91] |
| Korean Test Distribution System | [92] |
| American Elecric Power Substation | [8] |
| George Tripp (GTP) substation | [93] |
| Avista Based Distribution Network | [11] |

ergy consumption without violating the minimum acceptable voltage as prescribed by ANSI C84.1 [94].

### 2.2.2.2 VAr Optimization

The issue of voltage drop toward the end of a distribution feeder is commonly addressed by installing shunt capacitors close to the load center. In VAr optimization, the system communication platform is utilized to coordinate the operation of capacitors in order to limit the reactive power requirement at a distribution feeder and additionally at the substation. The reduction in reactive power at the distribution feeder prompts a decrease in the line current, in this manner line losses ($I^2R$) will be reduced in addition to power factor (PF) improvement. In the smart grid era, advanced automation, and communication technologies are facilitated together for the best possible coordination of VVC devices and other smart grid technologies.

### 2.2.3 VVC Devices and Smart Grid Technologies

The OLTC, VRs and Capacitor Banks (CBs) are traditional voltage regulation and VAr compensations devices. These devices are installed at the substation or potentially on the distribution feeder(s) to address the issues of voltage and reactive power (VAr) flow. These devices are operating or scheduled to achieve various objectives of VVO. Now in a smart grid environment, new technologies such as AMI, DGs, EVs, smart inverters, etc. are going to affect the operation and performance of traditional VVC devices.

### 2.2.4 Problem Statement

The VVO is a procedure of ideally managing voltage levels and reactive power (through VVC devices) to accomplish progressively efficient grid operation by reducing network losses, peak demand, energy consumption, and so on. These targets have been accomplished subjects to various operating constraints, DGs constraints, environmental constraints, and other system constraints. The typical VVO problem is a mixed integer non-linear type optimization problem.

### 2.2.5 Common Objectives

The VVO problem may have a single or multiple objectives. The common VVO objectives are as follows:

- Minimization of Power/Energy Losses (MOEL)

- Minimization of Peak Load (MOPL)

- Minimization of Switching Operations of VVC devices (MOSO)

- Minimization of Overall Energy Consumption (MOOE)

- Minimization of Voltage Deviation (MOVD)

- Minimization of Power Drawn from substation (MOPD)

- Minimization of Emission by DGs (MOED)

- Minimization of Energy Price offered by substation and DGs (MOEPSD)

VVO can likewise be defined as a multi-objective problem in which each objective assigned with a particular weight and then formulated as a single objective using a weighted sum of each objective (commonly known as weighted sum approach). Some times a trade-off between optimal solutions of objectives are obtained using multi-objective formulation in which each set of solution is optimal.

### 2.2.6 Load Models

There are various models available for representing loads of the distribution network. These can be broadly classified as classical models and mixed models. The classical models can be further classified as constant power ($PQ$), constant current ($I$), and constant impedance ($Z$) models. On the other part, the mixed models are of two types, i.e., Exponential Load Models ($ELM$), and Polynomial Load Models (also known as $ZIP$ model). Sometimes ZIP model does not have all three coefficients ($Z$, $I$, and $P$) and hence a particular share (in percentage) has been assigned to any of two $ZIP$ coefficient for representing the load of a distribution network. Table 2.2 shows a classifications of various load model alongside VVO applications.

### 2.2.7 VVO Constraints

The common VVO constraints are:

Table 2.2. Load models alongside VVO applications

| Type | Load Model | VVO Reference(s) |
|---|---|---|
| Classical | $PQ$ | $[30\text{–}32, 36\text{–}42, 53\text{–}57, 59\text{–}69, 71\text{–}73, 76\text{–}80, 82\text{–}85, 87, 89\text{–}92, 98\text{–}100]$ |
| | $I$ | $[31, 32, 39, 41, 42, 53\text{–}57, 81, 99]$ |
| | $Z$ | $[31, 32, 39, 41, 42, 53, 55\text{–}57, 93, 99]$ |
| Mixed | $ZIP$ | $[8, 11, 12, 28, 29, 31\text{–}33, 58, 74, 75, 88]$ |
| | $50\%PQ + 50\%Z$ | $[16\text{–}19, 70]$ |
| | $10\%PQ + 90\%Z$ | $[34]$ |
| | $50\%I + 50\%Z$ | $[86]$ |
| | $ELM$ | $[35, 72]$ |

- real and reactive power balance

- bus voltage limit

- PF limit

- DG output limits

- transformer regulation ratio

- VR regulation ratio

- VR taps operation limit

- capacitor output

- capacitor switching operation limit

- emission limit

## 2.3 Previous Methods and Work

### 2.3.1 Analytical Methods

In [66–68, 99], analytical methods have been utilized. The analytical solution of VVC problem was presented in [67], where the objectives are MOEL and MOPL. The numerical results

and economic benefits of the VVC were reported in [68]. An analytical solution of VVC problem was suggested using oriented decent method for MOEL in [99].

### 2.3.2 Numerical Methods

#### 2.3.2.1 Linear Programming (LP)

LP method incorporating algorithms, such as a random algorithm and deterministic algorithm is developed in [82] and Mixed Integer Linear Programming (MILP) in [78] for optimal co-ordination of capacitors and VRs. The method developed in [82] is faster than explicit search method in terms of execution time. The VVO problem of the Korean Distribution Management System (KDMS) [92] was solved using MILP. The objectives were MOVD, MOSO, MOEL, and minimization of emergency level by the optimal dispatch of VVC devices and DGs. The MILP was also used to solve a VVO problem in [31, 32, 101] including embedded generation (EG) in which real power output considered to be known and reactive power was treated as a control variable under capability limits. In [32], the unbalanced 3-phase distribution system was considered for solving VVO, where different types of transformer connections, presence of EG, delta and wye-connected loads with the possibility of capacitor banks operating in per-phase were considered in the modeling.

#### 2.3.2.2 Nonlinear Programming (NLP)

While considering the system behavior prediction, load-to-voltage dependencies and uncertainties of DG output, model predictive control (MPC) based VVO was proposed in [72]. In this, Mixed Integer Nonlinear Programming (MINLP) is utilized to formulate VVO problem in which different types of DGs such as WT, and PV were considered. In [76], MINLP problem of VAr and voltage control of the Chinese real distribution system was transformed into NLP problem. Thereafter, Interior Point Method (IPM) was applied to solve the problem considering daily operating switching limits of OLTC and capacitors.

As DG always have an impact on the system voltage, it may increase or decrease switching operations of VVC devices. Therefore, coordination in DG output and switching operation of VVC devices is necessary. To address this problem, a Prime Dual Interior Point Method (PDIPM) was suggested in [85] to deal with the constraints of MOSO. In [33], RE area of Vancouver, BC, Canada was taken for VVO study. In this, VVO was formulated as

17

Mixed Integer Quadratic Constrained Programming (MIQCP) problem and solved using the advanced branch-and-cut algorithm, which involves the use of a branch and bound algorithm and using cutting planes to tighten the LP relaxations. In [98], the original VVC problem was transformed into a convex problem, then Sequential Convex Programming (SCP) was applied for optimal dispatch of DGs connected in the distribution system in order to minimize injected VAr from all DGs.

*2.3.2.3 Dynamic Programming (DP)*

DP was used for optimal scheduling of VVC devices of substation of Taipei region of Taiwan Power Company (TPCo) in order to minimize reactive power flow from the main transformer and kept the distribution system voltage close to the rated value [30]. Thereafter fuzzy membership functions were developed in [88] for voltage deviation, PF, switching operation of transformer taps and capacitors, and then its combined effect was integrated to DP for scheduling VVC devices in order to achieve objectives. The VVC problem of a distribution feeder of the Yunlin District of TPCo was solved using DP [90], where VVC devices were scheduled for MOEL, MOVD in addition to the objectives of [30]. In [59], DP was also used to solve VVC problem of the distribution system, where actual problem was divided into two sub-problems, i.e., First, control of OLTC and CBs of the substation, and second, control of CBs of the feeder. The local and remote control for OLTC, substation capacitors and feeder's capacitors in coordination with DP was proposed for MOEL considering the effect of induction DGs on VVC devices [60].

*2.3.2.4 Ordinal Optimization (OO)*

In OO, order compared first and then estimate the value of the optimum (solution). An OO was proposed to solve the VVC problem for the purpose of MOEL in the distribution system and kept the system voltage near to rated value [86]. It relaxes the optimality definition and makes optimization simple.

### 2.3.3 Heuristic Methods

#### 2.3.3.1 Genetic Algorithm (GA) and its Variants

Capacitors were placed optimally under varying load levels using GA in [102, 103] for MOEL. GA based on integer string coding was proposed in [54] to solve VVC problem, where power losses were minimized through optimal scheduling of capacitor banks, OLTC and DGs. Optimal scheduling of OLTC and capacitors in changing load level was determined in [70] using GA for off-line VVC to minimizing energy losses. Here switching operation of OLTC was limited by time-interval based approach, therefore search space for GA was reduced.

To reduce peak-load and losses, a strategy based on Non-Sorting Genetic Algorithm (NSGA) was proposed in [34] for optimal allocation of capacitors in the distribution system. GA-fuzzy (GAF) was used in [104] as an optimization tool for real-time VVC of the Serbian distribution system. In this case, fuzzy rules for power loss, voltage deviation, PF, and degree of satisfaction were defined and then integrated into the GA environment to make it faster. The optimal trade-off among power losses and voltage deviation for the radial distribution network was evaluated in [62] using micro GA, where the optimal position of VRs was also determined.

In [71], GA was utilized for optimal coordination of VVC devices together with optimal control of distribution voltage in order to reduce voltage deviation and power losses. In [63], Gray-based GA was proposed to solve the VVC problem of the distribution system that includes DGs as wind farms, which is faster than conventional GA. The Multi-Objective Genetic Algorithm (MOGA) improved by fuzzy logic was used to solve VVC problem of the distribution system in [77], where search space was reduced (up to 92.5%) by identifying group of buses for allocation of VRs using fuzzy membership functions. In [17], the GAF optimization approach was utilized to solve VVC problem, including Total Harmonic Distortion (THD) for the purpose of MOEL and minimization of THD over a day. MOGA based VAr/Volt management for DGs and FACTS was proposed in [105] under smart grid environment to minimize power losses and investment cost of FACTS devices.

In [80], PDIPM is utilized for VVC with assumptions to treat a discrete variable as con-

tinuous, and relax the switching constraints. PDIPM based sensitivities provides lower and upper heuristic limits for control variables. The number of control combinations for the actual VVC problem was tremendously reduced due to sensitivity based heuristics, while keeping the solution space intact. Then GA was applied for solving VVC, which searches only the limited combinations of control. Volt/VAr/THD control problem was solved using MOGA in [18], where reactive power capability for DG's also considered for day-ahead scheduling of VVC devices for MOEL. In [106], GA was applied for optimal location and sizing of capacitors in the radial distribution system to minimize power losses and cost of VAr generated by capacitors.

A multiobjective NSGA-II based VVO framework was proposed in [35] for peak load reduction in the distribution network, where ELM was utilized. The Pareto front was obtained for MOEL and MOVD, hence DSO may use solution for specific purposes. In [19], MOGA was applied to solve Volt/VAr/THD control problem in which loads and output power of WTs were considered to be stochastic in nature, hence various scenarios were developed for loads and WTs output and then objectives MOEL and MOVD were solved in possible scenarios. An improved GA of a higher level of precision using two-mutation and two-crossover steps was proposed to solve a VVO problem in [58]. Impact of EVs with different penetration and charging levels on VVO was studied and usual objectives such as MOEL, etc. were also achieved by optimizing voltage of the distribution system.

*2.3.3.2 Particle Swarm Optimization (PSO)*

PSO integrated with fuzzy rules was applied in [64] to solve VVC problem of Thailand based distribution system. In this case, three objectives, i.e., MOEL, minimization of capacitor kVAr to be switched on, and MOSO were fuzzified using membership functions. In [65], DGs were integrated into the same distribution system and effect/benefits irrespective of objectives were studied for VVC problem. A fuzzy adaptive PSO for solving the daily VVC problem was presented in [83] considering DGs as one of the control variables in order to achieve the objective, i.e., MOEPSD under different load levels.

### 2.3.3.3 Teaching-Learning Algorithm (TLA)

A modified TLA was proposed in [39] to solve daily VVC problem considering the uncertainties of loads and output power of DGs. In this case, various objectives such as MOEL, MOED, MOVD, and MOEPSD were considered. The trade-off between conflicting objectives were also resolved by the proposed interactive fuzzy satisfying method.

### 2.3.3.4 Simulated Annealing (SA)

In [91], SA was applied to solve the VVC problem of a distribution system based on the Yunlin District of TPCo. In this case, VVC devices were optimally scheduled for MOEL, MOVD, MOSO, and minimization of reactive power intake from the substation. For all these objectives, membership functions were identified using fuzzy rules and then the overall objective was the minimization of a combined value of all memberships throughout the day.

### 2.3.3.5 Tabu Search (TS)

The capacitor placement problem was attempted using TS method to reduce power losses of Portuguese electric distribution system [84]. In this case, an optimal trade-off between power losses and cost of capacitors was also evaluated for decision making of DSO.

### 2.3.3.6 Shuffled Frog Leaping Algorithm (SFLA)

Modified/Improved SFLA was applied in [36, 37] to solve the daily VVC problem of a distribution system, where uncertainties due to load and the power output of WTs were modeled using Point Estimation Method (PEM). Using the proposed approach, optimal dispatch of real and reactive power of WTs and other DGs was ensured to achieve objectives, i.e., MOEL, MOED, and MOEPSD.

### 2.3.3.7 Memetic Algorithm (MA)

In [107], a fuzzy inspired MA was proposed to solve VVO the problem of the Yunlin District of TPCo, Taiwan in which system uncertainties were considered. VVC devices are coordinated with optimal scheduling to minimize power losses, voltage deviation, and reactive power intake from the substation. Due to consideration of the uncertainties of WTs and load, MA improves the results as compared to cases of without uncertainties and it is found to be better than PSO and GA.

### 2.3.3.8 Honey Bee Mating Optimization (HBMO)

The VVC problem of [83] was converted into multiobjective by including two new objectives as MOVD and MOEL, and then Chaotic Improved Honey Bee Mating Optimization (CIHBMO) was applied to solve the problem [38]. In this case, daily optimal dispatch of OLTC, capacitors, and active power output of DG's were determined for each hour. It has been shown that the proposed algorithm is more effective than HBMO, PSO, and GA.

### 2.3.3.9 Bacterial Foraging Algorithm (BFA)

In [79], Multiobjective $\theta$-Smart Bacterial Foraging Algorithm (M$\theta$-SBFA) was proposed to solve the VVC problem in which a wide variety of DGs was included (as in [39]). Total four objectives were considered, i.e., MOEL, MOVD, MOED, and MOEPSD, VVO problem first solved as a weighted combination of a single objective, and then optimal Pareto-front for various combinations of objectives was obtained.

### 2.3.3.10 Ant Colony Optimization (ACO)

The ACO was applied in [56] to solve VVC problem, including DGs, where VVC devices along with DGs were scheduled for MOEPSD.

### 2.3.3.11 Bee Swarm Optimization (BSO)

Modified BSO was proposed in [40] to solve multiobjective VVC problem considering uncertainties, where uncertainties were taken care of utilizing PEM based probabilistic load flow. Fuzzy clustering was used to control the size of the repository, where objective functions were converted into pseudo-objectives using fuzzy membership functions.

### 2.3.3.12 Gravitational Search Algorithm (GSA)

In [73], GSA was used for optimal allocation of capacitors in order to minimize power losses and cost of kVAr generated by capacitors. The sensitivity analysis was used to reduce the search space in order to make GSA faster. This method is faster and more effective as compared to SA and IPM.

### 2.3.4 Intelligent Methods

#### 2.3.4.1 Neural Network (NN)

Y-Y Hsu and F-C Lu [89] have overcome the problems of time and memory taken by methods presented in [30], [88] by applying Artificial Neural Network (ANN) for solving VVC problem. ANN was applied for preliminary dispatching of OLTC and capacitor then the dispatch was refined using fuzzy dynamic programming of [88] to achieve the best solution while the objectives remain the same as in [88]. ANN was also applied in [108] for optimal switching of CBs in the distribution system for reducing power losses, which is 100 times faster than traditional methods and suitable for online purpose.

#### 2.3.4.2 Adaptive Neuro-Fuzzy Inference System (ANFIS)

In ANFIS, classical artificial intelligence and expert systems have been combined together to make them suitable for real-time applications. The proposed ANFIS was applied to solve the VVC problem of the distribution network, where the scheduling of capacitor and taps of VRs was optimized for MOEL under changing peak load [69].

#### 2.3.4.3 Multi-Agent System (MAS)

A real-time VVO/CVR using MAS was suggested in [28] utilizing IEC 61850 and narrowband PLC communication platform. Here, real-time load profile was used to feed the VVO engine, which optimized the control settings of different VVC devices using improved GA for MOPD, MOEL, and minimization of VAr injection in real time.

## 2.4 Practical VVO and Applications

### 2.4.1 Siemens Power System and Control (SPSC)

A pilot VVC project for the distribution system of Northern State Power Company was developed by SPSC in order to achieve various objectives such as MOOE, revenue maximization, and maximization of VAr generated by capacitor switching. [12].

### 2.4.2 BC Hydro (BCH)

BCH conducted load-to-voltage dependency test for distribution feeders and reported up to 1% kWh and 3% kVArh reduction for a 1% reduction in voltage [93]. In [9], BCH shared

their experiences in terms of benefits, energy savings, deployment assessment, improvements in VVO with smart meters, etc. over the 12 years on VVO deployment in North America's distribution network. Recently BCH implemented VVO for the real-time distribution system, challenges and experiences in doing so are shared in [10].

### 2.4.3 American Electric Power (AEP)

As a part of AEP's smart grid initiative, an alternating day evaluation scheme (ADES) for conducting, and evaluating, the ability of VVO field deployment to reduce energy consumption and to optimize VAr flow was studied in [8]. In this ADES, $ZIP$ model was utilized for the residential load varies with time and voltage without a thermal loop. Transformer losses along with types of loading also studied for the reduced voltage. The overall energy consumption of loads with thermal loop (e.g. Water heater) also gets reduced by reducing voltage. It is also observed that energy consumption reduced when VVO in operation as compared with the case when VVO not in operation.

### 2.4.4 Avista Utilities (AUs)

Real-time VVC implementation was suggested in [11] and validated by an electric utility in Northwest USA. The operation of VVC program implemented by AUs, where demand reduction computed in various scenarios. The complete experiment was run for two weeks in order to minimize the uncertainties of customer behavior and temperature. The advantage of this VVC algorithm is utilities need not wait for a longer time to compute the energy savings of VVC implementations.

## 2.5 Scope of Research

Previous sections of this chapter discussed problem statement, common VVO objectives, constraints, outline of different techniques and work in the literature. From the above text, it can be stated that there is a lot of scope in this domain. With the inspiration to handle new difficulties, the exploration work exhibited in this thesis is divided into three parts, i.e., identifying a suitable load model for VVO, VVO framework considering DGs in presence of harmonics, and development of VVO strategies for the future distribution network. This section introduces a short background of significant works relating to the issues tended to in

this thesis, to legitimately justify the pertinence and need of the fundamental contributions of this work.

### 2.5.1 Impact of Load Models on Scheduling of VVC Devices

In previous research, different load models, such as $PQ$, $I$, $Z$, and mixed-load models ($ZIP$ and $ELM$) has been utilized for scheduling VVC devices while minimizing power and energy losses. The summary of existing literature in the area of minimizing power and energy losses using VVO is presented in Table 2.3. Here, $PQ$ and mixed of $PQ$, $I$, and $Z$ (shown with $PQ/I/Z$) modeling is widely used. However, few studies have also considered voltage-dependent models, such as $ELM$ [72] and $ZIP$ model [28, 29, 33, 58, 74, 75]. Most of the existing work considered balanced (B) distribution systems, and only few have focused on unbalanced (UB) characteristics. The common VVC devices used so far are OLTC, VRs, and CBs. However, some advanced devices, such as Static VAR Compensator (SVC) [63], DGs (PV, WT, and other generators) [18, 19, 41, 42], RES [40], EVs [58], and feeder re-configurations [109, 110] have also been included in the VVO.

### 2.5.2 VVO in Presence of DGs and Harmonics

In [112], network losses were minimized using VVO incorporating RE, CO, and Industrial (IN) customers in the distribution system. In [54], the impact of DGs on VVC has been studied first time on peak-loading conditions, where GA is used as an optimization tool. It is observed that loss reduction is higher when DGs are allowed to operate in the system. The VVC in presence of induction machine based DGs has been considered in [60, 113].

In [18,19,34,35,77], the VVO/CVR has been developed as a multi-objective problem and solved with a NSGA and its variant. The percentage reduction in peak-load was up to 7% and energy loss reduction was up to 33.87%. A real-time VVO/CVR method using a multi-agent system has been proposed in [28]. Here, improved GA has been utilized for scheduling taps of the transformer and capacitors so that apparent energy losses can be minimized. In [16–19], the harmonics are considered into the loads by incorporating nonlinear loads and therefore solved to minimize THD along with the energy losses. The problem of [18] (in which SPV generators along with the reactive power capability are considered) has been modified by considering WT generator into the network and results were reported in [19]. Here, up to 5%

Table 2.3. Summary of existing literature on minimization of power/energy losses using VVO

| Literature | Solution Method | Test System | Load Model | Characteristics | Volt/VAR Control Variables | | | |
|---|---|---|---|---|---|---|---|---|
| | | | | | OLTC | VR | CBs | Other |
| [60] | DP | 14-Bus | $PQ$ | B | ✓ | × | ✓ | × |
| [86] | OO | 120-Bus | $50\%I + 50\%Z$ | B | ✓ | × | ✓ | × |
| [71] | GA | Japanese Distribution System | $PQ$ | B | ✓ | ✓ | ✓ | kVAR of Reactor and SVC |
| [76] | IPM | 30-Bus | $PQ$ | B | ✓ | × | ✓ | × |
| [63] | GA | 17-Bus | $PQ$ | B | ✓ | × | × | DG voltage, SVC output |
| [77] | SPEA-2 | 69-Bus | $PQ$ | B | × | ✓ | ✓ | × |
| [38] | HBMO | 70-Bus | $PQ$ | B | ✓ | × | ✓ | Real Power of DG |
| [17] | GA | 30-Bus IEEE-123 Node | $50\%PQ + 50\%Z$ | B UB | ✓ | × | ✓ | × |
| [37] | SFLA | 70-Bus | $PQ$ | B | ✓ | × | ✓ | Real and Reactive Power of RES |
| [39] | TLA | 69-Bus IEEE-123 Node | $PQ$ $PQ/I/Z$ | B UB | ✓ | × | ✓ | Real and Reactive Power of RES |
| [78] | CPLEX Solver | 30-Bus, 120-Bus | $PQ$ | B | × | ✓ | ✓ | × |
| [79] | BFA | 69-Bus | $PQ$ | B | ✓ | × | ✓ | Real Power of RES |
| [80, 111] | Prime Dual IPM | 69-Bus, 119-Bus | $PQ$ | B | ✓ | × | ✓ | × |
| [18, 19] | GA | IEEE-123 Node | $50\%PQ + 50\%Z$ | UB | ✓ | × | ✓ | Reactive Power of PV WT |
| [40] | BSO | 69-Bus | $PQ$ | B | ✓ | × | ✓ | Real Power of RES |
| [28] | Genetic Algorithm | IEEE-34 Node | ZIP | UB | ✓ | ✓ | ✓ | × |
| [72] | DICOPT Solver | 33-Bus | $PQ$ and ELM | B | ✓ | × | ✓ | × |
| [53] | GNU Octave | 30-Bus, 69-Bus IEEE-13 Node | $PQ$ $PQ/I/Z$ | B UB | ✓ | × | ✓ | × |
| [33] | CPLEX Solver | 69-Bus | ZIP | B | ✓ | ✓ | ✓ | × |
| [61] | PSO | 14-Bus, 69-Bus | $PQ$ | B | ✓ | × | ✓ | × |
| [87] | Sensitivity Based DCDA | 135-Bus | $PQ$ | B | ✓ | × | ✓ | × |
| [57] | MAS | IEEE-34 Node | $PQ/I/Z$ | UB | × | ✓ | ✓ | × |
| [58] | GA | IEEE-123 Node | ZIP | B | × | ✓ | ✓ | Injected Reactive VAr of EVs |
| [29] | PSO | 33-Bus | ZIP | B | ✓ | × | ✓ | × |
| [74, 75] | GA | 33-Bus | ZIP | B | ✓ | × | ✓ | × |
| [42] | PSO | IEEE-123 Node IEEE-8500 Node | $PQ/I/Z$ $PQ$ | UB | ✓ | ✓ | ✓ | Real Power and PF of DG |
| [41] | PSO and NN | IEEE-37 Node | $PQ/I/Z$ | UB | ✓ | × | ✓ | Reactive Power of PV |
| [110] | PSO | 16-Bus, Taiwan Distribution System | $PQ$ | B | × | × | ✓ | Reconfiguration of Feeders |

reduction in THD and 28.75% reduction in peak hour losses have been reported. In [76], a Chinese distribution network has been considered with limited switching operations of VVC devices to minimize daily energy losses.

In [98, 114], BB and SCP has been applied to solve problems of VVC, where reactive kVAr are supplied by DGs while minimizing injected reactive power. A VVC problem considering RES, uncertainties of loads, and output power of RES has been solved with modified TLA and results in-terms of minimization of energy losses, energy demand, voltage deviation are reported in [39]. MPC-based VVO have been presented in [72], where 77% reduction in power losses has been reported. A VVO/CVR framework was presented in [33] to reduce the load demand, and up to 4.8% reductions in demand and 40% in losses have been reported.

Manbachi et. al [28, 29, 58, 74, 75] focused on real-time simulation platform of VVO in order to achieve various objectives such as minimization of energy losses, the cost incurred due to switching operations of control devices, cost of CVR, etc. In the literature, the VVO problem has been formulated to achieve a different set of objectives with various load models such as $PQ$, $I$, $Z$, $ELM$, and $ZIP$ load models. The $PQ$ model is widely used, where loss minimization was the prime objective. But, in actual practice, the active and reactive components of a load acts differently with variation in the terminal voltage [14, 115]. Some of the studies have considered this fact and utilized $ELM$ [35, 72, 116, 117], and $ZIP$ model [28, 29, 33, 58, 74, 75, 117] in the VVO.

### 2.5.3 Intelligent Volt/VAr Control for Maximum Energy Savings

In the past, a few researchers have worked on the VVO by considering RES in the distribution grid. The overview literature in this domain has been compiled in Table 2.4. In [36, 37], real and reactive power of wind farms are considered as control variables with real power of other RES. Whereas, only real power has been taken as a control variable in [38–40]. A few studies, [18, 19, 41], have also utilized converter capability to control reactive power. The dispatchable DGs are considered in [42], where both PF and active power have been taken as control variables. Thereafter, PF based reactive power control of SPV and/or WT generators has been studied in [43–46, 118–120].

In the literature, a very few studies have considered SPV systems operating with smart

inverters [47–50]. The full reactive power capability of a smart inverter has been utilized in [47]. In [48], the reactive power support of a SPV system is considered, where the reactive power capability of an inverter is determined based on Maximum Power Point Tracking (MPPT) and PF. Thereafter, the scheduling of reactive power has been ensured within the obtained capability of SPV unit. In [49], reactive power priority of a smart inverter has been utilized. The predefined intelligent volt/VAr control characteristic (IVVCC) of an inverter has been considered in [121]. The inverter supposed to follow the pre-specified IVVCC and inject or absorb reactive power based on local voltage signal. Thereafter, volt/VAr control considering IEEE Std.1547-2018 has been proposed in [50]. Here also, a predefined IVVCC of the smart inverter and local voltage signal were utilized for reactive power injection or absorption.

Table 2.4. Summary of existing literature on VVO with distributed generation

| Reference | Solution Technique | Volt/VAr control variables | | | Smart Inverter Consideration | | | | |
|---|---|---|---|---|---|---|---|---|---|
| | | OLTC/VR | CBs | Others | Inverter | Default IVVCC | Limited Q Capability | Optimal IVVCC | IEEE Std |
| [38] | HBMO | ✓ | ✓ | P of DG | ✗ | ✗ | ✗ | ✗ | ✗ |
| [36, 37] | SFLA | ✓ | ✓ | P and Q of RES | ✗ | ✗ | ✗ | ✗ | ✗ |
| [39] | TLA | ✓ | ✓ | P of RES | ✗ | ✗ | ✗ | ✗ | ✗ |
| [40] | BSO | ✓ | ✓ | P of RES | ✗ | ✗ | ✗ | ✗ | ✗ |
| [18] | GA | ✓ | ✓ | Q of PV | ✗ | ✗ | ✗ | ✗ | ✗ |
| [19] | GA | ✓ | ✓ | Q of WT | ✗ | ✗ | ✗ | ✗ | ✗ |
| [41] | PSO and NN | ✓ | ✓ | Q of PV | ✗ | ✗ | ✗ | ✗ | ✗ |
| [42] | PSO | ✓ | ✓ | P and PF of DG | ✗ | ✗ | ✗ | ✗ | ✗ |
| [43] | PSO | ✓ | ✓ | PF of WT | ✗ | ✗ | ✗ | ✗ | ✗ |
| [44] | PSO | ✓ | ✓ | constant PF of DG | ✗ | ✗ | ✗ | ✗ | ✗ |
| [45] | GA and PSO | ✓ | ✓ | constant PF of PV and WT | ✗ | ✗ | ✗ | ✗ | ✗ |
| [46] | CONOPT | ✓ | ✓ | unity PF of PV | ✗ | ✗ | ✗ | ✗ | ✗ |
| [47] | CPLEX | ✓ | ✓ | Q of PV | ✓ | ✗ | ✗ | ✗ | ✗ |
| [48] | OPTI | ✓ | ✓ | Pcurtail, and Q of PV | ✓ | ✗ | ✗ | ✗ | 1547-2003 |
| [49] | GA | ✓ | ✓ | Q of PV | ✓ | ✓ | ✗ | ✗ | 1547-2014 |
| [50] | CPLEX | ✓ | ✓ | Q of PV | ✓ | ✓ | ✗ | ✗ | 1547-2018 |
| Proposed | GA and PS | ✓ | ✓ | Q, IVVCC of Inverters | ✓ | ✓ | ✓ | ✓ | 1547-2018 |

# CHAPTER 3

# SELECTION OF LOAD MODEL FOR VOLT-VAR CONTROL

## 3.1 Introduction

Most of the literature in the domain of Volt/VAr Optimization (VVO) and control has considered minimization of real power losses (*kW*) and energy losses (*kWh*) with optimal coordination of Volt/VAr Control (VVC) devices. Nonetheless, a few studies [28, 29] have focused on minimization of *kVA* and *kVAh* losses. The existing works in the literature focuses only on impacts of different VVC devices scheduling on power and energy losses. However, no study is available on the impact of different load models on scheduling of these devices along with estimated losses (both power and energy) of the distribution network. Moreover, optimal scheduling obtained using a single load model can give misleading results. The settings obtained from the single load models cannot be considered for distribution feeder having the mix type of load. Different loads in the distribution network not only affect losses but also impact the voltage profile, energy intake, power factor, etc. Therefore, an investigation of effects of load model on planning or scheduling of VVC devices is necessary under VVO. Therefore, in this chapter, the impact of load models on the day-ahead scheduling of VVC devices in order to achieve minimal apparent power and energy losses have been considered. This chapter also demonstrates that how these parameters behave with different types of load models.

The rest of the chapter organized as follows. Section 3.2 describes various load models alongside their mathematical representation. The details of VVC devices and lines losses has been shown in section 3.3 and 3.4, respectively. Section 3.5 deals with the objective function considered in this chapter, and the required system and operational constraints have been defined in section 3.6. The simulation results of various case studies are discussed in section 3.7. Finally, the important findings of this chapter are summarized in section 3.8.

## 3.2 Modeling of Loads

There are various load models available for representing loads in a distribution system. These can be broadly classified as constant load models and voltage-dependent load models.

### 3.2.1 Constant Load Models

This category of model deals with constant impedance $(Z)$, constant current $(I)$, and constant power $(PQ)$ loads. [122] .

### 3.2.1.1  Constant Impedance Load (Z)

In this model, load impedance $(Z_i^l)$ is calculated using (3.1) and then load current is determined by (3.2) provided impedance calculated at rated voltage $(V_r)$ remains constant,

$$Z_i^l = \frac{|V_r|^2}{(S_i^l)^*} \tag{3.1}$$

$$I_i^l = \frac{V_i}{Z_i^l} \tag{3.2}$$

### 3.2.1.2  Constant Current Load (I)

In this model, current magnitude $(|I_i^l|)$ is determined using (3.3) and kept constant, whereas, $\delta_i$ is updated in each iteration of power-flow with update in voltage. Therefore, angle $(\angle\delta_i - \theta_i)$ of load current updated according to (3.4).

$$I_i^l = \left(\frac{S_i^l}{V_i}\right)^* \tag{3.3}$$

$$I_i^l = |I_i^l| \angle (\delta_i - \theta_i) \tag{3.4}$$

### 3.2.1.3 Constant Power Load (PQ)

For rated constant complex power $(S^l)$, load current is evaluated using (3.3), where $V_i$ is updated in every iteration of power flow.

### 3.2.2 Mixed Load Models

In actual practice, the active and reactive components of a load show different sensitivities to the terminal voltage [14, 96]. The load to voltage dependency is quite different for various categories of the load in which reactive power is more sensitive to voltage change [14]. This can be mathematically dealt with polynomial (ZIP) and exponential load model (ELM). In this work, the exact share of constant impedance (Z), constant current (I), and constant power (P) is not known for the studied test system. Therefore, we can not proceed with the ZIP model and hence ELM is utilized to represent the load-to-voltage dependencies. The real and reactive components of a load in ELM can be defined by (3.5) and (3.6), respectively.

$$P_{i,t}^l = P_{i,t}^r \left| \frac{V_{i,t}}{V_i^n} \right|^{k_i^p} \tag{3.5}$$

$$Q_{i,t}^l = Q_{i,t}^r \left| \frac{V_{i,t}}{V_i^n} \right|^{k_i^q} \tag{3.6}$$

## 3.3 Modeling of VVC Devices

The common VVC devices are on-load tap changer, substation and feeder capacitors, and voltage regulators. The scheduling of these devices is planned to accomplish a different set of VVO objectives. Details of these devices are as follows.

### 3.3.1 On Load Tap Changer (OLTC)

Transformers are equipped with a regulating or tap windings which are connected to the OLTC. The OLTC changes transformer ratio by adding or subtracting turns from either the primary or the secondary winding. A standard OLTC regulates the substation transformer voltage in the range of $\pm 5\%$ usually into 8 steps [35]. This results in $\frac{10}{8}\%$ or $1.25\%$ change in voltage per step. The regulation ratio for an OLTC transformer ($V^{oltc}$) can be defined by (3.7)

$$V^{oltc} = 1 \pm 0.0125 \times Tap^{oltc} \tag{3.7}$$

### 3.3.2 Voltage Regulator (VR)

The VR comprises of load tap changing mechanism and an auto-transformer. The voltage can be changed by changing taps of series winding of the auto-transformer. The VR requires

various settings such as *Voltage Level, Bandwidth, Time Delay, and Line Drop Compensator* [122]. VRs (single phase or three phase type) with tap changers are installed at various locations on distribution feeders to fine tune the voltage at a specific point. Tap position of a VR can be determined by a line-drop compensator circuit. A standard VR can regulate the voltage in the band of $\pm 10\%$ normally with 32 steps (16 taps for raising and 16 taps of lowering the voltage from nominal tap position) . This adds up to a $\frac{20}{32}\%$ or 0.625% change for every step. The regulation ratio of a VR ($V^{vr}$) can be determined using (3.8)

$$V^{vr} = 1 \pm 0.00625 \times Tap^{vr} \tag{3.8}$$

### 3.3.3 Capacitor Banks (CBs)

CBs are accommodated for power factor improvement and reactive power compensation. Therefore, capacitor banks are situated near the loads, on the feeder, and in the substation at distribution transformer. CBs are utilized to reduce the reactive power flows in the distribution network. Shunt CBs connected near the load will take leading current, which results in a reduction of total line current, thus decrease in line losses. Capacitor Banks that are installed in substation/or on feeders might be fixed or switched.

The capacitive VAr of a capacitor ($q^{cap}$) at rated voltage ($V^r$) can be written as

$$q^{cap} = |V^r|^2 \, \omega C \tag{3.9}$$

The reactive power supplied by a capacitor at terminal voltage $V$ (different than $V^r$), with frequency ($\omega$) and capacitance ($C$) constant, can be represented by (3.10)

$$Q^{cap} = q^{cap} \left| \frac{V}{V^r} \right|^2 \tag{3.10}$$

### 3.4 Line Losses

The power loss in $i - j$ section of a line can be mathematically expressed as

$$P_{loss} = |I_{ij}|^2 \times r_{ij} \tag{3.11}$$

The current in $i - j$ section can be evaluated using following relationship

$$I_{ij} = \frac{V_i - V_j}{z_{ij}} \tag{3.12}$$

Here, $z_{ij}$ is a complex impedance and can be written as $z_{ij} = r_{ij} + jx_{ij}$.

The line losses comprises real and reactive power losses. Therefore, the total apparent power loss at time $t$ can be expressed as

$$S_{loss,t} = \sum_{\substack{i \in N_b \\ i \neq j}} \sum_{\substack{j \in N_b \\ j \neq i}} (r_{ij} + jx_{ij}) \times \left| \frac{V_{i,t} - V_{j,t}}{z_{ij}} \right|^2 \tag{3.13}$$

Hence, the real power loss ($P_{loss,t}$) and reactive power loss ($Q_{loss,t}$) can be expressed by following equations.

$$P_{loss,t} = \sum_{\substack{i \in N_b \\ i \neq j}} \sum_{\substack{j \in N_b \\ j \neq i}} r_{ij} \times \left| \frac{V_{i,t} - V_{j,t}}{z_{ij}} \right|^2 \tag{3.14}$$

$$Q_{loss,t} = \sum_{\substack{i \in N_b \\ i \neq j}} \sum_{\substack{j \in N_b \\ j \neq i}} x_{ij} \times \left| \frac{V_{i,t} - V_{j,t}}{z_{ij}} \right|^2 \tag{3.15}$$

## 3.5 Objective Function

In VVO, both voltages and VAr flows in the distribution system are optimized. In the case of practical loads, the characteristics of active and reactive powers is distinct and vary with terminal voltage. Different classes of customer have different voltage sensitivities [14]. The apparent energy losses comprises the real as well as reactive energy losses. Therefore, the minimization of apparent energy losses leads to minimization of other two components as well. Accoridingly, minimization of apparent energy loss seems more appropriate than the minimization of real energy loss. The minimization of apparent energy losses ($SE_{kvah}^{loss}$) in *kVAh*, over a period of 24-hours, can be expressed by (3.16).

$$min \quad f = SE_{kvah}^{loss} = \sum_{t=1}^{24} |S_{loss,t}| \tag{3.16}$$

Here, $S_{loss,t}$ is evaluated based on mathematical expression in (3.13). The minimization of objective function is subjects to various system and operational constraints defined in the next section.

## 3.6 System and Operational Constraints

There are various operational and system constraints, which are defined by (3.17)-(3.23).

### 3.6.1 System Voltage Constraint

The voltage of the distribution system is constrained between $V^{min}$ and $V^{max}$

$$V_i^{min} \leq |V_{i,t}| \leq V_i^{max} \tag{3.17}$$

According to ANSI Std. C84.1-2016 [123], the maximum and minimum service voltage should be within $\pm 5\%$ of rated voltage.

### 3.6.2 Voltage Regulator Tap Setting and Daily Allowable Tap Operations

The more generalized form of regulation ratio for a regulator can be defined by (3.18)

$$V_{j,t}^{vr} = 1 + Tap_{j,t}^{vr} \frac{\triangle V_j}{100} \tag{3.18}$$

Here, $Tap_{j,t}^{vr} \epsilon \left\{ Tap_j^{min}, .., -1, 0, 1, .., Tap_j^{max} \right\}$. Since the tap changer of a voltage regulator is a mechanical device, the increased number of tap operations results in higher maintenance cost and decreased life. Therefore, daily tap operations of a voltage regulator needs to be limited. This limit can be mathematically expressed by (3.19)

$$\sum_{t=2}^{24} \left| Tap_{j,t}^{vr} - Tap_{j,t-1}^{vr} \right| \leq MT_j^{vr} \tag{3.19}$$

### 3.6.3 Switched Capacitor Bank and its Daily Allowable Switching Operations

In a practical system, capacitors are controlled with the help of a switch or tap changing mechanism. If a capacitor is control by a switch (either '*on*' or '*off*'), then kVAr supplied by $k^{th}$ capacitor at time $t$ can be written as in (3.10) with its switch status $(Sw_{k,t}^{cap})$

$$Q_{k,t}^{cap} = Sw_{k,t}^{cap} q_k^{cap} \left| \frac{V_{k,t}}{V^r} \right|^2 \tag{3.20}$$

Here, $Sw_{k,t}^{cap} \epsilon \{0, 1\}$. The constraint on number of daily switching operations of capacitor banks is necessary to avoid their frequent maintenance and replacements. This can be mathematically represented as (3.21)

$$\sum_{t=2}^{24} \left| Sw_{k,t}^{cap} - Sw_{k,t-1}^{cap} \right| \leq MS_k^{cb} \tag{3.21}$$

36

### 3.6.4 Capacitive kVAr Compensation Limit

Total reactive power support (*kVAr*) provided by the capacitor units should not exceed the total reactive power demand (load plus losses) of the network at any time slot $t$. Mathematically, this constraint is defined as (3.22)

$$\sum_{k=1}^{N_{cap}} Q_{k,t}^{cap} \leq \left( \sum_{m=1}^{N_b} Q_{m,t}^{l} + Q_{kvar,t}^{loss} \right) \tag{3.22}$$

### 3.6.5 Thermal Limit of Line

Overhead (OH) lines and underground (UG) cables in distribution systems have limits on current carrying capacities (ampicities). The maximum loading (*kVA*) limit is determined based on ampacity and rated voltage of a line or cable. The power flows through a line ($S_{line,t}$) at any point of time should be less than or equal to the maximum permitted loading limit of the line ($S_{line}^{max}$). This constraint can be mathematically represented by (3.23)

$$S_{line,t} \leq S_{line}^{max} \tag{3.23}$$

## 3.7 Simulation Results and Analysis

In this chapter, the IEEE-123 node radial distribution network shown in Fig. 3.1 [125], is considered for the study. The current carrying capacities of the lines and cables in the system are listed in Table 3.1. This system is suitably modified with three types of load, *i.e.*, Residential (RE), Commercial (CO) and Industrial (IN), and their locations in the network are

Table 3.1. Ampacity of lines and cables [124]

| Phases | Line or Cable | Conductor | Name | Ampacity |
|---|---|---|---|---|
| 3-phase and 2-phase | OH Line | Phase | 336,400 26/7 ACSR | 530 |
| | | Neutral | 4/0 6/1 ACSR | 340 |
| 1-phase | OH Line | Phase | 1/0 ACSR | 230 |
| | | Neutral | 1/0 ACSR | 230 |
| 3-phase | UG Cable | Phase and Neutral (1/3 Cu) | 1/0 AA CN | 175 |

given in Table 3.2. The total load connected to this system is $(3.49 + j1.92)$ MVA. In this study, the percentage of load shared by IN, CO, and RE customers is 44.72%, 20.77%, and 34.51%, respectively. Moreover, according to ANSI Std. C84.1-2016 [123], the operational voltage limits for this network are $V^{min} = 0.95$ p.u. and $V^{max} = 1.05$ p.u. The maximum number of switching operations per day for voltage regulators and capacitors are $MT^{vr} = 60$ and $MS^{cb} = 6$, respectively [89].

Table 3.2. Location of various load in the distribution system

| Load Type (No. of Loads) | Location in the distribution network (a,b,c are phases at which load is connected) |
|---|---|
| Commercial (22) | 10(a), 11(a), 31(c), 32(c), 33(a), 87(b), 88(a), 90(b), 92(c), 94(a), 95(b), 96(b), 102(c), 103(c), 104(c), 106(b), 107(b), 109(a), 111(a), 112(a), 113(a), 114(a) |
| Residential (28) | 62(c), 63(a), 64(b), 65(a), 65(b), 65(c), 66(c), 68(a), 69(a), 70(a), 71(a), 73(c), 74(c), 75(c), 76(a), 76(b), 76(c), 77(b), 79(a), 80(b), 82(a), 83(c), 84(c), 85(c), 86(b), 98(a), 99(b), 100(c) |
| Industrial (45) | 1(a), 2(b), 4(c), 5(c), 6(c), 7(a), 9(a), 12(b), 16(c), 17(c), 19(a), 20(a), 22(b), 24(c), 28(a), 29(a), 30(c), 34(c), 35(a), 37(a), 38(b), 39(b), 41(c), 42(a), 43(b), 45(a), 46(a), 47(a), 47(b), 47(c), 48(a), 48(b), 48(c), 49(a), 49(b), 49(c), 50(c), 51(a), 52(a), 53(a), 55(a), 56(b), 58(b), 59(b), 60(a) |
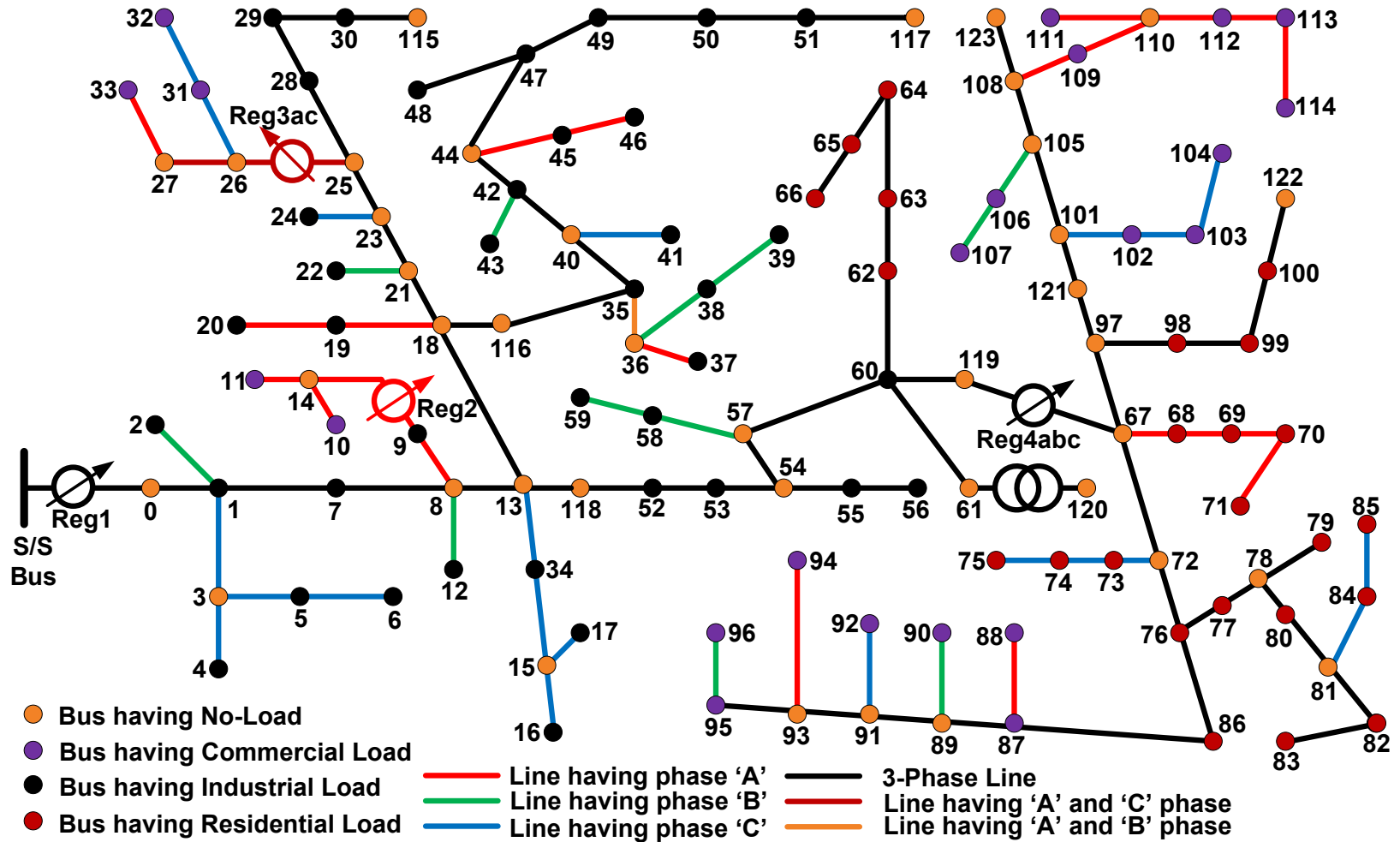
Fig. 3.1. Network topology of the modified IEEE-123 node radial distribution system

For the purpose of time-series power flow solutions, the daily load-shapes are adopted from a distribution utility based in Gujarat (India). The per unit (p.u.) load curves are shown in Fig. 3.2 [126, 127]. All the time-series load flow calculations are performed by utilizing MATLAB COM interface of OpenDSS [128]. The VVO is a kind of mixed integer non-linear programming problem and Genetic Algorithm (GA) has been broadly acknowledged for tackling this type of problem (Table 2.3). Therefore, GA is utilized for hourly scheduling of VVC devices in order to minimize apparent energy losses of the network. The interfacing of the optimization engine and OpenDSS is displayed in Fig. 3.3, where control commands of the network and initialization parameters of an optimization method are defined in MATLAB environment. Whereas, information related to the distribution system (such as, transformer data, load data, line data, capacitor data, etc.) is defined in the OpenDSS environment. As shown in Fig. 3.3, all load-flow calculations are performed in OpenDSS and then results fed to MATLAB, where the objective function and constraints are evaluated. And, based on the objective function value, control variables are updated for next iteration. This iterative procedure continued until minimum objective function value is achieved.
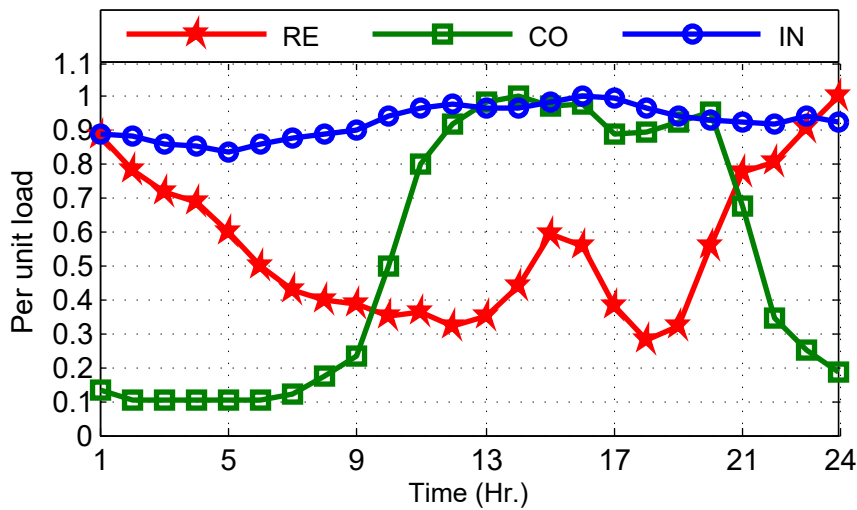


Fig. 3.2. Daily-load curves for different types of load
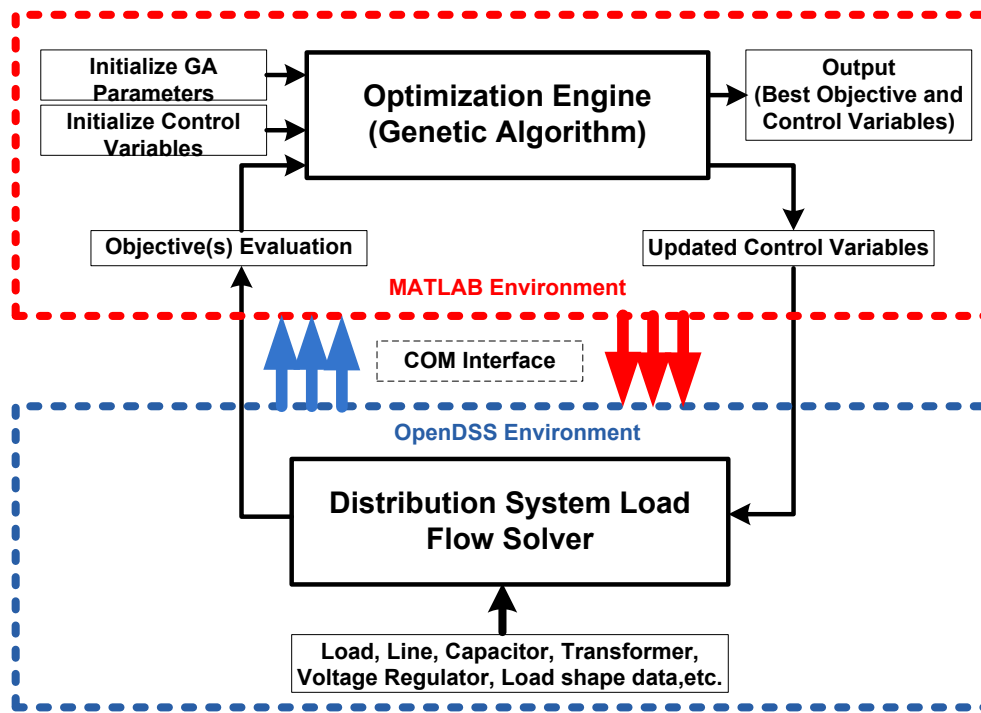
Fig. 3.3. Interfacing of an optimization engine (genetic algorithm) defined in MATLAB and OpenDSS load-flow solver

**3.7.1 Case Studies**

In order to study the impact of load models on the scheduling of VVC devices, this study has been conducted using constant load models ($PQ$, $I$, and $Z$) as well as mixed load model (represented by $ELM$). Four cases are considered and their description is given in Table 3.3. In first three cases, loads of the distribution network are modeled as $PQ$, $I$, and $Z$, respectively. But, the practical loads are of mixed type (combination of $PQ$, $I$, and $Z$). The exact combination of $PQ$, $I$, and $Z$ is not known for IN, CO, and RE loads connected to the network. Therefore, the last case deals with a mixed load model. For this situation, $ELM$ is utilized for modeling practical loads of the network. The voltage exponents ($k^p$ and $k^q$) required to represent each class of load model can be found in Table 3.3 [14].

Table 3.3. Studied cases and required $k^p$ and $k^q$ parameters for different load models

| Load Model | Industrial | | Commercial | | Residential | |
|---|---|---|---|---|---|---|
| | $k^p$ | $k^q$ | $k^p$ | $k^q$ | $k^p$ | $k^q$ |
| $PQ$ | 0 | 0 | 0 | 0 | 0 | 0 |
| $I$ | 1 | 1 | 1 | 1 | 1 | 1 |
| $Z$ | 2 | 2 | 2 | 2 | 2 | 2 |
| $ELM$ | 0.18 | 6.00 | 1.50 | 3.15 | 1.04 | 4.19 |

**3.7.2 Impact of Load Models During Peak-Loading Condition**

In this case, the objective is to minimize the apparent power losses (absolute value calculated using eq. (3.13)) of the network, when loads are operating at their peak value. The results obtained for peak-loading conditions are displayed in Table 3.4. The voltage profile of IN, CO, and RE loads is shown in Fig. 3.4.
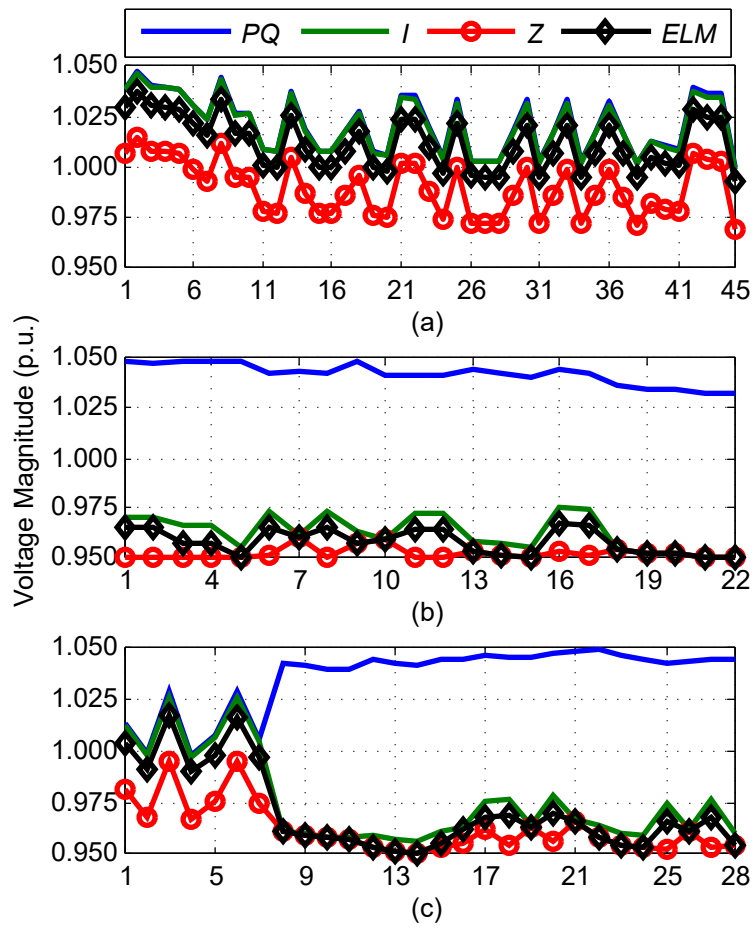
Fig. 3.4. Voltage profile of various customers with different load models, (a) Industrial Loads, (b) Commercial Loads, (c) Residential Loads

Table 3.4. Results obtained with peak-loading condition

| Load Model | System Losses | | | Load Consumption | | | Capacitor | Substation Parameters | | | | Optimal Tap Positions of Regulators | | | | | | |
|---|---|---|---|---|---|---|---|---|---|---|---|---|---|---|---|---|---|---|
| | kVA | kW | kVAr | kVA | kW | kVAr | kVAr | kVA | kW | kVAr | pf | VR1 | VR2a | VR3a | VR3c | VR4a | VR4b | VR4c |
| PQ | 177.95 | 91.21 | 152.80 | 3983.62 | 3490.26 | 1920.24 | 825.12 | 3792.66 | 3581.47 | 1247.91 | 0.944 | 16 | 4 | 7 | 5 | 7 | 2 | 5 |
| I | 177.24 | 91.07 | 152.06 | 3962.72 | 3471.67 | 1910.68 | 705.43 | 3812.53 | 3562.74 | 1357.31 | 0.934 | 16 | -8 | -8 | -8 | -5 | -8 | -8 |
| Z | 169.55 | 87.11 | 145.46 | 3776.36 | 3308.43 | 1820.77 | 691.56 | 3626.91 | 3395.53 | 1274.67 | 0.936 | 6 | -7 | -4 | -6 | -1 | -7 | -4 |
| ELM | 173.89 | 89.51 | 149.09 | 3894.93 | 3416.85 | 1869.66 | 698.48 | 3746.69 | 3506.36 | 1320.27 | 0.936 | 13 | -8 | -8 | -8 | -5 | -8 | -8 |

*3.7.2.1 Scheduling of VVC Devices*

The optimal tap-positions of voltage regulators, for different cases, are shown in Table 3.4 . It can be seen that there is significant variation in tap positions. Most of the regulators (asides VR1) attains the same schedule for $I$ and $ELM$ models, though very surprising settings are acquired in the case of $PQ$ and $Z$ models. In spite of the fact that all capacitors are '*on*' in each case, *kVAr* provided by them is not same. This is a result of different terminal voltages at the capacitor units.

*3.7.2.2 Voltage Profile*

The voltage profile acquired in various cases is altogether different. The industrial loads having higher voltage magnitudes (Fig. 3.4a) than commercial and residential loads. It is also demonstrated that voltage magnitude is highest for $PQ$ model and lowest for $Z$ model to achieve minimum loss. The voltage profile of the commercial loads (Fig. 3.4b) is in the range of 0.95 p.u. to 0.975 p.u. (except for $PQ$ model). Furthermore, residential loads also having similar voltage range (with the exception of first few loads, *i.e.*, from 62c to 66c) and displayed in Fig. 3.4c.

*3.7.2.3 Other Distribution System Parameters*

The system losses, load consumption, *kVAr* supplied by the capacitors, and substation parameters, all are highest for $PQ$ model and lowest for $Z$ model (Table 3.4). Due to the voltage-dependency of the capacitors, *kVAr* supplied by them is highest in the case of $PQ$ model as the voltage is higher than rated. Though, *kVAr* provided by capacitor units is least in $Z$ model as a result of lower voltage (Fig. 3.4). In the case of $ELM$, the voltage exponents of active and reactive power are different for IN, CO, and RE loads. In this case, the total reactive power consumed by loads and losses is more sensitive to voltage change than the real power.

**3.7.3 Impact of Load Models with Variable-Loading Condition**

In the previous section, the impact of load models on the scheduling of VVC devices along with various distribution parameters (power losses, power consumption, etc.) has been discussed for the peak-loading condition. But in actual practice, loads are varying throughout

the day. Therefore, this section deals with the variable-loading condition, where loads are varying according to the load-curves.

The daily scheduling of taps of voltage regulators for the variable-loading conditions is displayed in Fig. 3.5, while '*on-off*' schedule of capacitor units is shown in Fig. 3.6. The tap operations of regulators and switching operations of capacitor units are greatly affected in time-series analysis. Therefore, operations of these devices are also discussed in this section. The surface of voltage profile for a period of 24-hr is shown in Fig. 3.7. Besides, Table 3.5 represents the energy dissipated in losses, consumed by the loads, and supplied at the substation.

Table 3.5. Energy consumption and power factor in different cases with variable-loading condition

| Load Model | Energy Losses | | | Energy consumed by Loads | | | Capacitor | Substation Energy and Power Factor | | | | |
|---|---|---|---|---|---|---|---|---|---|---|---|---|
| | *kVAh* | *kWh* | *kVArh* | *kVAh* | *kWh* | *kVArh* | *kVArh* | *kVAh* | *kWh* | *kVArh* | $pf_{min}$ | $pf_{max}$ |
| *PQ* | 2159 | 1110 | 1852 | 68505 | 59803 | 33061 | 8718 | 66644 | 60913 | 26195 | 0.8687 | 0.9689 |
| *I* | 2144 | 1101 | 1840 | 67389 | 58828 | 32524 | 12019 | 64180 | 59929 | 22346 | 0.8758 | 0.9656 |
| *Z* | 2053 | 1054 | 1762 | 63909 | 55794 | 30840 | 11251 | 61056 | 56848 | 21351 | 0.8644 | 0.9796 |
| *ELM* | 2126 | 1092 | 1824 | 65121 | 58374 | 28566 | 10140 | 63037 | 59466 | 20250 | 0.8886 | 0.9763 |
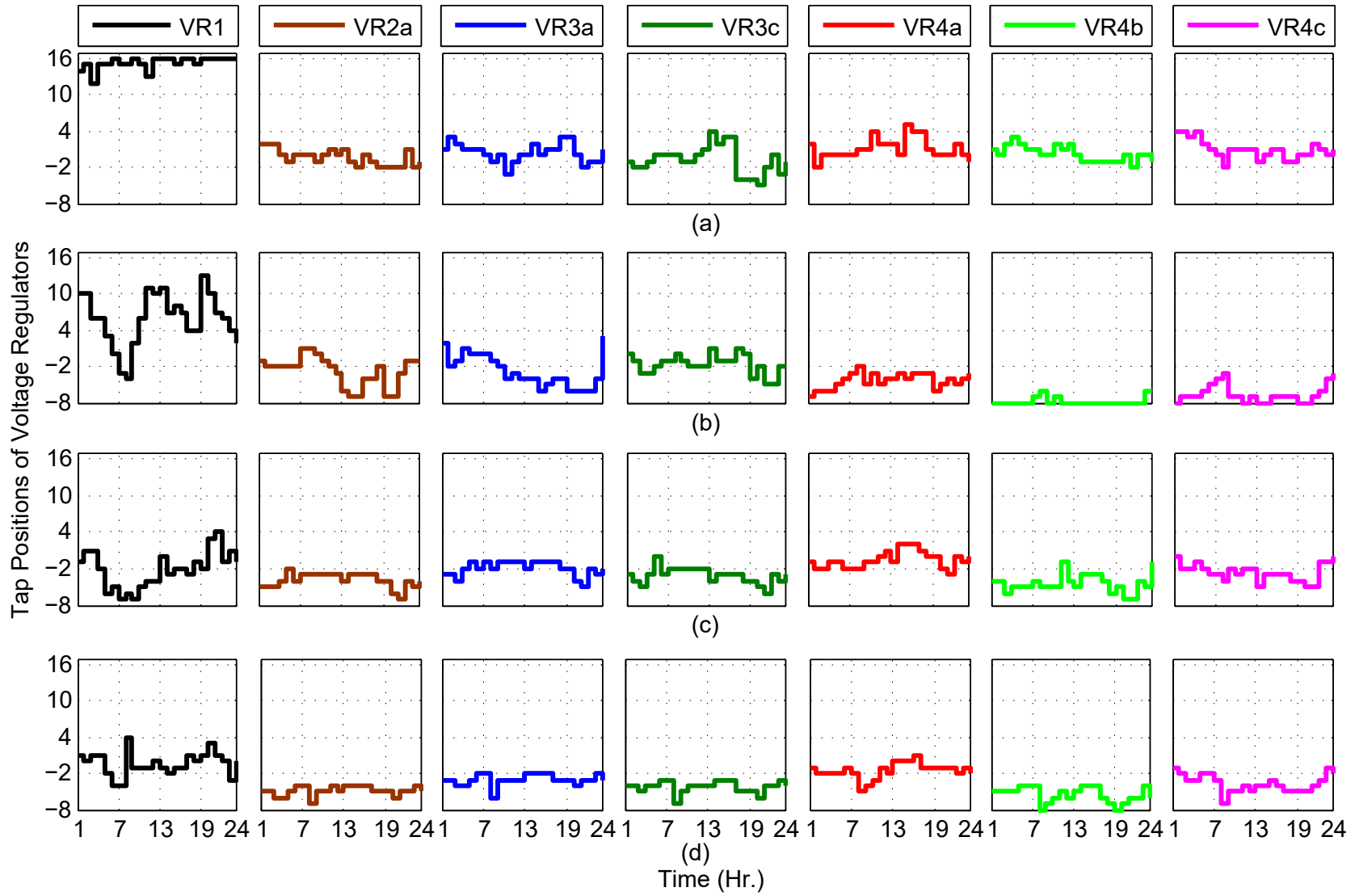
Fig. 3.5. Optimal tap scheduling of voltage regulators for different load models, (a) $PQ$, (b) $I$, (c) $Z$, (d) $ELM$

### 3.7.3.1 Daily Scheduling of VVC Devices

The optimal tap settings of regulators for various load models are displayed in Fig. 3.5. In the case when loads are modeled as $PQ$, taps are settled to higher positions (Fig. 3.5a) to keep up high voltage magnitude. Here, it is also observed that daily highest positions of all regulators have occurred for $PQ$ load model. However, lowest position is distributed among different load models and can be noticed in Fig. 3.5a to Fig. 3.5d. The range of tap operation of individual regulator unit is almost same for $Z$ model and $ELM$ model, but positions (with respect to time) are distinct.

The 'on-off' schedule of capacitor units is displayed in Fig. 3.6. This schedule is unique for different load models. Therefore, active participation time (number of hours for which capacitor status is 'on') of each unit is different. Here, *Cap#83* (600 kVAr) having highest capacity as compared to other units (50 kVAr). Therefore, 'on-off' status of this unit can greatly affect performance of distribution network. From Fig.3.6a to Fig.3.6d, it is clear that *Cap#83* having maximum participation hours than other units (except for $PQ$ model).

### 3.7.3.2 Daily Taps and Switching Operations of VVC Devices

In daily scheduling, switching operation of VVC devices is an important aspect. These operations are calculated based on mathematical expressions given in (3.19) and (3.21). In addition, total tap operations of regulators and switching operations of capacitor units can be evaluated using (3.24) and (3.25), respectively.

$$REG_{oper} = \sum_{j=1}^{N_{vr}} \sum_{t=2}^{24} \left| Tap_{j,t}^{vr} - Tap_{j,t-1}^{vr} \right| \tag{3.24}$$

$$CAP_{oper} = \sum_{k=1}^{N_{cap}} \sum_{t=2}^{24} \left| Sw_{k,t}^{cap} - Sw_{k,t-1}^{cap} \right| \tag{3.25}$$

The number of switching operations with respect to different models are displayed in Table 3.6. The maximum number of operations are highlighted with red color and minimum with yellow color. It is observed that total operations is highest for constant current model ($I$) and lowest for mixed load model ( *i.e.*, $ELM$). It can also be noticed that tap operations of main regulator (*VR1*) are more (except for $PQ$ model) as compared to other regulators.
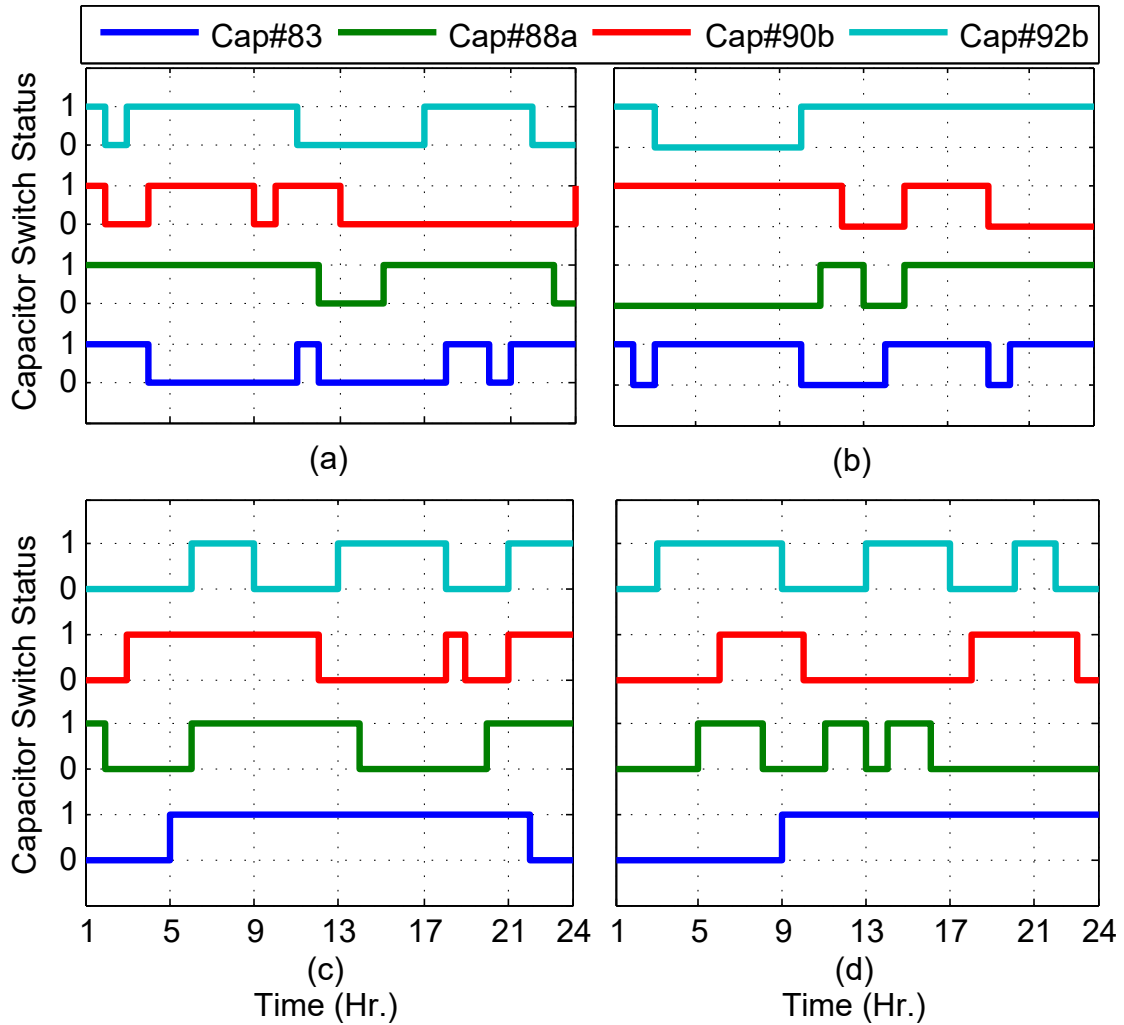
Fig. 3.6. Daily optimal '*on-off*' status of capacitor units in different cases, (a) $PQ$, (b) $I$, (c) $Z$, (d) $ELM$

Table 3.6. Switching operations of voltage regulators and capacitor units with different load models

| Load Model | Tap Operations of Regulators | | | | | | | Switching Operations of Capacitors | | | |
|---|---|---|---|---|---|---|---|---|---|---|---|
| | VR1 | VR2a | VR3a | VR3c | VR4a | VR4b | VR4c | Cap83 | Cap88a | Cap90b | Cap92c |
| $PQ$ | 20 | 23 | 28 | 30 | 29 | 20 | 23 | 6 | 3 | 6 | 5 |
| $I$ | 60 | 28 | 29 | 28 | 24 | 8 | 19 | 6 | 3 | 3 | 2 |
| $Z$ | 44 | 17 | 19 | 22 | 21 | 29 | 22 | 2 | 4 | 5 | 5 |
| $ELM$ | 39 | 16 | 16 | 18 | 19 | 21 | 21 | 1 | 6 | 4 | 6 |
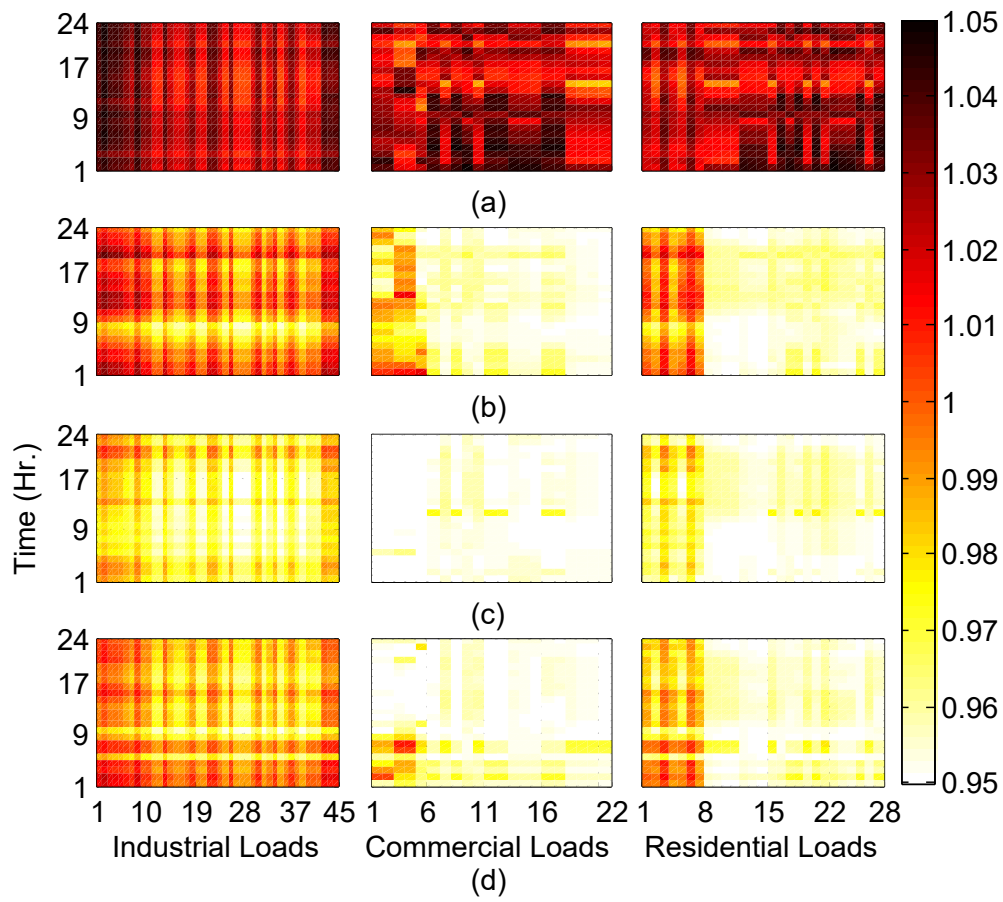
Fig. 3.7. Surface plot of daily voltage profile for various types of customer with different load model, (a) $PQ$ (b) $I$, (c) $Z$, (d) $ELM$

*3.7.3.3 Daily Voltage Profile*

The surface plots of voltage profiles are displayed in Fig. 3.7. It can be seen that voltage magnitudes are highest for $PQ$ model throughout the day (Fig. 3.7a). This is because of tap positions of regulators are at higher positions (Fig. 3.5a) to minimize the losses. On the contrary, the voltage levels are near minimum limit in the case of $Z$ model. This property of $Z$ models is utilized in Conservation Voltage Reduction (CVR) to reduce the energy losses in a distribution system. Except $PQ$, other load models lead to reduced voltage profile (Fig. 3.7b, Fig. 3.7c, and Fig. 3.7d). However, the industrial loads still holds higher voltage than CO and RE loads. The voltage profile of first seven nodes of RE loads also having high magnitudes during peak-loading condition, since they are connected just after the industrial loads and voltage regulation is not possible. In this case, all CO loads having low voltage (0.95-0.96 p.u.). The RE loads also showing the same behavior (except first seven loads). When loads are modeled as mix loads ($ELM$), they attain higher voltage magnitudes as compared to $Z$ model (Fig. 3.7d).

*3.7.3.4 Various Parameters of the Distribution Network*

The various energy parameters along with minimum and maximum substation power factor are shown in Table 3.5. The energy consumption in all domains (losses, loads, and substation) is high when loads are modeled as $PQ$. In the case of $I$ model, the voltage magnitude for IN, CO, and RE customer is reduced and hence energy consumption decreases. The overall energy-consumption of network is minimum in case of $Z$ model. This reduction can be directly correlated to the voltage profile in this case (Fig. 3.7c), and due to decreased voltage profile, the energy consumption is minimum. But, substation parameters acts very differently in the case of mixed-load model ($ELM$). Although, voltage profile in these two cases ($Z$ model and $ELM$ model) is not so different (Fig. 3.7c and Fig. 3.7d), but reactive power consumption is more sensitive to voltage change and, hence, more reduction is achieved in load and substation *kVArh*. In this case, *kVArh* supplied by capacitors are also less as compared to case where $I$ and $Z$ modeling is considered. This is due to '*on-off*' schedule of capacitor units and their terminal voltage.
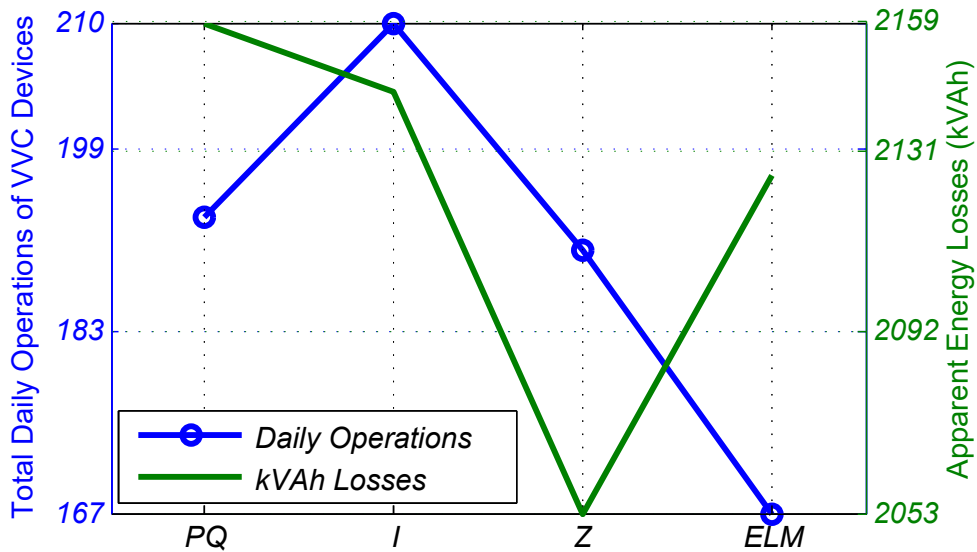
Fig. 3.8. Total operations of VVC devices verses kVAh losses of the network

### 3.7.4 Final Remarks on Selection of Load Model for Volt/VAr Control

It is observed in both peak and variable loading conditions that power and energy consumed by loads and losses is maximum when loads are modeled as $PQ$. This is because power remains constant in $PQ$ model, and network losses can be minimized if current drawn by the loads is minimum. It can be possible by raising the terminal voltage of the loads and injecting leading current in to the system. Therefore, surface of voltage profile shows higher range as compared to other cases. If the loads are modeled as $I$, the current remains constant. Here, the current drawn by loads cannot be reduced, and losses can only be reduced if some leading currents (due to capacitors) injected in the system. Hence, reactive *kVArh* supplied by the capacitor units is highest in this case. Apart from this, constant impedance loads consumed less power with reduced terminal voltage. Therefore, DSO tries to reduce the voltage to its minimum permissible limit so that current drawn by loads can be reduced and hence minimum losses can be obtained. The energy consumed by loads and losses is minimum when loads are modeled as $Z$.

In order to minimize energy losses, optimal scheduling of capacitors and voltage regulators is required. This will results in optimized voltages and reactive power flow throughout the distribution network. The controlled voltage over a different types of load (IN, CO, and

RE) have distinct range of voltage magnitudes and varies with load models. The voltage sets to a maximum value with $PQ$ model and minimum with $Z$ model. In all studied cases, IN customers holds higher voltage magnitudes as compared to CO and RE loads.The behavior of various parameters of the network (such as energy, power factor, etc.) is totally different when loads are modeled as $ELM$. In this model, the voltage exponents ($k^p$ and $k^q$) displayed in Table 3.3 are unique and distinct for industrial, commercial, and residential loads. However, they are same when considering classical load model, e.g., $k^p = k^q = 0$ for $PQ$ model, $k^p = k^q = 1$ for $I$ model, and $k^p = k^q = 2$ for $Z$ model. Therefore, active and reactive components of various types of load acts distinctly with the change in the terminal voltage when considering $ELM$ model. Henceforth, different parameters of the network such as energy, losses, power factor, and so on will also be different with ELM model. Here, it is found that reactive energy (*kVArh*) consumed is more sensitive to voltage change than real energy (*kWh*) and same has been noticed in the results. This is due to the voltage exponents of different loads in $ELM$ model.

The taps and switching operations of VVC devices is an important aspect while scheduling them on daily basis. They are largely affected by the load models and same has been seen in the results (Table 3.6). The total switching operation with respect to *kVAh* losses has been displayed in Fig. 3.8. The operations are minimum with $ELM$ model and maximum with $I$ model. However, the losses are minimized with $Z$ model and maximum for $PQ$ model.

The results show that optimal scheduling of VVC devices is different for various load models. The scheduling obtained with one model cannot be applied to a network having a different kind of load. This may provide misleading information about the expectation of different set of network parameters. As seen in the results, the overall performance of $Z$ model is better than other (in terms of energy consumption and losses). However, optimal settings obtained in this case cannot be considered for the same network having a different kind of load. In order to validate the same, if optimal settings of VVC devices obtained with $Z$ model, applied on the same distribution system having different loads (let, $PQ$, $I$, and $ELM$), then, it will give ambiguous results and can be seen in Table 3.7. Here, it is observed that power and energy consumed by loads and substation are reduced and losses increased. But, voltage solution in all the cases is violating its lower permissible limit (highlighted with

red color). Similarly, if scheduling obtained with $PQ$ model applied to a network having practical loads then energy and losses would be more than expected due to voltage-dependent loads.

Table 3.7. Various parameters of distribution network when settings obtained with $Z$ load model applied on other models

(Upper and lower rows indicate the values of parameters during peak-loading and variable loading conditions, respectively)

| | Power/Energy Loss | | | Power/Energy of Loads | | | Capacitor | Power/Energy and p.f. of substation | | | | | Minimum voltage of network | | |
|---|---|---|---|---|---|---|---|---|---|---|---|---|---|---|---|
| | kVA | kW | kVAr | kVA | kW | kVAr | kVAr | kVA | kW | kVAr | pf | pf | Phase A | Phase B | Phase C |
| | kVAh | kWh | kVArh | kVAh | kWh | kVArh | kVArh | kVAh | kWh | kVArh | $pf_{min}$ | $pf_{max}$ | $min(V_a)$ | $min(V_b)$ | $min(V_c)$ |
| PQ | 200.07 | 102.55 | 171.79 | 3993.14 | 3489.99 | 1919.98 | 684.79 | 3858.67 | 3592.53 | 1406.98 | 0.931 | 0.931 | 0.9426 | 0.9471 | 0.9446 |
| | 2401.0 | 1230.0 | 2062.0 | 68504.7 | 59803.2 | 33061.0 | 11186.7 | 65860.1 | 61033.2 | 23936.3 | 0.864 | 0.973 | 0.9431 | 0.9478 | 0.9445 |
| I | 183.26 | 94.02 | 157.30 | 3852.59 | 3367.13 | 1852.42 | 688.45 | 3704.53 | 3461.15 | 1321.27 | 0.934 | 0.934 | 0.9467 | 0.9486 | 0.9476 |
| | 2212.4 | 1135.0 | 1899.0 | 66083.2 | 57690.2 | 31890.8 | 11220.4 | 63322.0 | 58825.2 | 22569.4 | 0.864 | 0.977 | 0.9469 | 0.9489 | 0.9475 |
| ELM | 177.93 | 91.34 | 152.69 | 3778.34 | 3387.93 | 1655.16 | 692.93 | 3653.31 | 3479.27 | 1114.92 | 0.952 | 0.952 | 0.9507 | 0.9507 | 0.9496 |
| | 2156.8 | 1107.0 | 1851.0 | 64865.5 | 58350.9 | 28025.1 | 11265.5 | 62659.2 | 59457.9 | 18610.7 | 0.888 | 0.991 | 0.9505 | 0.9504 | 0.9492 |

## 3.8 Summary

In this chapter, the effect of load models on the scheduling of VVC devices has been studied under VVO framework. This effect has been studied considering constant power, constant current, constant impedance, and mixed load models. From the results, it is observed that these models provide different scheduling of VVC devices and, hence, voltage profile, losses, energy consumption, power factor, etc., are different. The constant $PQ$ load model shows slightly higher losses, whereas constant $Z$ load model results in the least energy losses. Moreover, it is ascertained that daily operations of VVC devices are greatly affected by different types of loads and their models. Therefore, a solution obtained from a particular model cannot be applied to the same network having another types of loads. This may generate misleading results, such as higher losses, voltage violation, line congestion, etc. This may also lead to a wrong estimation of life of switching devices because each device has fixed number of operations.Thus, it is very important to choose suitable load models for proper scheduling of VVC devices. It can also be concluded that the exponential load models with a proper choice of exponents accurately emulate the practical loads.

# CHAPTER 4

# VOLT-VAR OPTIMIZATION IN PRESENCE OF DISTRIBUTED GENERATION

## 4.1 Introduction

It has been observed in chapter 3 that exponential load models can accurately represent the practical loads with appropriate choice of voltage exponents. Moreover, the real and reactive energy demand of the distribution network is altogether influenced by the scheduling of volt/VAr Control (VVC) devices. The vast majority of the research performed in the domain of VVC has considered minimization of real power ($kW$) and energy losses ($kWh$) for optimal coordination of VVC devices. However, minimization of apparent energy losses ($kVAh$) has also been studied in the previous chapter and a few past research [28, 29]. But as reported in [8], 5% energy losses have occurred in the distribution system. This has been focused in many studies [11, 12, 30–35, 116], where the prime objective was the minimization of active energy demand.

But, the characteristics of active and reactive loads are distinct and varies with the terminal voltage. Each class of customer having different voltage sensitivities [14]. Therefore, voltage control and VAr flow in the distribution system affects both real and reactive powers in a distinct way. Moreover, the presence of a shunt capacitor provides a leading current, and hence, both active and reactive power losses will also be affected. This gives the motivation to focus on minimization of apparent energy demand or apparent energy losses instead of active energy demand and losses. There is no literature on minimization of apparent energy demand. Apart from energy demand, the impact of distributed generation (DG) and Conservation Voltage Reduction (CVR) has been studied [15] for the perspective of voltage profile on peak-loading condition. However, its impacts on energy savings under the Volt/VAr Optimization (VVO) framework needs to be studied.

Aside from the consideration of the apparent energy demand of a distribution network, the harmonics have also been considered in this chapter. Because of complexity, the harmonics have received less attention in VVO problem formulation. Ref. [16–19] deals with the har-

monics considering non-linear loads. However, the voltage reliance on the real and reactive components of the load has been neglected. In this chapter, the harmonics are considered on the load-side along with the distinctive voltage-dependency of the active and reactive load of various customers. The main contributions of this chapter are as follow:

1) Due to different voltage dependence of active-reactive powers of the loads and losses, minimization of apparent energy of the distribution system is considered instead of minimization of active energy or losses.

2) The distributed generation is considered to increase the savings in-terms reduction of substation apparent energy demand.

3) The harmonics are considered on the load-side while maintaining the voltage-dependence of different practical loads.

4) The impact of harmonics with and without local generation has been studied in order to minimize substation apparent energy demand.

Therefore, this chapter particularly focuses on the VVO model with and without DGs in order to minimize daily substation apparent energy. The study is conducted into two scenarios, i.e., with and without DGs. Here, non-dispatchable DGs are considered in the study. Each scenario is having three cases, such as (1) base case, (2) voltage control case, and (3) volt/VAr control case.

The rest of chapter is organized as follows. Section 4.2 describes problem formulation by describing load model, DG model, loss model, objective function, and constraints. Results and discussion along with modifications in the test systems and case studies are described in section 4.3, whereas complete study is summarized in section 4.4.

## 4.2 Problem Formulation

### 4.2.1 Load Models

In previous chapter, it has been shown that the exponential load models with a proper choice of voltage exponents accurately emulate the practical loads such as Industrial (IN), Residential (RE) and Commercial (CO). Therefore, in this chapter, the exponential load models have

been utilized to represent the voltage dependencies of the practical loads. Mathematical expression of exponential load model to represent the real and reactive components of a load have been directly utilized from (3.5) and (3.6), respectively. The required voltage exponents ($k^p$ and $k^q$) for IN, CO, and RE loads will be same as in Table 3.3.

### 4.2.2 Distributed Generator Models

In this chapter, Solar Photovoltaic (SPV) and Wind Turbine (WT) generators are assumed to be connected at various locations in the distribution system [129, 130]. Their mathematical modeling is discussed in the following subsections.

#### 4.2.2.1 Solar Photovoltaic Generator

In this chapter, SPV generators are assumed to be connected at various locations in the distribution grid. The power generated by a SPV generator is basically a mathematical function of two factors, i.e., solar irradiance ($G$) and cell temperature ($T^c$). These factors vary over geographical locations and time of the day. The mathematical expression for the output power can be defined by (4.1) [131].

$$P_{m,t}^{pv} = P_m^{rated} \frac{G_t}{G^{std}} [1 + k_m^{Temp}(T_{m,t}^c - T)] \tag{4.1}$$

The real power obtained using (4.1) is directly fed to the distribution grid with the help of an inverter operating on unity power factor.

The total power available is directly fed to the distribution system as a negative PQ load.

#### 4.2.2.2 Wind Turbine Generator

The output of a WT generator is a function of wind speed. Wind speed varies throughout the day. Therefore, the output power of WT generator will also vary. This variation can be

59

represented by following equation [39].

$$P_{n,t}^{wt} = P_{n,max}^{wt} \times \begin{cases} r_1(w_t - v_{ci}), & v_{ci} \leq w_t \leq v_1 \\ r_1(v_1 - v_{ci}) + r_2(w_t - v_1), & v_1 \leq w_t \leq v_2 \\ r_1(v_1 - v_{ci}) + r_2(v_2 - v_1) + r_3(w_t - v_2), & v_2 \leq w_t \leq v_r \\ 1 & v_r \leq w_t \leq v_{co} \\ 0 & otherwise \end{cases} \quad (4.2)$$

where $v_{ci}$ =4 m/s, $v_r$ =14 m/s, $v_{co}$ =25 m/s, $v_1$ =7 m/s, $v_2$ =12 m/s, $r_1 = \frac{0.2}{(v_1 - v_{ci})}$, $r_2 = \frac{(0.96 - 0.2)}{(v_2 - v_1)}$, and $r_3 = \frac{(1 - 0.96)}{(v_r - v_2)}$. $r_i$ and $v_i$ are the slope and break-point of the $i^{th}$ piece of the wind power generation curve, respectively.

Total real power generated by SPV and WT generators can be mathematically written as

$$P_t^{DG} = \sum_{m \in N_{pv}} P_{m,t}^{pv} + \sum_{n \in N_{wt}} P_{n,t}^{wt} \quad (4.3)$$

Based on power factor of each generator, total reactive power generation can also be formulated using equation (4.4)

$$Q_t^{DG} = \sum_{m \in N_{pv}} P_{m,t}^{pv} tan\phi_m^{pv} + \sum_{n \in N_{wt}} P_{n,t}^{wt} tan\phi_n^{wt} \quad (4.4)$$

Therefore, total complex power of all DGs at time $t$ can be defined by (4.5)

$$S_t^{DG} = P_t^{DG} + jQ_t^{DG} \quad (4.5)$$

### 4.2.3 Capacitor kVAr Model

The load in a distribution system is continuously varying throughout the day. Therefore, the voltage across the feeders where capacitors are associated will likewise affected, and subsequently, a voltage-dependent capacitor model is utilized. Referring (3.10), a total capacitive VAr injected into the distribution system at time $t$ can be mathematically written as

$$Q_t^{CBs} = \sum_{k \in N_{CB}} q_{k,t}^{cap} \left| \frac{V_{k,t}}{V_k^r} \right|^2 \quad (4.6)$$

### 4.2.4 Loss Model

The power from a substation to different loads will flow through distribution lines, transformers, and voltage regulator (if any). Mathematical models of losses in these components are discussed in the following sections.

*4.2.4.1 Line Losses*

The line losses (defined earlier using 3.14, 3.15, and 3.13) can be redefined by considering line admittance ($y_{ij} = 1/z_{ij}$). The mathematical expression for total real and reactive power losses in the lines at time $t$ are defined by (4.7) and (4.8).

$$P_{loss,t} = \sum_{\substack{i \in N_b \\ i \neq j}} \sum_{\substack{j \in N_b \\ j \neq i}} r_{ij} \times \left( |V_{i,t} - V_{j,t}| \times |y_{ij}| \right)^2 \tag{4.7}$$

$$Q_{loss,t} = \sum_{\substack{i \in N_b \\ i \neq j}} \sum_{\substack{j \in N_b \\ j \neq i}} x_{ij} \times \left( |V_{i,t} - V_{j,t}| \times |y_{ij}| \right)^2 \tag{4.8}$$

Similarly, complex power losses at time $t$ can also be written as

$$S_{loss,t} = \sum_{\substack{i \in N_b \\ i \neq j}} \sum_{\substack{j \in N_b \\ j \neq i}} (r_{ij} + jx_{ij}) \times \left( |V_{i,t} - V_{j,t}| \times |y_{ij}| \right)^2 \tag{4.9}$$

*4.2.4.2 Transformer Losses*

Transformer losses are composed of no-load losses ($P_{NLL}$) and load losses ($P_{LL}$). In a practical distribution system, the load varies with time. Therefore, transformer secondary side voltage will also vary to meet the requirement of a change in voltage at the load end. This will lead to a change in $P_{NLL}$ as well as $P_{LL}$. If the frequency and other parameters of a transformer are assumed to be constant then $P_{NLL}$ at the applied voltage ($V$) can be defined by (4.10).

$$P_{NLL}(V) = P_h^r \left( \frac{V}{V^r} \right)^{ks} + P_e^r \left( \frac{V}{V^r} \right)^2 \tag{4.10}$$

As $ks$ is varying from 1.4 to 1.8, approximate function can be written as

$$P_{NLL} \approx (P_h^r + P_e^r) \left( \frac{V}{V^r} \right)^2$$

61

No-load losses at time $t$ can be re-written as

$$P_{NLL,t} = P^r_{NLL} \left( \frac{V_t}{V^r} \right)^2 \qquad (4.11)$$

Thus, complex no-load losses of a transformer at time $t$ can be represented as

$$S_{NLL,t} = P_{NLL,t} + jQ_{NLL,t} \qquad (4.12)$$

$Q_{NLL,t}$ are reactive no-load losses of the transformer, and this is very less as compared to $P_{NLL,t}$ and can be neglected in calculations.

Solution obtained from equation (4.11) represent approximate no-load losses. The percentage error is varying from -2.5% to 2.5% for voltage variation in the range of 0.9 p.u. to 1.1 p.u. This error is negligible if it compared with overall distribution system losses.

Load losses ($P_{LL}$) of a transformer at time $t$ can be evaluated using (4.13)

$$P_{LL,t} = |I_{ht,t}|^2 R_{ht} + |I_{lt,t}|^2 R_{lt} \qquad (4.13)$$

Here $I_{ht,t}$, $I_{lt,t}$ are current of HT and LT sides of the transformer at time $t$, whereas $R_{ht}$ and $R_{lt}$ are resistances of HT and LT side and each is 50% of specified resistance.

Similarly, reactive load losses of a transformer can also be written as

$$Q_{LL,t} = |I_{ht,t}|^2 X_{ht} + |I_{lt,t}|^2 X_{lt} \qquad (4.14)$$

In (4.14), $X_{ht}$ and $X_{lt}$ are reactances of HT and LT sides of the transformer and each is 50% of specified reactance.

Hence, total complex load-losses of a transformer at time $t$ can be written as

$$S_{LL,t} = P_{LL,t} + jQ_{LL,t} \qquad (4.15)$$

Here, $S_{NL,t}$ and $S_{LL,t}$ are complex no-load and load losses of the transformer over time $t$.

### 4.2.5 Inclusion of Harmonics

*4.2.5.1 Line Parameters and Admittance Matrix in Presence of Harmonics*

At higher frequencies, the distribution network is modeled by a harmonic frequency admittance matrix ($Y(f_h)$) and harmonic current sources ($I(f_h)$). In this, $Y(f_h)$ is evaluated by

modifying the conventional admittance according to the harmonic order. The distribution lines or cables are considered as lumped parameters connected in a nominal-$\pi$ model. The longitudinal ($y_{longitudinal}^{(h)}$) and shunt ($y_{shunt}^{(h)}$) parameters of the overhead lines or underground cables are incorporated into off-diagonal ($y_{ij}^{(h)}$) and diagonal ($y_{ii}^{(h)}$) elements of the modified matrix $Y^{(h)}$, respectively:

$$y_{ij}^{(h)} = \frac{1}{r_{ij} + j2\pi f_h L_{ij}} \tag{4.16}$$

The harmonic frequency ($f_h$) can also be written as $h \times f$. Where, $f$ is fundamental frequency and $h$ is harmonic order. Hence, equation (4.16) can be rewritten as follows:

$$y_{ij}^{(h)} = \frac{1}{r_{ij} + jh(2\pi f L_{ij})} = \frac{1}{r_{ij} + jh x_{ij}} \tag{4.17}$$

$$y_{ii}^{(h)} = j2\pi f_h C_{ii} \tag{4.18}$$

Apart from this, the capacitors connected into the network are also shunt element. Therefore, shunt CBs connected at node $k$ can also be modeled similar to (4.18) and it can be written as in (4.19)

$$y_{cap,k}^{(h)} = h y_{cap,k} \tag{4.19}$$

Here, $y_{cap,k}$ is evaluated based on mathematical equation (3.9).

*4.2.5.2 Load Modeling in Presence of Harmonics*

When higher order of harmonics frequencies ($f_h$) are considered in the distribution network, then loads are modeled as admittance to take the effect of harmonics into the loads. The load connected at node $i$ can be modeled using (4.20)

$$y_{load,i}^{(h)} = \frac{P_i^l(V(f_h))}{|V_i(f_1)|^2} + j\frac{Q_i^l(V(f_h))}{h\,|V_i(f_1)|^2} \tag{4.20}$$

Here, $P_i^l(V(f_h))$ and $Q_i^l(V(f_h))$ are determined using equations (4.21) and (4.22).

$$P_i^l(V(f_h)) = P_i^n \left| \frac{V_i(f_h)}{V_i^n(f_1)} \right|^{k_i^p} \tag{4.21}$$

$$Q_i^l(V(f_h)) = Q_i^n \left| \frac{V_i(f_h)}{V_i^n(f_1)} \right|^{k_i^q} \tag{4.22}$$

The nonlinear loads are modeled as current sources that inject harmonic current into the system. The fundamental and the $h$ order harmonic current of the nonlinear load connected at bus $i$ are modeled as [16–18]

$$I_i(f_1) = \left(\frac{P_i + jQ_i}{V_i(f_1)}\right)^*$$

(4.23)

$$I_i(f_h) = I_i(f_1) \times C(h)$$

(4.24)

The voltage at harmonic frequency $V(f_h)$ can be determined using following equation

$$[Y(f_h)][V(f_h)] = [I(f_h)]$$

(4.25)

### 4.2.5.3 Calculation of Line Losses and Power Consumed by Loads

The line-losses will also be affected when considering harmonics in the system. Therefore, total real power loss occurred at time instant $t$ can be mathematically written as

$$P_{loss,t} = \sum_{\substack{i \in N_b \\ i \neq j}} \sum_{\substack{j \in N_b \\ j \neq i}} \sum_{h \in N_h} r_{ij} \times \left(|V_{i,t}(f_h) - V_{j,t}(f_h)| \times \left|y_{ij}^{(h)}\right|\right)^2$$

(4.26)

Similarly, reactive power losses can also be written as

$$Q_{loss,t} = \sum_{\substack{i \in N_b \\ i \neq j}} \sum_{\substack{j \in N_b \\ j \neq i}} \sum_{h \in N_h} hx_{ij} \times \left(|V_{i,t}(f_h) - V_{j,t}(f_h)| \times \left|y_{ij}^{(h)}\right|\right)^2$$

(4.27)

However, complex power losses can be determined using (4.28)

$$S_{loss,t} = \sum_{\substack{i \in N_b \\ i \neq j}} \sum_{\substack{j \in N_b \\ j \neq i}} \sum_{h \in N_h} (r_{ij} + jhx_{ij}) \times \left(|V_{i,t}(f_h) - V_{j,t}(f_h)| \times \left|y_{ij}^{(h)}\right|\right)^2$$

(4.28)

Apart from losses, the power consumed by loads gets affected due to voltage dependency of the loads. The load power of $i^{th}$ node at time $t$ considering harmonics effect can be expressed by following mathematical relations

$$P_{i,t}^l = \sum_{h \in N_h} P_{i,t}^n \left|\frac{V_{i,t}(f_h)}{V_i^n(f_1)}\right|^{k_i^p}$$

(4.29)

$$Q_{i,t}^l = \sum_{h \in N_h} Q_{i,t}^n \left|\frac{V_{i,t}(f_h)}{V_i^n(f_1)}\right|^{k_i^q}$$

(4.30)

Similarly, the mathematical expressions representing output of DGs (4.5) and capacitor kVAr (4.6) will also be modified.

*4.2.5.4 Transformer Losses in Presence of Harmonics*

In the harmonic environment, load, no-load, and stray losses in a transformer get affected differently. According to IEEE standard C57.110-2008 [132], total load losses can be divided into three components, *i.e.*, copper loss ($P_{cu-loss}$), winding eddy current loss ($P_{ec-loss}$) and other stray losses ($P_{os-loss}$). However, the percentage of $P_{ec-loss}$ and $P_{os-loss}$ is 33% and 67% [133], respectively, in total stray load losses of the transformer (for oil-immersed distribution transformer). Once all these losses at rated conditions are known, losses in the harmonic environment are determined using (4.31)-(4.33).

$$P_{cu-loss,t} = \frac{P^r_{cu-loss}}{(I^r)^2} \sum_{h \in N_h} I_t^2(f_h) \tag{4.31}$$

$$P_{ec-loss,t} = \frac{P^r_{ec-loss}}{(I^r)^2} \sum_{h \in N_h} h^2 \times I_t^2(f_h) \tag{4.32}$$

$$P_{os-loss,t} = \frac{P^r_{os-loss}}{(I^r)^2} \sum_{h \in N_h} h^{0.8} \times I_t^2(f_h) \tag{4.33}$$

Therefore, total load losses at time $t$ can be written as

$$P_{LL,t} = P_{cu-loss,t} + P_{ec-loss,t} + P_{os-loss} \tag{4.34}$$

The effect of harmonics can also be considered for no-load losses of the transformer by utilizing mathematical expression (4.11). This equation will be modified in harmonic environment and can be written as

$$P_{NLL,t} = P^r_{NLL} \sum_{h \in N_h} \left| \frac{V_t(f_h)}{V^r} \right|^2 \tag{4.35}$$

## 4.2.6 Objective Function

Volt-VAr optimization affects real as well as reactive power consumption. Thus, the significance of Volt-VAr optimization will be reflected, when minimization of apparent energy

(*kVAh*) is considered. This objective function can be mathematically defined by (4.36).

$$min \quad f = SE_{kvah} =$$
$$\sum_{t=1}^{24} \left| \left( \left( \sum_{i \in N_b} \left[ P_{i,t}^l + jQ_{i,t}^l \right] \right) - \left[ S_t^{DGs} + jQ_t^{CBs} \right] + \left[ S_{loss,t} \right] + \left[ S_{NLL,t} + S_{LL,t} \right] \right) \right|$$
(4.36)

Here, $P_{i,t}^l$, $Q_{i,t}^l$, $S_t^{DGs}$, $Q_t^{CBs}$, $S_{loss,t}$, $S_{NLL,t}$, and $S_{LL,t}$ are evaluated using (3.5), (3.6), (4.5), (4.6), (4.9), (4.12), and (4.15), respectively. In the case of harmonics considerations, the objective function will be modified using mathematical formulation presented in the previous subsection utilizing mathematical expressions presented in (4.16) to (4.35).

### 4.2.7 System and Operational Constraints

In addition to constraints defined in previous chapter (3.17, 3.18, 3.19, 3.22, and 3.23), the additional constraints are given below:

#### 4.2.7.1 Root Mean Square Voltage

In case of harmonics consideration, the root mean square (RMS) voltage can be evaluated using (4.37)

$$V_{i,t}^{rms} = \sqrt{\sum_{h \in N_h} |V_{i,t}(f_h)|^2}$$
(4.37)

This RMS voltage is also constrained between the same min-max bounds as defined in (3.17). This can be mathematically defined using (4.38)

$$V_i^{min} \le V_{i,t}^{rms} \le V_i^{max}$$
(4.38)

#### 4.2.7.2 Total Harmonic Distortion (THD) of Voltage

The corresponding THD of voltage at time $t$ can also be evaluated using following mathematical relation

$$THD_{V_{i,t}} = \left( \sqrt{\sum_{\substack{h \in N_h \\ h \neq 1}} |V_{i,t}(f_h)|^2} \middle/ V_{i,t}(f_1) \right) \times 100\%$$
(4.39)

There are some limitations on allowable voltage THD as per IEEE Standard 519-2014 [134]. Hence, $THD_{V_{i,t}}$ should satisfy this limitation. This can be defined using (4.40)

$$THD_{V_{i,t}} \leq THD_{V_{i,t}}^{max} \tag{4.40}$$

*4.2.7.3 Capacitor Bank Tap Settings*

The total reactive power supplied by capacitors can be evaluated using (4.6). However, capacitors considered in this chapter are controlled by a tap changing mechanism. Therefore, the effective kVAr of $k^{th}$ capacitor bank can be determined using (4.41).

$$q_{k,t}^{cap} = Tap_{k,t}^{cap} \triangle q_k^{cap} \tag{4.41}$$

Here $Tap_{k,t}^{cap} \in \{0, 1, ...., Tap_k^{cap.max}\}$ and $\triangle q_k^{cap} = 50$ kVAr. The tap operations limit of capacitor bank can be defined as

$$\sum_{t=2}^{24} \left| Tap_{k,t}^{cap} - Tap_{k,t-1}^{cap} \right| \leq MS_k^{cap} \tag{4.42}$$

### 4.2.8 Selection of Optimization Technique

The objective function considered in the problem formulation is a nonlinear function along with nonlinear constraints. The control variables are transformer taps, voltage regulator taps, and capacitor taps. All these variables are of integer type. Therefore, the fitness function cannot be differentiated with respect to control variables. Hence, heuristic techniques are more suitable for this type of problem. There are various heuristic methods available in the literature and can be seen in Table 4.1. Here, it can be noticed that GA and PSO methods are widely accepted to deal with this type of problem. However, other methods like TLA, SA, TS, SFLA, HBMO, BFA, ACO, and BSO have also been used. Due to popularity of GA and PSO, they are selected for the optimization.

## 4.3 Results and Discussion

In this study, modified IEEE-33 bus radial distribution system [135] and IEEE-123 node test system [125] are considered. The daily load-shapes are adopted from previous chapter and shown in Fig. 3.2. These per unit load curves have been utilized for both the systems. In this

Table 4.1. Literature review on heuristic optimization techniques used for VVO problems

| Method | Reference |
|---|---|
| GA and its variants | [16–19, 28, 34, 35, 54, 58, 63, 70, 71, 74, 75, 77, 116, 117] |
| PSO | [29, 41, 42, 61, 83] |
| TLA | [39] |
| SA | [91] |
| TS | [84] |
| SFLA | [36, 37] |
| HBMO | [38] |
| BFA | [79] |
| ACO | [56] |
| BSO | [40] |

chapter also, Matlab COM Interfacing of OpenDSS (displayed in Fig. 3.3) has been utilized for hourly power-flow solutions and optimization methods (as discussed earlier) were utilized for optimal scheduling of VVC devices.

Solar irradiance, temperature and wind speed data are adopted from Suthari, Gujarat (India) and shown in Fig. 4.1.

### 4.3.1 Case Study

The study presented in this chapter has been carried out into two scenarios, i.e., Without DGs, and With DGs. Each scenario consists of three cases. Therefore, total six cases are considered and listed in Table 4.2. Case 1 is the base case. In this, the hourly power-flow solution in presence of loads has been obtained without violating voltage limits (0.95 p.u.-1.05 p.u.). Case 2 is a voltage control case, where optimal tap positions of OLTC/VRs has been obtained in order to minimize substation apparent energy. Whereas, Case 3 deals with the optimal coordination of taps of OLTC/VRs and CBs so that energy consumption can be minimized and this case named as Volt-VAr control case.

Case 4, Case 5, and Case 6 are similar to Case 1, Case 2, and Case 3, respectively. In these cases, DGs are connected in the distribution system. The VVC devices considered in various cases are shown in Table 4.2. All the results of all cases have been compared with
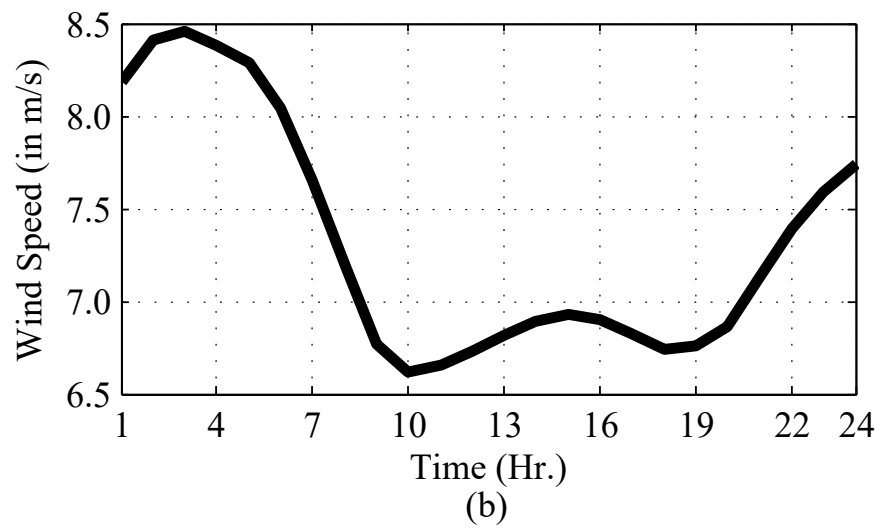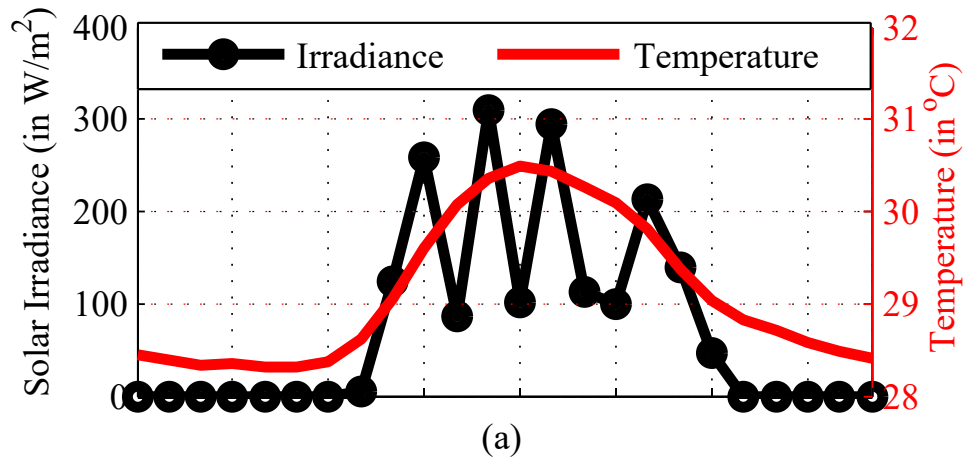
Fig. 4.1. Input parameters for SPV and WT generator, (a) Solar Irradiance and Temperature, (b) Wind Speed

Table 4.2. Different scenario along with its cases and assumptions

| Scenarios | System | IEEE 33-Bus System | | | IEEE-123 Bus System | | | | Optimal Solution |
|---|---|---|---|---|---|---|---|---|---|
| | VVC Devices | OLTC/VRs | CBs | DGs | OLTC | VR | CBs | DGs | |
| Without DGs | Case 1 | ✓ | ✗ | ✗ | ✓ | ✓ | ✗ | ✗ | ✗ |
| | Case 2 | ✓ | ✗ | ✗ | ✓ | ✓ | ✗ | ✗ | ✓ |
| | Case 3 | ✓ | ✓ | ✗ | ✓ | ✓ | ✓ | ✗ | ✓ |
| With DGs | Case 4 | ✓ | ✗ | ✓ | ✓ | ✓ | ✗ | ✓ | ✗ |
| | Case 5 | ✓ | ✗ | ✓ | ✓ | ✓ | ✗ | ✓ | ✓ |
| | Case 6 | ✓ | ✓ | ✓ | ✓ | ✓ | ✓ | ✓ | ✓ |
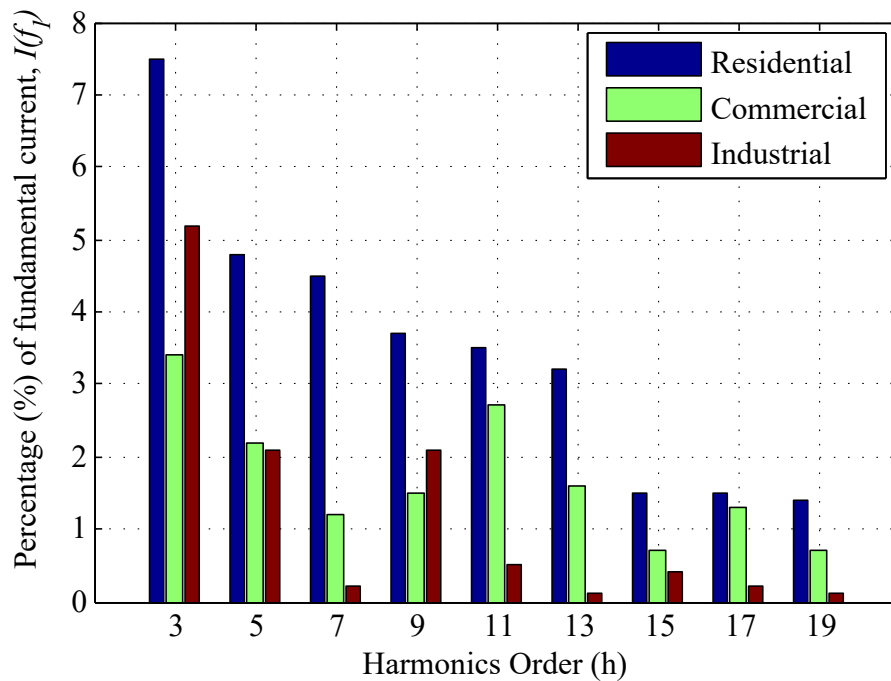


Fig. 4.2. Current harmonics spectrum of various load connected in the systems
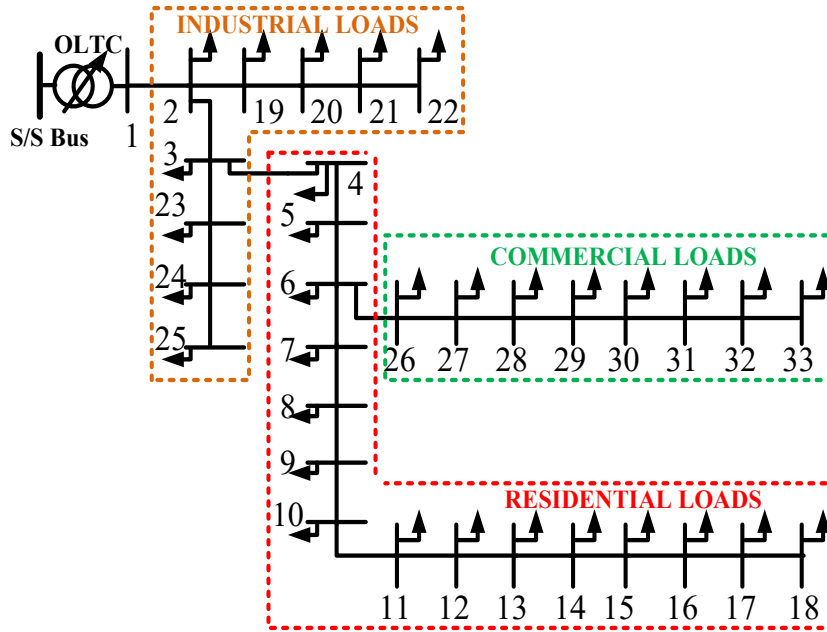
Fig. 4.3. IEEE-33 bus radial distribution system with residential, commercial, and industrial loads

Case 1 (base case).

All these cases have also been studied when current harmonics are considered in the loads. To add the harmonics effect to load current, the harmonic spectrum of residential, commercial, and industrial loads has been measured using a power quality analyzer. In this study, the load connected to a node of the network is varying according to given load-shape (Fig. 3.2), where load category remains the same. Therefore, it is assumed that the measured current harmonics spectrum will not vary in hourly power flow calculations. The harmonics spectrum of various loads (RE, CO, and IN) used in the analysis is shown in Fig.4.2.

### 4.3.2 Modified IEEE-33 Bus Radial Distribution System

The original IEEE-33 bus system does not have any transformer, VR and CBs. Therefore, the system is suitably modified to consider these VVC devices. An OLTC transformer is assumed to be connected at the substation (start bus). This modified system also contains variable CBs and DGs at different locations as given in Table 4.3. Each capacitor can inject reactive power in 50 kVAR/step. The loads of the modified distribution network are of voltage-dependent, which are of constant power type in original system. Moreover, RE, CO,

Table 4.3. Location of CBs and DGs in the distribution networks

| Test System | Locations of CBs (Capacity in kVAR) | DG Location (Each of 250 kW) |
|---|---|---|
| IEEE 33-Bus | 12 (250), 21 (100), 24 (500), 26 (900), 30 (400) | WT: 14, 17 PV: 31, 32 |
| IEEE 123-Bus | 83a (200), 83b (200), 83c (200), 88a (50), 90b (50), 92c (50) | WT: 115, 117, PV: 95, 122 |

and IN loads (represented by voltage-dependent model) connected at various locations in the distribution system are shown in Fig. 4.3.

### 4.3.2.1 Variation in Tap Positions of a Transformer and Capacitor Banks

Transformer tap positions obtained in all six cases are displayed in Fig. 4.4. In this, Fig. 4.4 (a) represents an hourly variation of taps when DGs are not participating. In Case 1, variation can be seen from +4 to +9 and these positions are higher among other cases. When optimization is considered (Case 2), these have been settled down on lower positions. This is because of voltage-dependencies of the loads. As soon as CBs are active in the distribution system along with transformer taps (Case 3), these positions again settled down on the lower position in order to optimize the system voltage from the substation node.

Impacts on transformer tap position in presence of DGs can be seen in Fig. 4.4 (b). Tap positions in Case 4 have settled down on lower positions (-1 to +6) as compared to Case 1 as local power has been injected by the DGs. And in Case 5, when optimization is considered, these tap positions again reduced (-8 to +4). In Case 6, when all the VVC devices are considered to be active in the network, these taps are at its lowest position (-11 to +2) among all the cases. Considering harmonics into the system influences planning of taps of transformer and can be effortlessly seen in Fig.4.4 (c) and Fig.4.4 (d). For this situation, a totally different scheduling is obtained from Case 1 to Case 6.
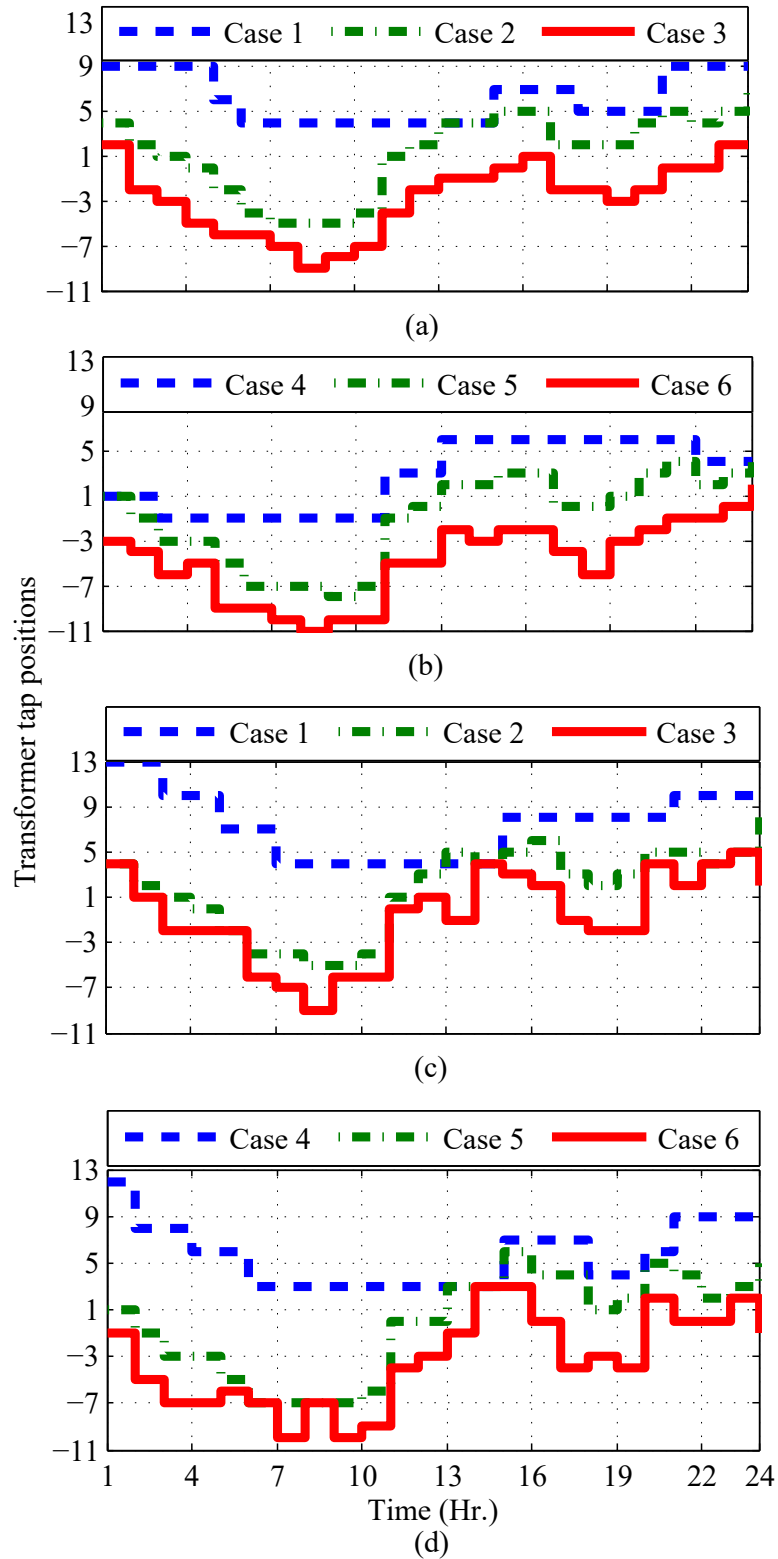
Fig. 4.4. Transformer tap positions for IEEE 33-bus distribution system, (a) Without DGs (No Harmonics), (b) With DGs (No Harmonics), (c) Without DGs (With Harmonics), (d) With DGs (With Harmonics)
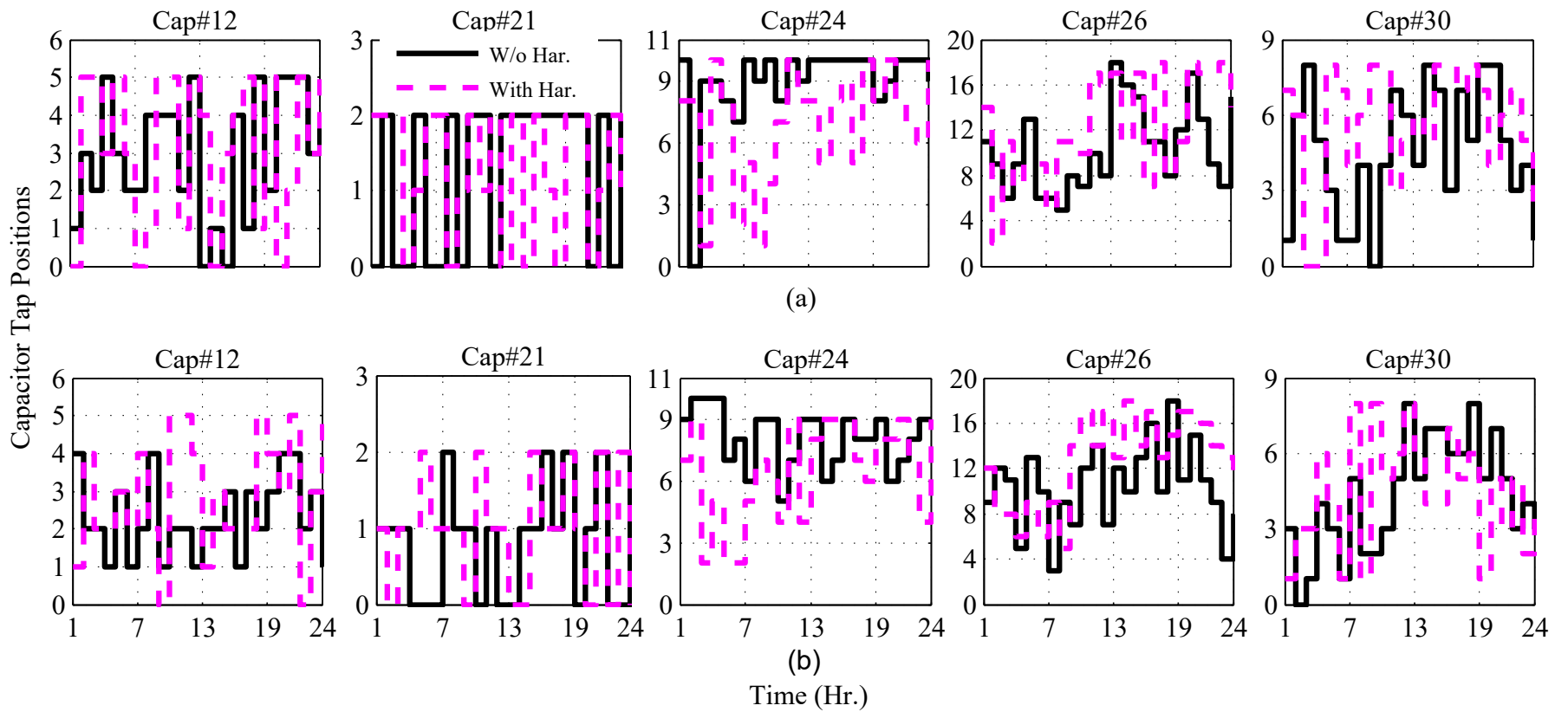
Fig. 4.5. Capacitor tap positions for IEEE-33 bus system (With and without Harmonics), (a) Case 3, (b) Case 6

Capacitors banks are included into the system only in Case 3 and Case 6. Hourly tap positions of all the CBs are displayed in Fig. 4.5. In Case 6, switching operations of all the CBs are less (except Cap#26) as compared with Case 3. It is also observed that reactive VArs (through CBs) provided here is 29.15 MVArh, whereas, it was more (31.98 MVArh) when DGs were not connected to the system. This is because of voltage profile, and capacitors are under-performing due to its voltage-dependent behaviour. The CBs taps are likewise influenced when harmonics are there in the system. This effect can also be seen on the tap scheduling of capacitors (shown with dotted pink lines).

*4.3.2.2 Effect on Distribution System Voltage*

Hourly variation in the system voltage can be seen in Fig. 4.6. In Case 1, the voltage is only controlled with the help of OLTC, therefore higher voltages (i.e., $> 1.0$ p.u.) are observed on the buses near to substation bus and can be seen in Fig. 4.6 (a). Whereas in Case 2 (Fig.4.6(b)), voltage is relatively low because of optimal settings of substation transformer taps. Here, more reductions in the voltage have been observed for Case 3 and shown Fig. 4.6 (c). The overall voltage is quite low (almost area is covered with $0.98$ p.u. to $0.95$ p.u.). This is because of simultaneous control of CBs and OLTC taps.

Once DGs are connected in the system, there will be more room for the operator to optimize the tap positions of the transformer and hence overall voltage in Case 4 is relatively low (Fig. 4.6 (d)) as compared with Case 1. Further reduction in the system voltage can also be observed in Fig. 4.6 (e) for optimal scheduling of transformer taps as in case 5. In case 6, CVR is effectively applied as mostly voltages are near to 0.95 p.u. and can be seen in Fig. 4.6 (f). This is because of optimal coordination of taps of transformer and CBs in the presence of DGs.

*4.3.2.3 Energy and Volt-Amperes Supplied from Substation*

Minimized substation apparent energy is shown in Table 4.4 along with energy consumed by loads and losses. Up to 14.48% savings in-terms of substation *kVAh* has been achieved when DGs are not connected in the distribution network and harmonics are not considered. Apart from this, major reductions in losses has also been observed. These savings are increased when DGs are connected in the system. By connecting DGs, 5.55% reduction in substation

75
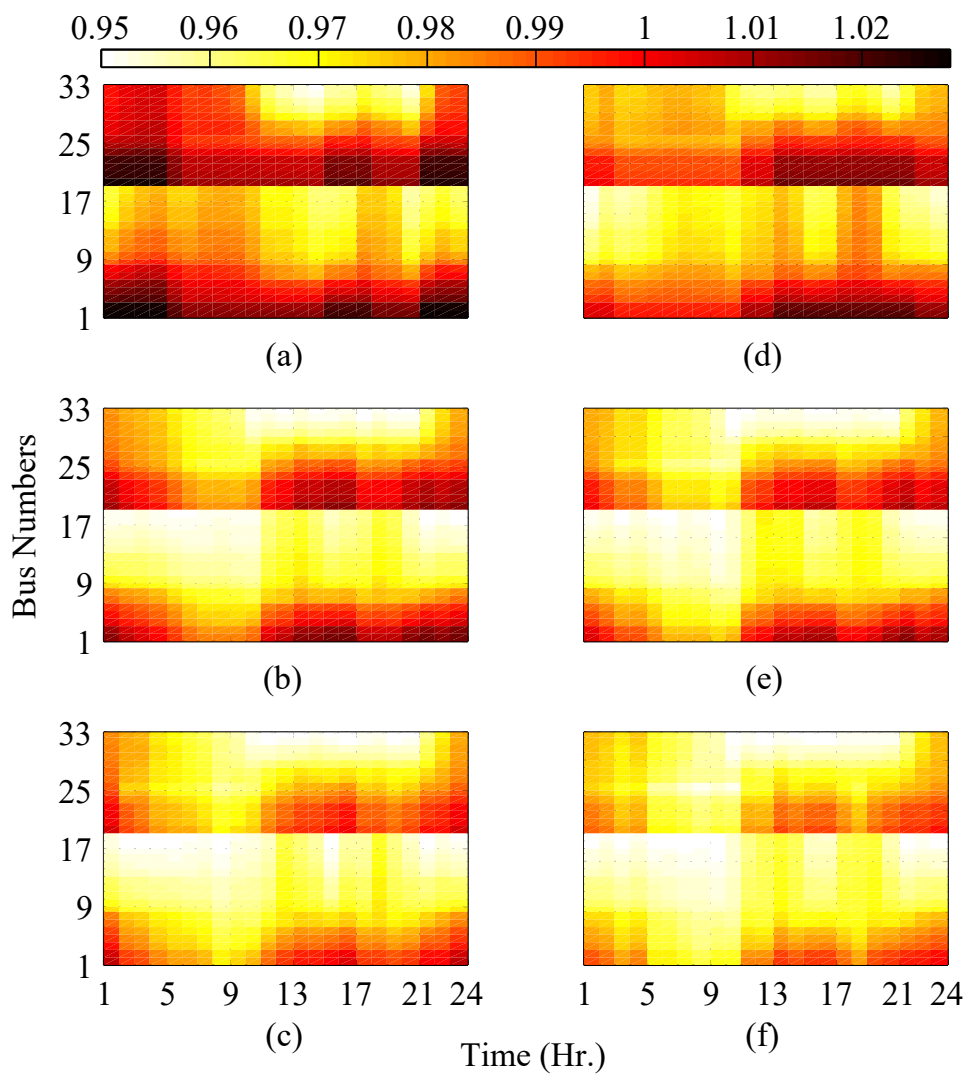
Fig. 4.6. Voltage surface plot of IEEE 33-bus distribution system for different control cases, (a) Case 1, (b) Case 2, (c) Case 3, (d) Case 4, (e) Case 5, (f) Case 6

Table 4.4. Energy consumption for IEEE 33-Bus system in different cases (% savings w.r.t. Case 1)

| Cases | Substation Apparent Energy (*kVAh*) | | Energy consumed by Loads (*kWh*) | | Energy Losses (*kWh*) | |
|---|---|---|---|---|---|---|
| | W/o Har. | With Har. | W/o Har. | With Har. | W/o Har. | With Har. |
| Case 1 | 72494 | 72950 | 61165 | 59434 | 1702 | 3600 |
| Case 2 | 70994 (2.07%) | 71112 (2.51%) | 60649 (0.84%) | 58842 (1.00%) | 1677 (1.51%) | 3532 (1.89%) |
| Case 3 | 61997 (14.48%) | 62266 (14.65%) | 60519 (1.06%) | 58935 (0.84%) | 1303 (23.48%) | 3185 (11.53%) |
| Case 4 | 68470 (5.55%) | 69383 (4.89%) | 60928 (0.39%) | 59353 (0.14%) | 1481 (13.01%) | 2939 (18.36%) |
| Case 5 | 65800 (9.23%) | 67500 (7.47%) | 60557 (0.99%) | 58767 (1.12%) | 1374 (19.29%) | 2865 (20.42%) |
| Case 6 | 57767 (20.31%) | 57802 (20.76%) | 60432 (1.20%) | 58769 (1.12%) | 1062 (37.63%) | 2481 (31.08%) |
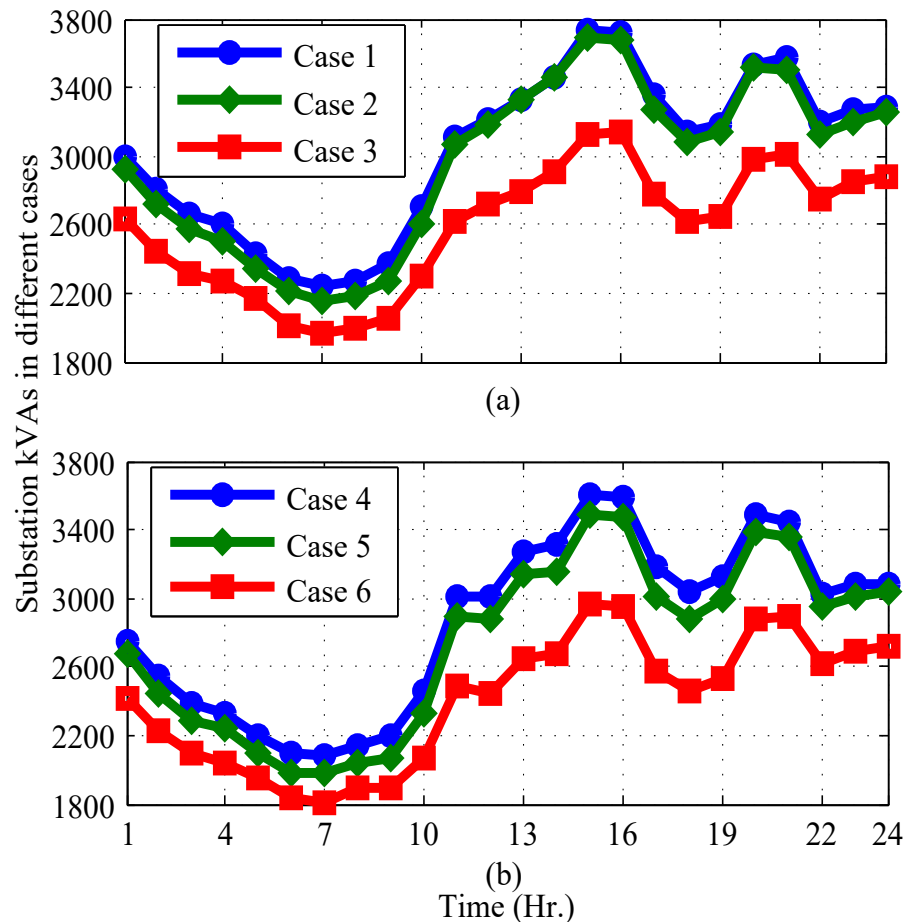


Fig. 4.7. Hourly substation kVAs of IEEE 33-bus distribution system for different cases, (a) Without DGs, (b) With DGs

*kVAh* and 13.01% in losses have been reported. These savings further improved in subsequent cases (Case 5 and Case 6) and reduction up to 20.31% in substation *kVAh* and 37.63% in loss *kWh* have been obtained. The substation *kVAh* is slightly increased when considering harmonics in the network. However, savings (compared to Case 1) are similar. The energy consumed by loads is slightly decreased (because of the predominance of admittance type of load), however, losses are drastically increased. Further, reduction in losses is similar to the situation when no harmonics are there in the system. Indeed, up to 31% reductions in energy losses have also been acquired for this case.

Due to voltage dependency of loads, hourly substation *kVAs* are also affected and can be seen in Fig. 4.7. Hourly profile of substation *kVAs* when DGs are not connected in the system is shown in Fig. 4.7 (a), where peak occurs at 1500 hours. There is marginal reduction in *kVAs* for Case 2. This effect is more in the lightly loading period as compared with other time. Moreover, a major reduction in hourly substation *kVAs* is observed in Case 3. Here, reduction in peak-time is higher as compared with other periods of time and can be seen with the red curve in Fig. 4.7 (a).

When local power through DG is available, good reduction in the substation kVAs is observed (Case 4) during the lightly loaded period (i.e., from 0100 Hrs to 1000 Hrs) and shown in Fig. 4.7 (b). In Case 5, significant reductions on an entire day are observed and shown with a green curve. These reductions are highest for Case 6 and the behavior is exactly same as in Case 3 but with major energy savings. The substation *kVA* profile is almost similar when harmonics are there in the system (therefore, not shown). But, the magnitude is slightly more, which results in increased substation *kVAh*.

*4.3.2.4 Peak Shaving*

Asides from reduction in substation energy, peak-hour *kVA* ($SS_{kVA}$) is additionally reduced (Fig. 4.7). The peak shaving is maximum in Case 6. Percentage savings (when no harmonics in the system) in terms of load and losses during the peak hour period are shown in Fig. 4.8 (a). Here, up to 21% reductions have been observed in substation *kVA*. Both real ($P_{Loss}$) and reactive power ($Q_{Loss}$) losses having a higher reduction as compared to other parameters. Reduction up to 41% in $P_{Loss}$ and 44% in $Q_{Loss}$ have been achieved. It is also clear

Table 4.5. Energy consumption for IEEE123-bus system in different cases (% savings w.r.t. Case 1)

| Cases | Substation Apparent Energy (*kVAh*) | | Energy consumed by Loads (*kWh*) | | Energy Losses (*kWh*) | |
|---|---|---|---|---|---|---|
| | W/o Har. | With Har. | W/o Har. | With Har. | W/o Har. | With Har. |
| Case 1 | 72352 | 72609 | 58720 | 58551 | 1296 | 3028 |
| Case 2 | 69437 (4.03%) | 69618 (4.29%) | 57546 (2.00%) | 56949 (2.73%) | 1222 (5.71%) | 2990 (1.25%) |
| Case 3 | 62530 (13.57%) | 63368 (12.72%) | 56632 (3.56%) | 56658 (3.23%) | 1060 (18.22%) | 2923 (3.47%) |
| Case 4 | 69409 (4.07%) | 69665 (4.05%) | 58745 (-0.04%) | 58561 (-0.01%) | 1202 (7.19%) | 2931 (3.20%) |
| Case 5 | 64705 (10.57%) | 64849 (10.68%) | 56797 (3.28%) | 56546 (3.42%) | 1089 (15.92%) | 2906 (4.03%) |
| Case 6 | 60893 (15.84%) | 61194 (15.72%) | 56841 (3.20%) | 57444 (1.89%) | 998 (23.00%) | 2797 (7.63%) |

that major savings/reductions have been obtained for Case 3 and Case 6 as compared with other cases, and highest for Case 6. However, peak hour savings are different in the case of harmonics considerations and shown in Fig.4.8 (b). Here, the percentage savings in-terms of loads ($P_{Load}$ and $Q_{Load}$) increases as compared to previous case. Unlike previous operating conditions, the reductions in $SS_{KVA}$, $P_{Loss}$, and $Q_{loss}$ are highest in Case 5.

### 4.3.3 IEEE-123 Node Test System

The topology of the modified IEEE-123 node feeder is exactly same as shown in previous chapter (Fig. 3.1). Here, different loads (RE, CO, and IN) are shown with different color coding. The loads connected at various locations in the network are assumed to be voltage-dependent (as in IEEE-33 bus system), which are of constant power, constant current, and constant impedance type in the original system. This modified system also consists of variable CBs and DGs at different locations as shown in Table 4.3. The savings obtained from this system are tabulated in Table 4.5. The trends are similar to IEEE 33-bus system. The maximum savings are achieved in case of Volt/VAr control.
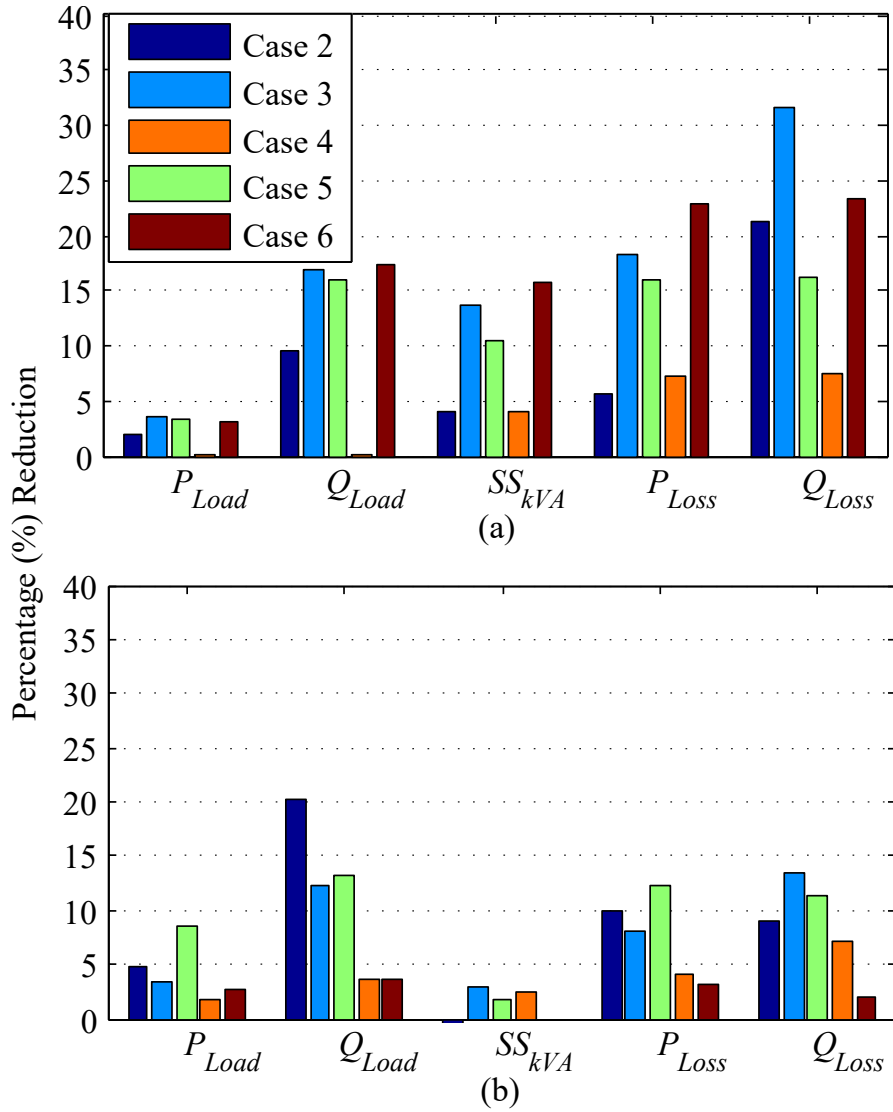
Fig. 4.8. Reduction of various parameters at peak-hour for IEEE 33-bus system, (a) Without Harmonics, (b) With Harmonics
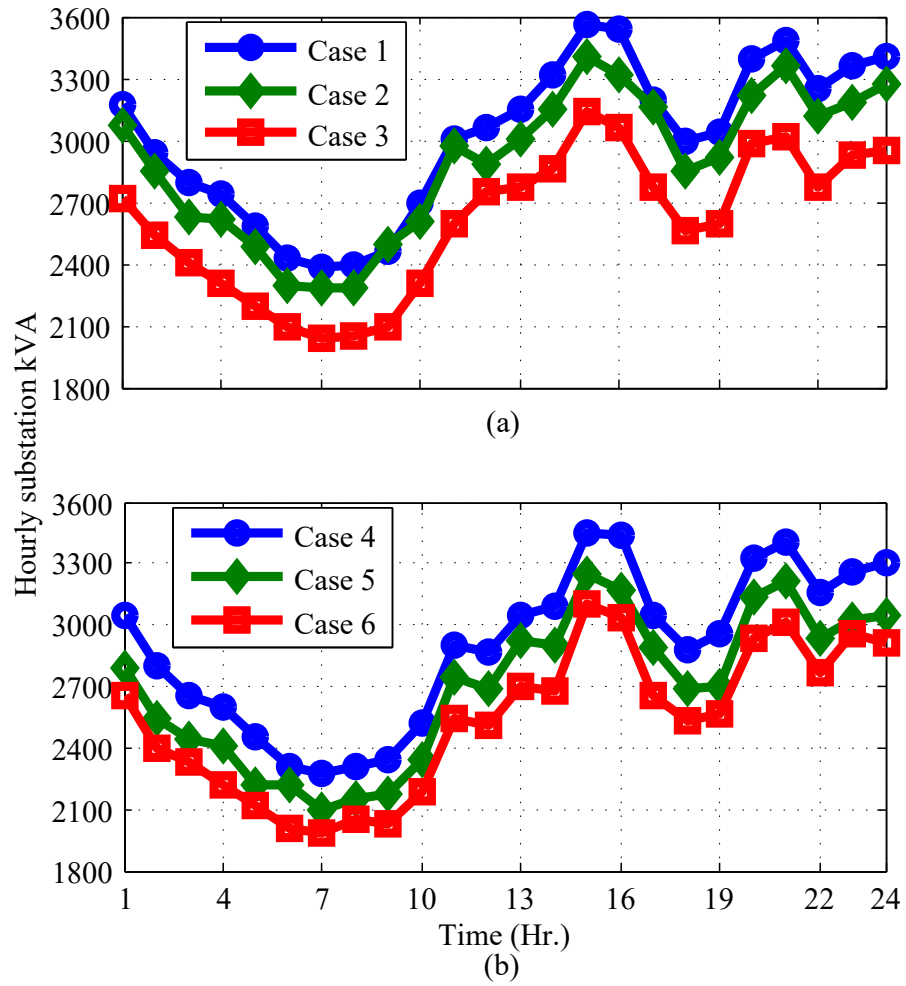
Fig. 4.9. Hourly substation kVAs for IEEE-123 bus system in different control cases, (a) Without DGs (b) With DGs
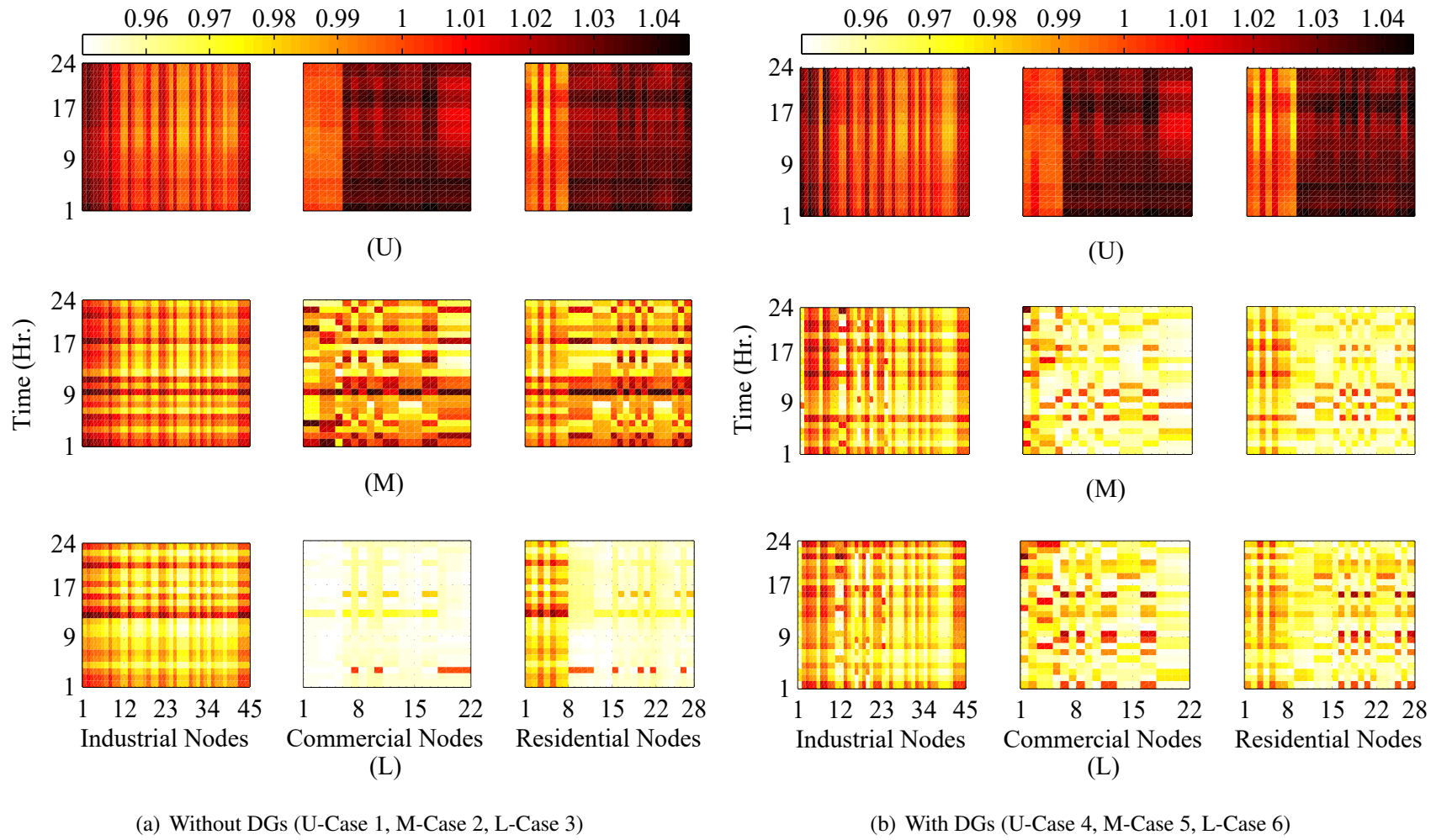
Fig. 4.10. Voltage surface plot of various customers connected in IEEE-123 bus system

Hourly substation kVAs is also following the same trend as in the IEEE 33-bus system, where less kVAs are supplied for voltage control (Case 2 and Case 5) and the minimum of these two were supplied when volt/var control (Case 3 and Case 6) is applied (Fig. 4.9). Daily voltage profile of both the scenarios is displayed in Fig. 4.10. Because of a large distribution network, these profiles are shown with respect to industrial, commercial and residential load connected nodes. Here, effective voltage reduction has been observed for commercial and residential loads. Therefore, it can be stated that these are the potential customers where CVR can be effectively applied. For the scenario, when DGs are connected in the system, savings in terms of load kWh are almost same (Table 4.5) for Case 5 and Case 6. This is happening because of voltage profile and can be seen in Fig. 4.10. This distribution network also follows the same trend in reduction of parameters at peak hour (except $Q_{Loss}$) as in the IEEE 33-bus system and it can be seen in Fig. 4.11. Here, substation kVAs at peak hour is reduced by 16% for Case 6. Major reduction in $Q_{Loss}$ has been observed for Case 3 (i.e., 32%), whereas 23% reduction has been obtained for Case 6.

### 4.3.4 Comparison of GA and PSO

All the studied cases have been solved with both GA and PSO. The convergence graphs of GA and PSO are displayed in Fig. 4.12 for Case 3 and Case 6. Here it is observed that PSO is converging faster than that of GA, but solution obtained using PSO is a suboptimal solution and can be easily observed in Fig.4.12. Although, the percentage error in both the solution is less still GA is giving a global solution. If one can compromise on global solution then PSO can be a good choice. Apart from this, when harmonics are induced in the system, the time taken by both the techniques is drastically increased and shown in Table 4.6, but solution obtained with GA is still better than PSO. Once the number of control variables increase (as in IEEE-123 Bus), the time taken by both optimization techniques is increased and the same has also been noticed in this study. Here, time taken to solve cases of IEEE-123 Bus system is higher than what in IEEE-33 Bus system.
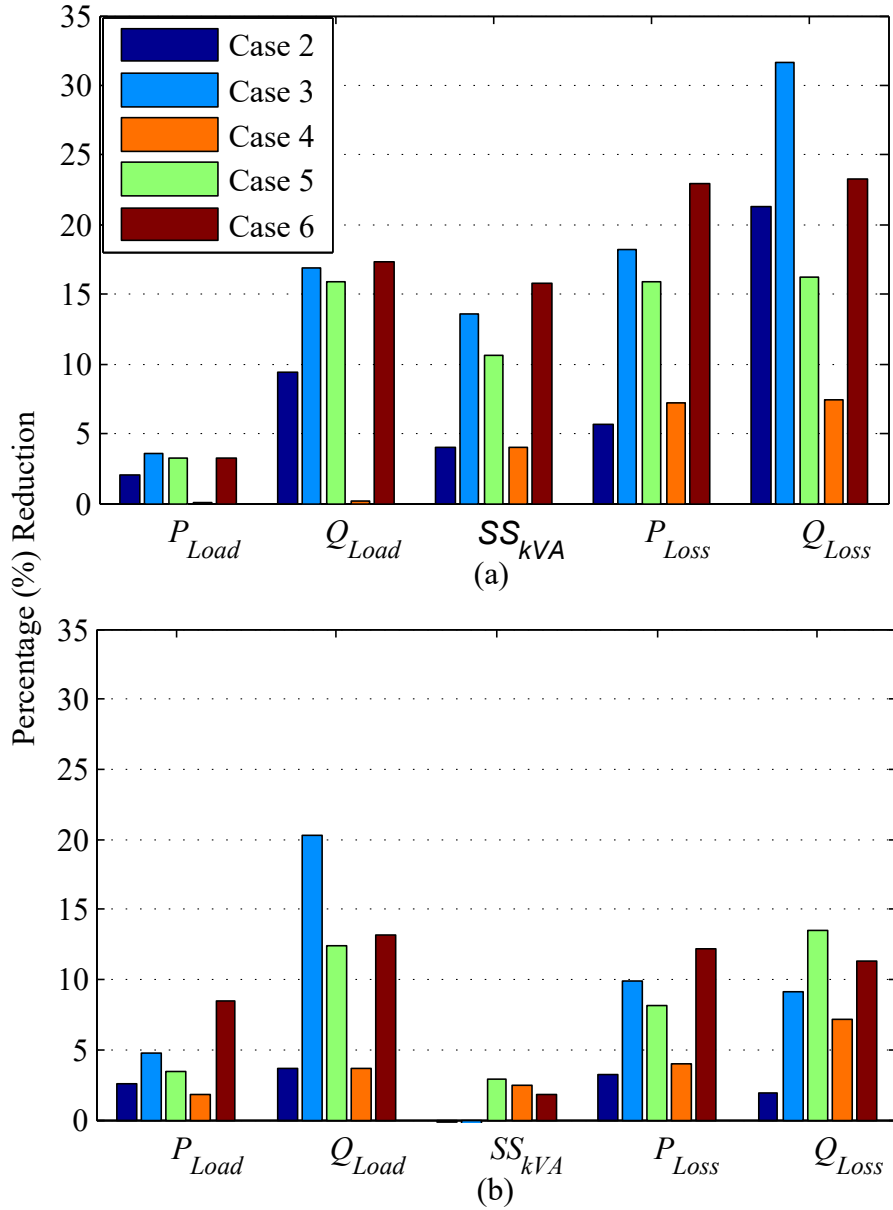
Fig. 4.11. Reduction in various parameters at peak-hour for IEEE-123 bus system, (a) Without Harmonics, (b) With Harmonics
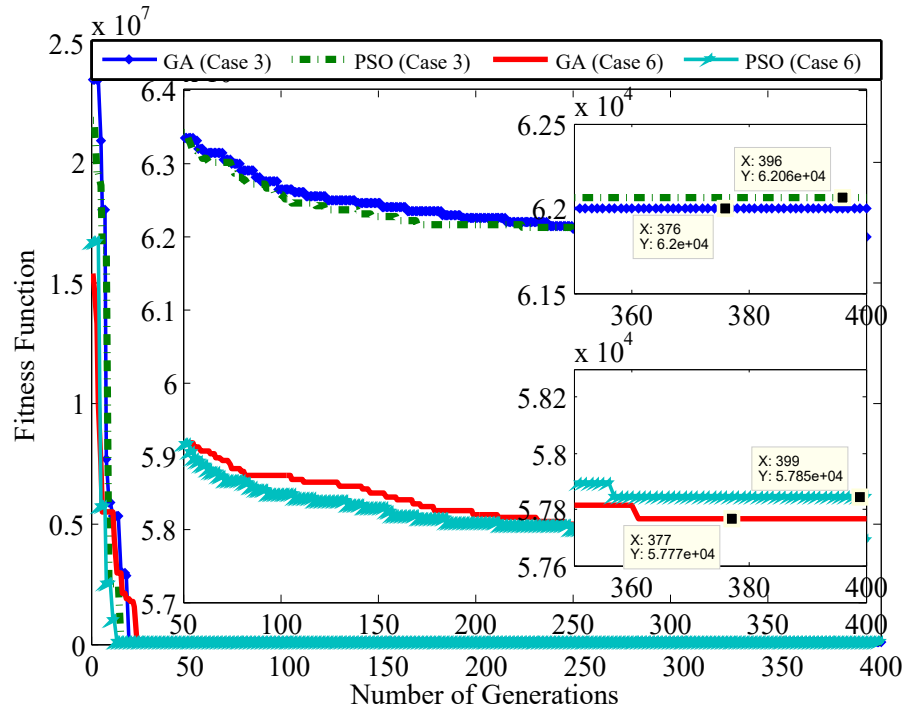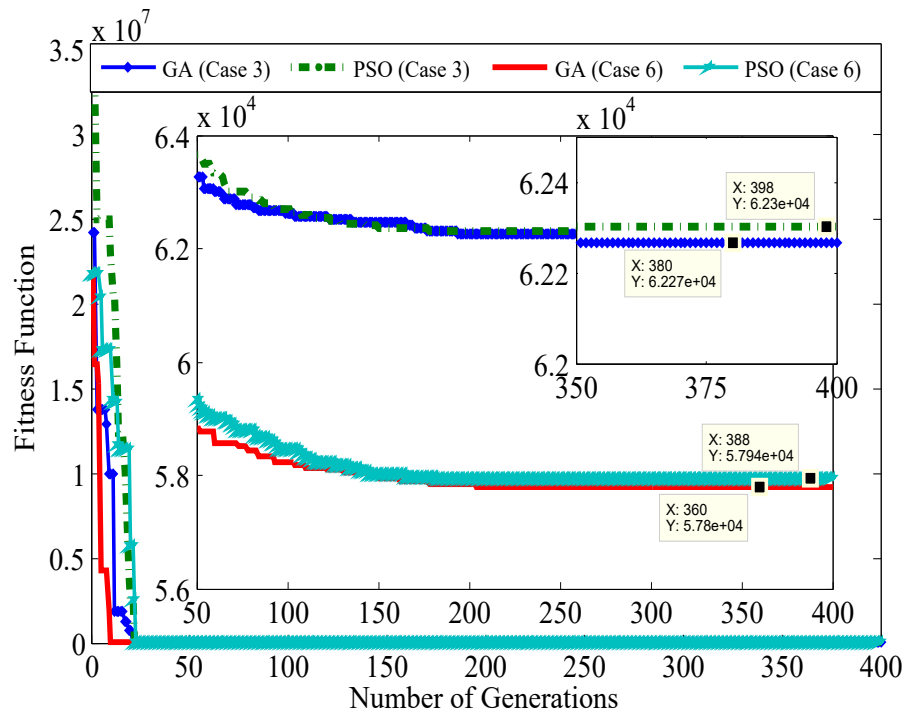
Fig. 4.12. Convergence graph of GA and PSO for Case 3 and Case 6 (IEEE-33 Bus), (a) Without Harmonics, and (b) With Harmonics

Table 4.6. Time taken by GA and PSO (in seconds) to solve different cases of the studied systems

(All computations are done on Intel Core i7 3.40 GHz processor)

| | | Without Harmonics | | With Harmonics | |
| --- | --- | --- | --- | --- | --- |
| | | GA | PSO | GA | PSO |
| IEEE-33 Bus | Case 2 | 299 | 90 | 2843 | 2519 |
| | Case 3 | 270 | 267 | 4197 | 3889 |
| | Case 5 | 651 | 128 | 3283 | 2717 |
| | Case 6 | 394 | 289 | 5574 | 3920 |
| IEEE-123 Bus | Case 2 | 2499 | 2938 | 76714 | 61233 |
| | Case 3 | 3964 | 1801 | 77105 | 63079 |
| | Case 5 | 2544 | 3749 | 103092 | 47575 |
| | Case 6 | 2262 | 2306 | 134880 | 80677 |
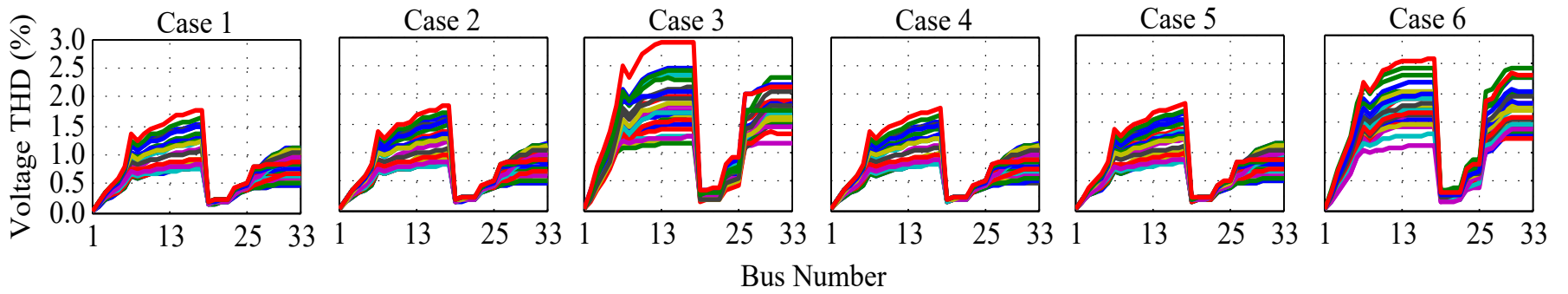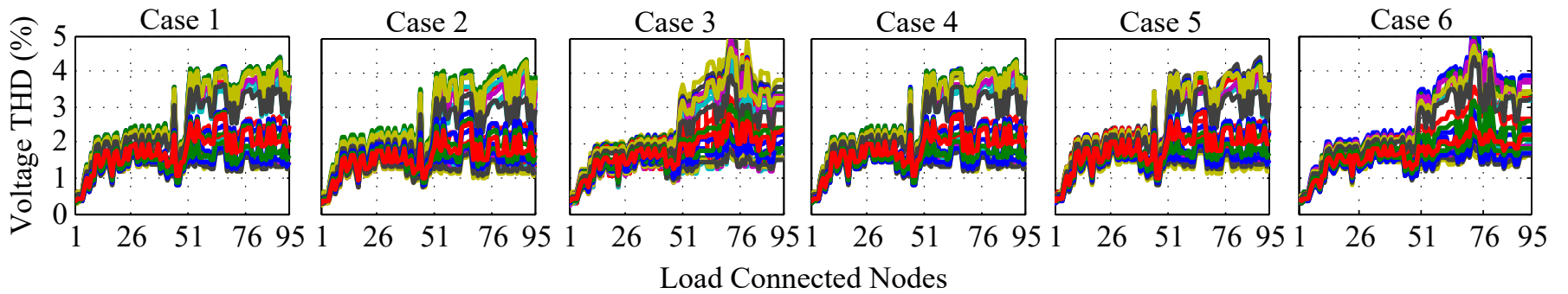
Fig. 4.13. Daily total harmonic distortion of voltages in different cases (a) For IEEE-33 Bus System, and (b) For IEEE-123 Bus System

### 4.3.5 Impact of Harmonics

The energy savings (as compared to base case) are almost similar when harmonics are considered in the load currents. However, substation *kVAh* are somewhat increased comparing to the case when there are no harmonics. In the case when harmonics are considered, all loads consists of harmonic spectrum. Therefore, the RMS load current is higher than what in case of no harmonics. Apart from load currents, transformer losses are likewise increased.This ultimately increases the overall losses of the distribution network. Therefore, energy losses (*kWh*) are increased. The power consumed by loads is decreased because of dominating admittance type of load. The daily profile of total harmonic distortion (THD) of voltage is shown in Fig.4.13. Here, it is observed that THD at any point of time is within allowable limits (i.e., $\leq 5\%$) as per IEEE Std. 519-2014. The daily profile of THD is more in the case of Volt/VAr control (Case 3 and Case 6). However, the overall THD profile having higher magnitudes for IEEE-123 bus system as compared to IEEE-33 bus system. From the perspective of optimization, the problem formulation is complex and evaluating each component of the objective function (4.36) is very time consuming. Therefore, the time required for solving any of the case in this situation (see Table 4.6) is drastically increased as compared with no harmonics in the system.

## 4.4 Summary

In this chapter, volt/VAr control in order to minimize the substation energy has been solved for two different scenarios, i.e., without DGs and with DGs. These two scenarios have also been formulated with harmonics in the load currents. Results obtained have been compared with base case and voltage control case. It was observed that PSO converges faster than GA, but sometimes it converges to a sub-optimal solution. In other words, GA is a time-consuming optimization technique but gives near-global solutions in each studied case. Therefore, results presented in this chapter are obtained with GA.

From the technical point of view. it is observed that when DGs are connected to the system, an operator has more chances to optimize the voltage profile. Therefore, more energy savings was observed when DGs are connected. Drastic reductions in substation *kVAh* and losses (*kWh*) were observed in volt/VAr control case. It is also observed that voltage reduction

is not so effective in voltage control case but proper conservation voltage reduction has been applied in volt/VAr control case. With the inclusion of harmonics, the substation *kVAh* is slightly increased as compared to no harmonics. However, there is a drastic increase in losses of the network.

The switching operations of VVC devices are less in the base case, but as we move towards an optimal solution, then switching operations increases. Therefore, it can be stated that more energy savings can be obtained if VVC devices are allowed to operate frequently as much as required. But this will reduce the life of VVC devices as every device has fixed number of operations. Therefore, there is a trade-off between energy savings and number of switching operations.

# CHAPTER 5

# VOLT-VAR OPTIMIZATION FOR FUTURE DISTRIBUTION SYSTEM

## 5.1 Introduction

As seen in previous chapters, On Load Tap Changer (OLTC), Voltage Regulators (VRs), and Capacitor Banks ( CBs) have been utilized to perform Volt/VAr Optimization (VVO) in a traditional distribution network. In chapter 3, a passive (or a traditional) distribution network is considered, where selection of load model alongside minimization of apparent energy losses have been obtained. Nowadays, many Distributed Energy Resources (DERs) are integrated in a distribution grid. In 2012, the global installed capacity of solar PV was 100 GW, which have crossed 390 GW by the end of 2017 [136]. Many of DERs are distributed Solar Photovoltaic (SPV) systems operating with conventional inverters at unity power factor (UPF). These inverters can only supply active power (operating at UPF) to the grid. The VVO formulations alongside SPV systems operating at UPF considered in chapter 4 in order to accomplish minimization of apparent energy demand of the substation. However, nowadays, SPV systems are increasingly paired with smart inverters, which can inject as well as absorb reactive power and control the voltages at the Points of Common Coupling (PCC). These smart inverters have the capabilities to take decisions based on local or distributed measurements (in terms of voltage, power factor etc.).

Earlier, DERs were not allowed to participate in the voltage regulation. However, in 2014 an amendment was made in IEEE Std.1547-2003 [137] to allow smart inverter based generation to participate in the voltage regulation [20]. Thereafter, in 2018, Std.1547-2003 was revised and certain new operational constraints have been introduced for smart inverter based SPV generators [21]. In a span of five years (2012 to 2017), the global PV installation shows an approximately 400% growth [136]. This gives an indication to consider SPV based generation for the future distribution grid. Therefore, utilities have new challenges to consider their effects in the planning and operations of distribution grids. The following research gaps have been identified based on the review presented in Table 2.4.

It has been observed that the most of the existing literature does not comply with IEEE Std. 1547-2018, except [50]. A few works have considered reactive power support at constant power factor and full apparent power capability of the smart inverter. However, IEEE Std. 1547-2018 recommends a limited ($44\%$ of inverter's kVA rating) reactive power capability. Moreover, in the available literature, a set of predefined operating points of IVVCC has been utilized while dealing with reactive support through smart inverters. Sometimes, the default operating points are incompatible with the local voltage signals. Because the distribution grid may demand reactive power support through smart inverters in the dead-band range of IVVCC. But, it will not be possible due to the default operating settings. Therefore, an optimal IVVCC for each smart inverter is necessary to support the dynamic reactive demand.

The focus of this chapter is to consider the participation of the DER in the voltage and reactive power management. Thus, a VVO formulation has been developed in accordance with IEEE Std. 1547-2018. The scope of research presented in this chapter is limited to reactive power capability and voltage/power control requirements. The important contribution of this chapter are as follows:

1 The volt/VAr optimization is performed on a traditional as well as an active distribution network.

2 The VVO formulation of a future distribution system has been done as per the DER interconnection guidelines of IEEE Std. 1547-2018.

3 The limited reactive power capability of a smart inverter has been taken into account while dealing with the reactive power dispatch.

4 Each smart inverter has been considered to operate on a different IVVCC. Therefore, the determination of an optimal IVVCC has also been taken into account while achieving the VVO objectives.

The rest of chapter is organized as follows. The problem formulation has been described in section 5.2. Section 5.3 deals with the various case and their details description alongside mathematical modelling of reactive power provided by the smart inveters. The proposed algorithm supported with objective function, constraints, and solution techniques is discussed

in section 5.4. Results and discussion alongside modifications in the distribution system have been covered in section 5.5, whereas complete study is summarized in section 5.6.

## 5.2 Problem Formulation

The mathematical models presented in (3.5) and (3.6) have been directly utilized to represent the load to voltage dependency. The conventional VVC devices are OLTC, VRs, and CBs utilized in the previous two chapters. The mathematical formulation for regulation ratio of OLTC and VR can be found in (3.7), and (3.8), respectively. Whereas, voltage-dependent kVAr provided by the capacitor is given in (3.10).

Apart from mathematical modeling of loads and VVC devices, the active, reactive, and apparent losses can also be determined using (4.7), (4.8), and (4.9), respectively.

In the future distribution grid, the smart inverters are capable of injecting/absorbing reactive power. Therefore, in this chapter, smart inverters have also been considered as reactive power compensation devices.

### 5.2.1 SPV Generator

In this study, SPV generators are assumed to be connected at various locations in the distribution grid. The mathematical expression for the real power output can be obtained from (4.1). The output calculated using (4.1) is directly fed to the distribution grid with the help of an inverter. Traditionally, an inverter is operated at unity power factor (as in chapter 4). However, future distribution grid will be having smart inverters, which are capable of injecting/absorbing reactive power. Therefore, in this chapter, the functionality of smart inverter has been considered and discussed in the next section.

## 5.3 Proposed Study

The purpose of this chapter is to access the energy savings in compliance with IEEE Std 1547-2018. Here, only cases have been considered which are related to voltage and reactive powers in the network. Therefore, volt/watt and watt/VAr modes of the smart inverters have not been given attention. Here, a total of five cases have been considered and their description is as follows:

### 5.3.1 Case1: VVO without SPV Systems

The VVO is performed by the utility to schedule VVC devices in order to achieve the desired objective. In this case, the SPV systems are not considered in the distribution grid. Therefore, VVO is performed just by utilizing voltage regulators and switched capacitors connected at different locations in the network.

### 5.3.2 Case2: VVO with SPV Inverters Operating at Unity Power Factor (UPF)

This case deal with the VVO performed in an active distribution grid where SPV systems are connected at various locations. These SPV units are interfaced with traditional inverters which are operating at UPF. Therefore, the inverters are considered to dispatch only real power to the network.

### 5.3.3 Case3: VVO with Smart Inverters with Local Control

In this case, SPV systems with smart inverters are considered. These inverters operate based on local voltage measurements. In this case, utility performed VVO by coordinating VVC devices. At the same time, SPV systems are participating in reactive power dispatch using a predefined volt/VAr curve. Here, smart inverters can absorb or supply reactive power from/to the grid based on intelligent volt/VAr control (IVVC) characteristics shown in Fig. 5.1. This IVVC characteristics (IVVCC) have to obey certain guidelines as specified in IEEE Std 1547-2018. The IVVCC is a piece-wise linear curve. Thus, it is combination of centralized (scheduling of VVC devices) and local (rule-based control of the smart inverter) control. The IVVC characteristics is described by (5.1).

The operating points of IVVCC as per IEEE Std. 1547-2018 are given in Table 5.1. The actual reactive power dispatch of a smart inverter depend on these operating points (where $V_{ref} = 1$) and reactive power capability ($Q^{max} = 0.44 S_n^{rated}$). In this case, the default IVVCC will remain the same for each smart inverter.
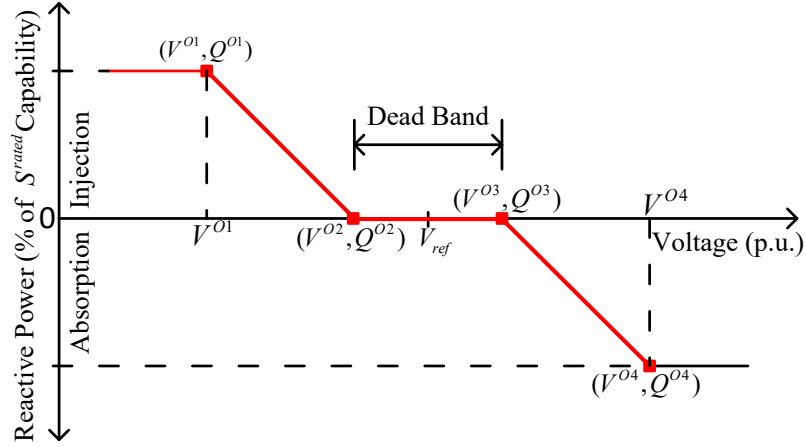
Fig. 5.1. Intelligent volt/VAr control (IVVC) characteristics for smart inverter

$$
Q_{m,t}^{pv}(V) = Q_m^{max} \times
\begin{cases}
+1 & |V_{m,t}| < V_m^{O1} \\[2mm]
+\frac{V_m^{O2} - |V_{m,t}|}{V_m^{O2} - V_m^{O1}} & V_m^{O1} \leq |V_{m,t}| < V_m^{O2} \\[2mm]
0 & V_m^{O2} \leq |V_{m,t}| \leq V_m^{O3} \\[2mm]
-\frac{|V_{m,t}| - V_m^{O3}}{V_m^{O4} - V_m^{O3}} & V_m^{O3} < |V_{m,t}| \leq V_m^{O4} \\[2mm]
-1 & |V_{m,t}| > V_m^{O4}
\end{cases}
\tag{5.1}
$$

Table 5.1. Operating points of IVVCC for local control

| $V^{O1}$ | $V^{O2}$ | $V^{O3}$ | $V^{O4}$ | $Q^{O1}$ | $Q^{O2}$ | $Q^{O3}$ | $Q^{O4}$ |
|------|------|------|------|-------------|------|------|-------------|
| 0.92 | 0.98 | 1.02 | 1.08 | $+Q^{max}$ | 0 | 0 | $-Q^{max}$ |

### 5.3.4 Case4: VVO with Smart Inverters with Optimal IVVCC

In this case, the optimal IVVCC is obtained to support the volt/VAr optimization. In the previous case, default set points of IVVCC are used (see Table 5.1) that can be utilized for the local control purposes. However, the IVVCC (5.1) indicates that the extent of reactive power injection or absorption depends on the set points ($V_m^{O1}$, $V_m^{O2}$, $V_m^{O3}$, and $V_m^{O4}$) of the

95

characteristics. These set points have certain limits (specified in IEEE Std 1547-2018) and described by (5.2), (5.3), (5.4), and (5.5).

$$0.82 \leq V_m^{O1} \leq 0.95 \tag{5.2}$$

$$0.97 \leq V_m^{O2} \leq 1.00 \tag{5.3}$$

$$1.00 \leq V_m^{O3} \leq 1.03 \tag{5.4}$$

$$1.02 \leq V_m^{O4} \leq 1.18 \tag{5.5}$$

$$V_m^{O2} \leq V_m^{O3} < V_m^{O4} \tag{5.6}$$

The variations of these settings impacts reactive power generation and absorption by the inverters. Therefore, the SPV systems can be effectively utilized for reactive power injection or absorption. Distribution System Operators (DSOs) can schedule the VVC devices along with optimal voltage settings of the smart inverters with the information of operating parameters (such as voltage, current, taps of regulators, switch positions of capacitors). In this case, the DSOs are responsible for coordinated optimal IVVCC settings and VVC devices in order to achieve maximum energy savings. The operational and system constraints also include the boundary constraints of the voltage set points for IVVCC of smart inverters installed in the distribution network. For stable operation of inverters an additional inequality constraint has also been defined in (5.6). Thus, there are a few additional control variables ($V_m^{O1}$, $V_m^{O2}$, $V_m^{O3}$, and $V_m^{O4}$) alongside voltage regulators and capacitors settings.

### 5.3.5 Case5: VVO with Smart Inverters with Reactive Capability Curve

In this case, the inverters of SPV systems are considered to be capable of injecting (+) and absorbing (−) reactive power for real power output levels as per capability characteristics shown in Fig. 5.2. It can be mathematically described by (5.7). Mathematically it can be
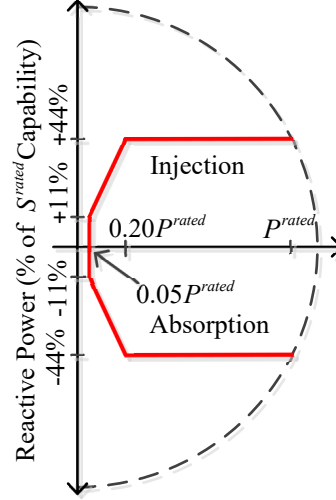
Fig. 5.2. Reactive power capability characteristics for smart inverter

described as follows:

$$Q_{m,t}^{pv}(P) = Q_m^{max} \times \begin{cases} \pm \frac{P_{m,t}^{pv}}{0.20 \times P_m^{rated}} & 0.05 P_m^{rated} \leq P_{m,t}^{pv} \leq 0.20 P_m^{rated} \\ \pm 1 & P_{m,t}^{pv} > 0.20 P_m^{rated} \end{cases} \tag{5.7}$$

Therefore, in this case, the reactive power of inverters is considered as a control variable and supposed to be scheduled by the utility within the boundary conditions as defined in (5.7). Here, the optimal dispatch of reactive power of inverter has been ensured in coordination with VVC devices.

## 5.4 Proposed Algorithm

### 5.4.1 Objective Function

The active and reactive power components of a practical load show distinct characteristics with variation in the terminal voltage. The voltage sensitivities of each class of customer are different [14]. Therefore, volt/VAr control in a distribution network influences both active and reactive load demands.

The objective of this chapter is the minimization of apparent energy demand of the distribution network. The minimization of apparent energy demand leads to minimization of both real as well as reactive components. The objective function can be mathematically defined

by (5.8).

$$min \quad f = SSE_{apparent} =$$

$$\sum_{t=1}^{24} \left| \left( \left( \sum_{i \in N_b} \left[ P_{i,t}^l + jQ_{i,t}^l \right] \right) + [S_{loss,t}] - \sum_{m \in N_{pv}} \left[ P_{m,t}^{pv} + jQ_{m,t}^{pv} \right] - j \sum_{k \in N_{cb}} Q_{k,t}^{cap} \right) \right|$$

$$(5.8)$$

In the above equation, the first part $(\sum_{i \in N_b} \left[ P_{i,t}^l + jQ_{i,t}^l \right])$ represents the apparent load of different customers in the distribution system, the second part is the apparent power loss $(S_{loss,t})$, the third part $(\sum_{m \in N_{pv}} \left[ P_{m,t}^{pv} + jQ_{m,t}^{pv} \right])$ is the apparent power generated by solar photovoltaic (SPV) generators in the network, and the fourth part $(\sum_{k \in N_{cb}} Q_{k,t}^{cap})$ is the kVAr supplied by capacitor units. Therefore, the objective is to get the optimal schedule of VVC devices alongside intelligent volt/VAr control characteristics (IVVCC) of smart inverters such that the daily apparent energy demand of the distribution network can be minimized.

**5.4.2 System and Operational Constraints**

The constraints presented earlier in this chapter (5.1, 5.2, 5.3, 5.4, 5.5, 5.6, and 5.7) are case specific. In addition to them, other operational and system constraints can be directly referred from (3.17, 3.18, 3.19, 3.22, and 3.23). The constraint defined by (3.22) will be modified due to local availability of reactive power through smart inverters and capacitor banks. Therefore, total reactive power provided by the capacitor units and SPV generators does not exceed the required reactive demand of the network at any point of time $t$. This constraint can be defined as

$$\left( \sum_{k \in N_{cap}} Q_{k,t}^{cap} + \sum_{m \in N_{pv}} Q_{m,t}^{pv} \right) \leq \left( \sum_{i \in N_b} Q_{i,t}^l + Q_{kvar,t}^{loss} \right) \quad (5.9)$$

**5.4.3 Solution Technique**

The objective function considered here is a nonlinear function along with nonlinear constraints. The control variables are taps of voltage regulators (integers), switch positions of capacitors (binary), operating points of IVVCC (continuous) and kVAr output of photovoltaic generators (continuous). Therefore, the fitness function cannot be differentiated with respect
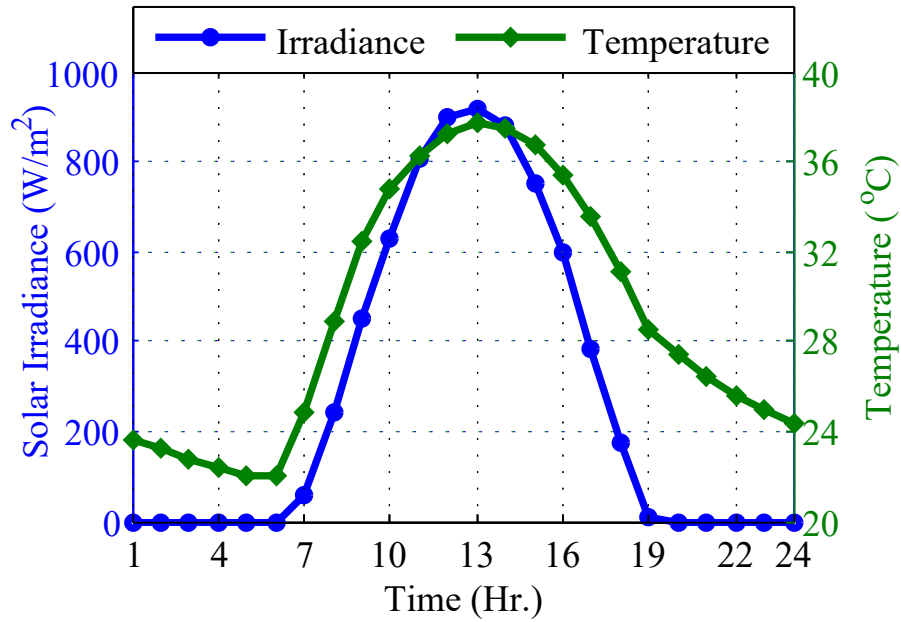
Fig. 5.3. Input parameters for SPV generators

to control variables. Hence, heuristic techniques are more suitable to deal with such a problem. Many works of literature on VVO have utilized heuristic methods and shown in Table 2.3 and 2.4. It can likewise be seen that PSO and GA have been broadly acknowledged to handle VVO problems. However, it has also been concluded in chapter 4 that PSO converges faster than GA, but sometimes it converges to a sub-optimal solution. Therefore, in this research GA has been used as an optimization technique. In order to make it fast, the initial solution (maybe sub-optimal) has been obtained with GA and then the pattern search algorithm has been utilized for obtaining the global solution.

## 5.5 Results and Discussion

The IEEE-123 node test system shown in Fig. 3.1 is considered to test the proposed study. Here, various customers like residential, commercial, and industrial are also assumed to be connected similarly to the previous two chapters. Their locations can be seen in Table 3.2. The hourly load variation of these customers has been adopted from Fig. 3.2. This modified system consists of some SPV generators and capacitors. Their locations and capacities are displayed in Table 5.2. The required solar irradiance and temperature profile are displayed in Fig. 5.3. In this chapter also, Matlab COM interfacing of OpenDSS (as displayed in

99

Table 5.2. Size and location of capacitors and SPV generators in the distribution networks

| Locations of CBs (Capacity in kVAR) | SPV generator Location (Each Inverter rated 275 kVA) |
|---|---|
| 83 (600), 88a (100), 90b (100), 92c (100) | 95, 115, 117, 122 |

Fig. 3.3) has been utilized for time-series load flow calculations. Here, in a very first step, the initial operating point (maybe a local solution) is determined using GA. Thereafter, the pattern search algorithm has been utilized for obtaining optimal settings of various control variables.

### 5.5.1 Energy Savings

The energy savings obtained for different cases are shown in Table 5.3. Firstly, it can be noticed that substation input energy is more in Case-1 and there is a substantial reduction in the demand (MWh and MVArh) when penetration of SPV system is considered. In Case-2, the MVArh demand has been reduced by 6% where inverters are operating at UPF. The overall savings increased when the operations of smart inverters are taken into the account. The savings in Case-4 are the highest among all the cases. It is also observed that utilizing a predefined IVVCC is a less efficient practice for the purpose of utility energy savings. The more savings can be attained by selecting optimal IVVCC for each smart inverter. Thus, up to 52% MVArh savings have been obtained with optimal IVVCC. The utilization of inverter's limited reactive capability (Case-5) is found to be the second most efficient method. However, the highest reduction in energy losses has been obtained in this case.

Table 5.3. Substation energy intake and corresponding losses along with percentage savings in different studied cases

|  |  | Case-1 | Case-2 | Case-3 | Case-4 | Case-5 |
|---|---|---|---|---|---|---|
| Substation Energy | MVAh | 61.11 | 57.63 | 54.24 | 53.51 | 53.73 |
|  | MWh | 59.75 | 56.35 | 53.18 | 53.15 | 53.16 |
|  | MVArh | 12.83 | 12.06 | 10.65 | 6.22 | 7.78 |
|  | $\Delta$ MVAh | _ | 5.70% | 11.24% | 12.44% | 12.34% |
|  | $\Delta$ MWh | _ | 5.69% | 11.00% | 11.05% | 11.04% |
|  | $\Delta$ MVArh | _ | 5.98% | 17.04% | 51.56% | 39.34% |
| Line Energy losses | MVAh | 2.43 | 2.20 | 2.06 | 2.09 | 2.03 |
|  | MWh | 1.09 | 0.99 | 0.93 | 0.94 | 0.91 |
|  | MVArh | 2.17 | 1.97 | 1.84 | 1.86 | 1.81 |
|  | $\Delta$ MVAh | _ | 9.22% | 15.30% | 14.05% | 16.31% |
|  | $\Delta$ MWh | _ | 9.00% | 14.96% | 13.82% | 16.03% |
|  | $\Delta$ MVArh | _ | 9.27% | 15.39% | 14.10% | 16.38% |
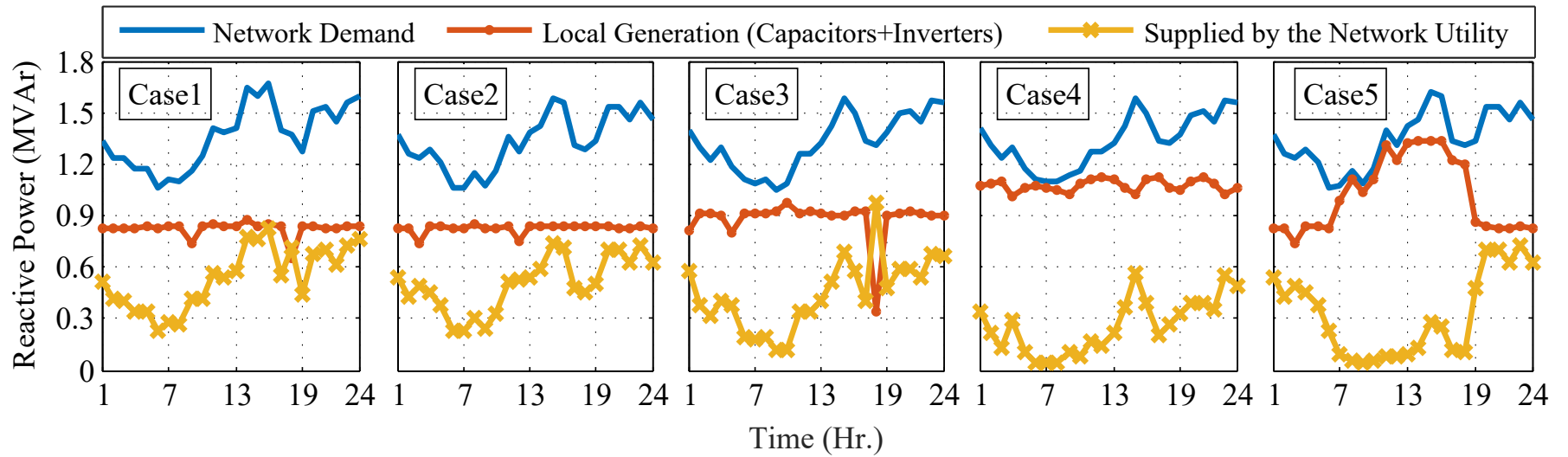
Fig. 5.4. Reactive power demanded by the network and supplied by the local generation (through capacitors and inverters) and utility in different cases
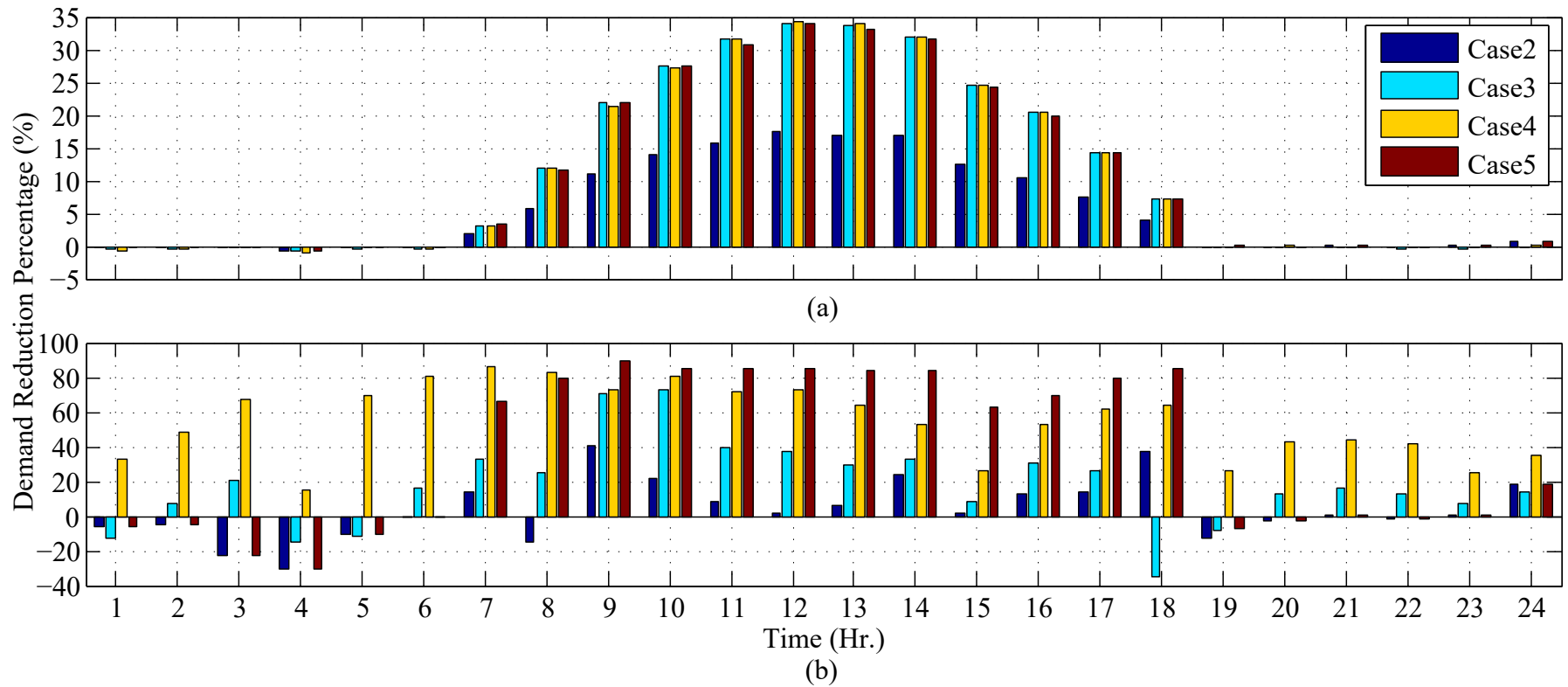
Fig. 5.5. The hourly demand reductions (compared to Case1) of an utility responsible for power supply (a) real Power, (b) reactive power

The hourly MVAr demand of the distribution system, and corresponding supply by the utility and local generators are displayed in Fig. 5.4. In Case1 and Case-2, the reactive power supplied by the utility is more, since a limited (local) MVArs supplied by the capacitor banks. However, the reactive power supplied by the SPV system and capacitors has been utilized in the other cases. It can also be observed that MVAr support received from the SPV system is subsequent when considering smart inverters. In Case-4, the local reactive power supply is varying from 1.0 to 1.2 MVAr (highest energy supply). This variation is quite fluctuating in Case5 because in the night time capacitors can only supply MVAr as no smart inverters allowed for it. Whereas in the day time (when the proper sun shines), both capacitors and inverters (under limited capability) are supplying MVAr.

The hourly reductions in the utility's active and reactive demand can be seen in Fig. 5.5. The active demand increases (shown with negative bar) during a period when none of the smart inverters producing real power (Fig.5.5(a)), whereas a significant reduction (5-35%) has also recorded during the day time. This reduction pattern is almost similar in Case3 to Case-5. Apart from this, the reactive demand is greatly affected and its percentage reduction is shown in Fig. 5.5(b). Like an increase in active demand, the reactive demand also increased at some hours (mostly when no sun shines). But it can also be noted that there will be no increase in the supplied reactive power if all the inverters are following the optimal IVVCC (Case-4). The demand reductions are highest at few hours when limited reactive capability of smart inverters have been utilized (Case-5). However, the overall demand reduction has been achieved in Case4 and varying from 15-85% (approx).

### 5.5.2 Optimal Dispatch Schedule of VVC devices and kVAr of Smart Inverters

The optimal dispatch of various VVC devices and reactive power of generators have been ensured to achieve the maximum energy savings. The hourly schedule of different regulators corresponding to the studied cases has been displayed in Fig. 5.6. It is observed that tap schedule of each regulator is unique and get affected with the studied cases. The daily tap operations of each regulator are less than the allowable operations and shown in Table 5.5. Apart from the regulators, capacitors are also switched 'on' and 'off' along with the time of a day. The optimal 'on-off' schedule of capacitor units is shown in Fig. 5.7. Here, it can be

noticed that all capacitor units remain in 'on' position in Case4 for the complete day. The daily switching operations of the capacitor units are less than the allowable operation (can also be observed in Table 5.5).

The kVAr output of smart inverters when utilizing a predefined IVVCC (Table 5.1) is displayed in Fig.5.8 . Here, the kVAr variation of the first two generators is from 18 to 43 kVAr, whereas the reactive energy supplied by the second one is more (PV1: 643 kVArh and PV2: 811 kVArh). The remaining generators are producing only a few units of reactive energy (PV3: 42 kVArh and PV4: 114 kVArh) for a complete day. This is happened because of the fixed operating points of the IVVCC, where kVAr dispatch is not allowed in the dead-band (0.98 to 1.02) of the characteristics even if it is demanded by the network. This problem has been overcome in Case4, where optimal IVVCC has been considered. In this case, the IVVCC is unique for each inverter and shown in Table 5.4. The graphical representation of the optimal IVVCC alongside kVAr dispatched by each inverter is depicted in Fig. 5.9. Here, the operating points of IVVCC have been determined along with optimal dispatch schedule of VVC devices for achieving the desired objective function. Because of optimal operating points, the kVAr dispatched by the smart inverters increased. Now, the reactive energy produced by PV1 generator is more than three times as compared to the previous case, i.e., 2000 kVArh. The other three generators have also supplied a major portion of reactive energy demand by the system (PV2: 2198 kVArh, PV3: 597 kVArh, and PV4: 807 kVArh).

In Case5, the kVAr dispatched by the smart inverter is based on the signal received from the utility. The optimal kVAr dispatch is shown in Fig. 5.10. Here, all inverters (except PV1) are injecting reactive power to the distribution network up to the allowable capability. The reactive power is not produced when there is no sunshine. There are some hours in a day when PV1 is absorbing reactive power from the network. The daily kVArh energy supplied by PV1, PV2, PV3, and PV4 is 446, 1324, 1358, and 1357, respectively. Therefore, energy supplied by the PV3 and PV4, in this case, is more than the previous two cases but overall local reactive energy is more in Case4.
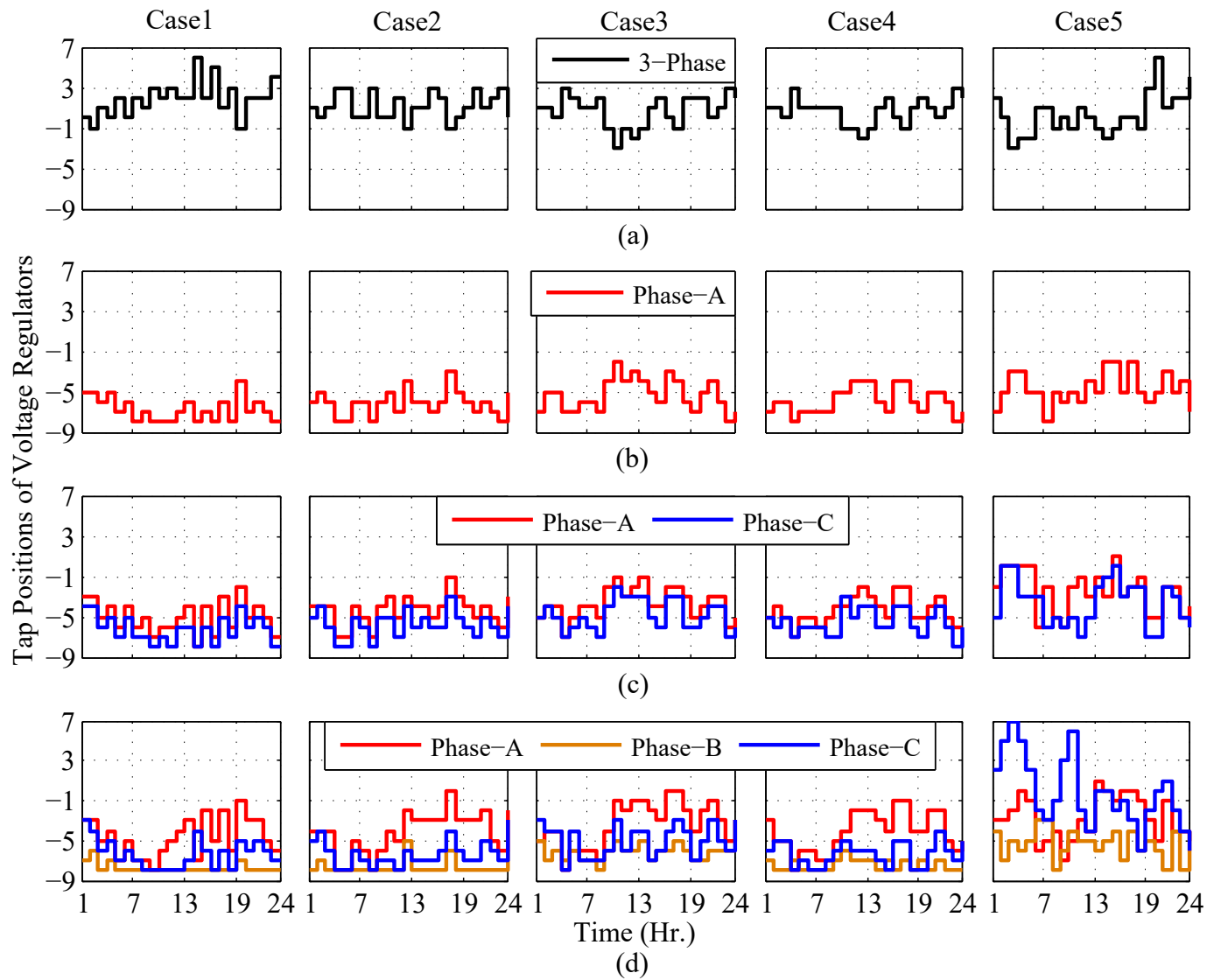
Fig. 5.6. The optimal schedule of tap positions of voltage regulators in various cases (a) Reg1 (3-phase regulator), (b) Reg2 (1-phase regulator), (c) Reg3 (Bank of two 1-phase regulators), (d) Reg4 (Bank of three 1-phase regulators)
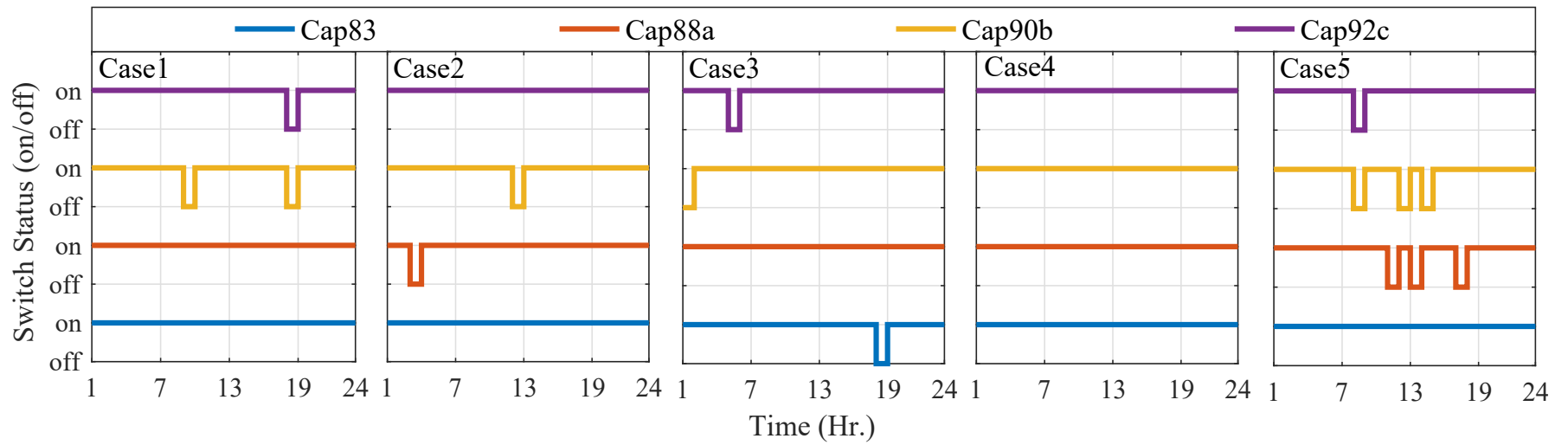
Fig. 5.7. The optimal switch status of capacitors in various cases

### 5.5.3 Final Remarks on VVO for Future Distribution Network

It is observed that active (real) energy savings are just 5.69% when SPV generators are allowed to penetrate the network (Case2). These savings are further increased by approximately 5% with the use of smart inverters. The smart inverters lead to a huge reduction in the substation kVAr demand (Fig.5.4). Therefore, a big saving in the reactive energy supplied by the utility (up to 52%) has been recorded. Here, it is also noticed that maximum energy savings (MVAh, MWh, and MVArh) can be accomplished if an optimal intelligent volt/VAr control characteristics have been allowed for the dispatch schedule of kVAr supplied by the smart inverters (Case4). The consideration of centralized dispatch of kVAr supplied by the inverters (utilizing limited reactive capability) is observed as the second most efficient approach for energy savings estimation (Case5).

There is a considerable reduction in the energy lost in terms of line losses. The losses are greatly reduced (up to 16.38%) when centralized dispatch of kVAr supplied by the inverters is an approach for energy savings. Other approaches also show a significant reduction (9-15%) in energy losses.

The hourly reduction in the utility's kW demand (Fig. 5.5(a)) is varying from -0.7% to 34% (-ve sign shows an increase in the demand). This means at some hours there is an increase (0 to 0.7%) in the kW demand but in the day time (from 7th to 18th hour) a significant reduction in the demand has been achieved. On the other side, reactive power (Fig. 5.5(b)) shows a reduction from -35% to 89%. Here, an increase up to 35% is recorded for a few hours (Case2, Case3, and Case5). The same has been mitigated with the introduction of the optimal intelligent volt/VAr control characteristics, where the kVAr demand reduction is varied from 15 to 86%.

In order to achieve energy savings, VVC devices are scheduled on a daily basis. Therefore, taps and switching operation of these devices are important to avoid frequent replacement or maintenance. The total operation of VVC devices is maximum in Case5 and minimum in Case4 (shown in Fig. 5.11). It is also observed that both demand (MVAh) and operation (of VVC devices) are minimum for the case when optimal intelligent volt/VAr control characteristics have been taken into the account (Case4). Here, it is obvious that Case5 is the second most efficient approach for energy savings estimation but at the cost of maximum
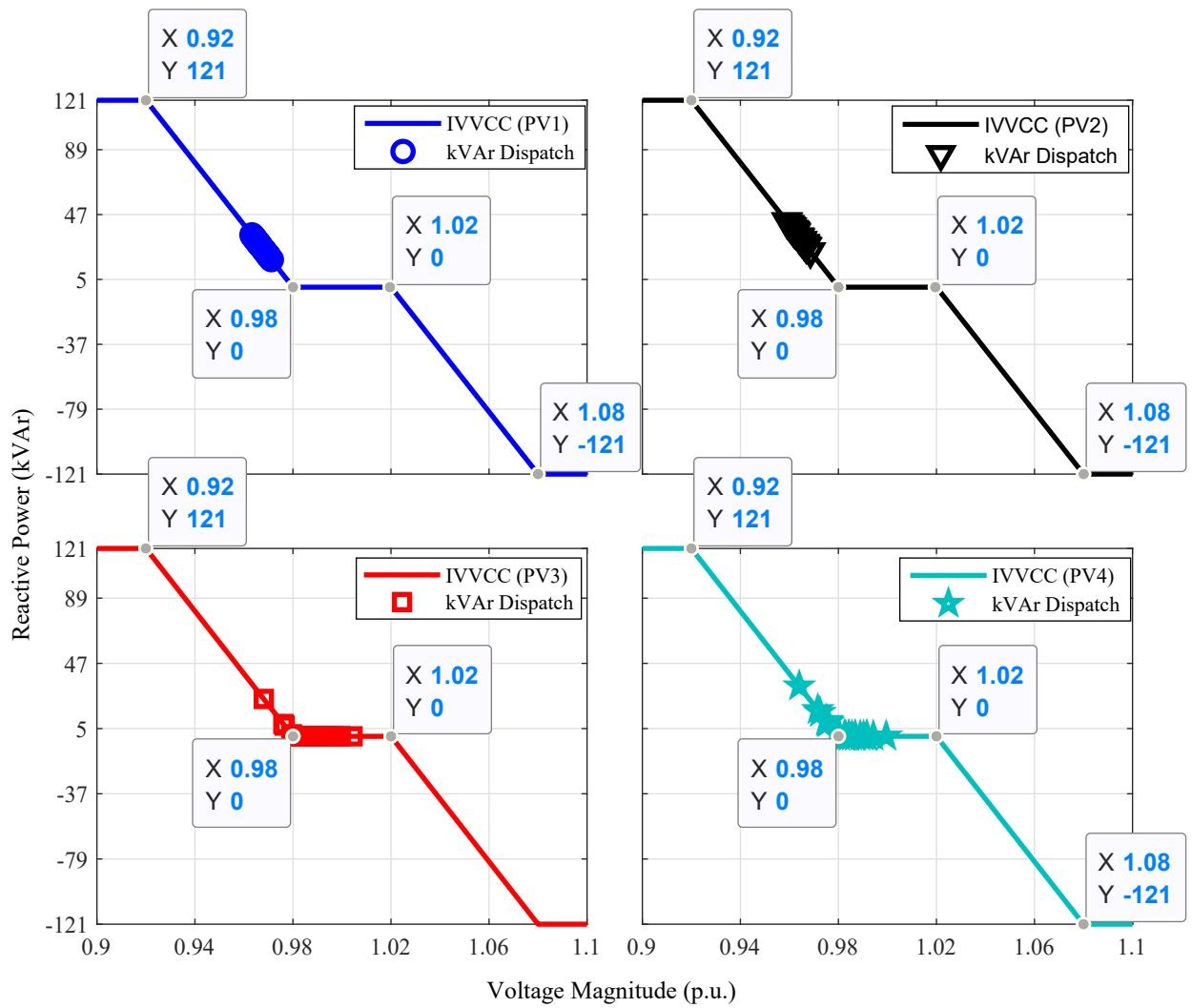
Fig. 5.8. The reactive power dispatch followed by predefined IVVCC of smart inverters

Table 5.4. Optimal operating points of IVVCC for different SPV inverters (Case4)

| SPV Inverter (Location) | $V^{O1}$ | $V^{O2}$ | $V^{O3}$ | $V^{O4}$ | $Q^{O1}$ | $Q^{O2}$ | $Q^{O3}$ | $Q^{O4}$ |
|---|---|---|---|---|---|---|---|---|
| PV1(95) | 0.9486 | 0.9995 | 1.0103 | 1.0395 | 121 | 0 | 0 | -121 |
| PV2(115) | 0.9481 | 1.0000 | 1.0140 | 1.0422 | 121 | 0 | 0 | -121 |
| PV3(117) | 0.9482 | 0.9999 | 1.0221 | 1.0574 | 121 | 0 | 0 | -121 |
| PV4(122) | 0.9492 | 0.9988 | 1.0250 | 1.0261 | 121 | 0 | 0 | -121 |
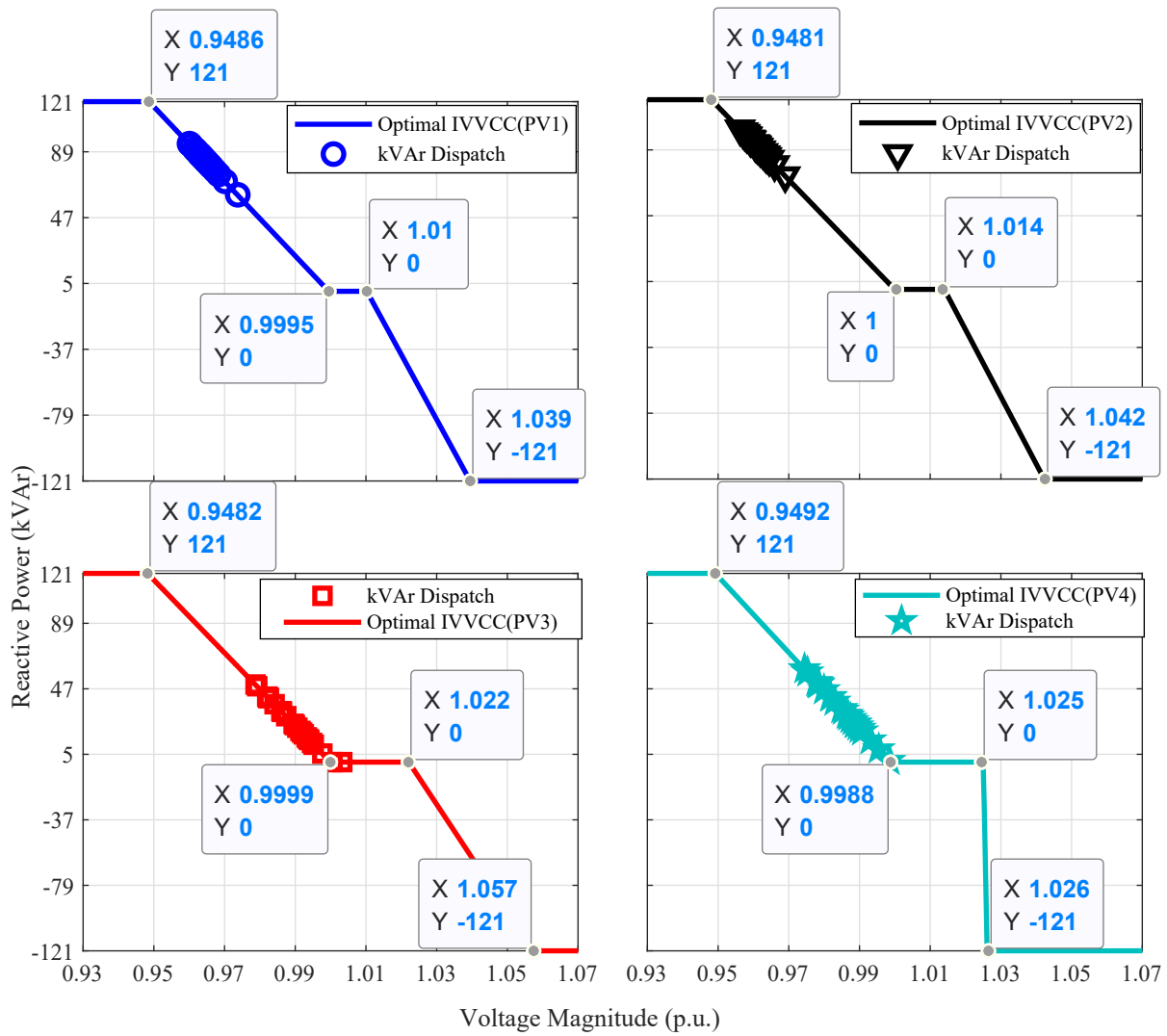
Fig. 5.9. The reactive power dispatch followed by optimal IVVCC of smart inverters
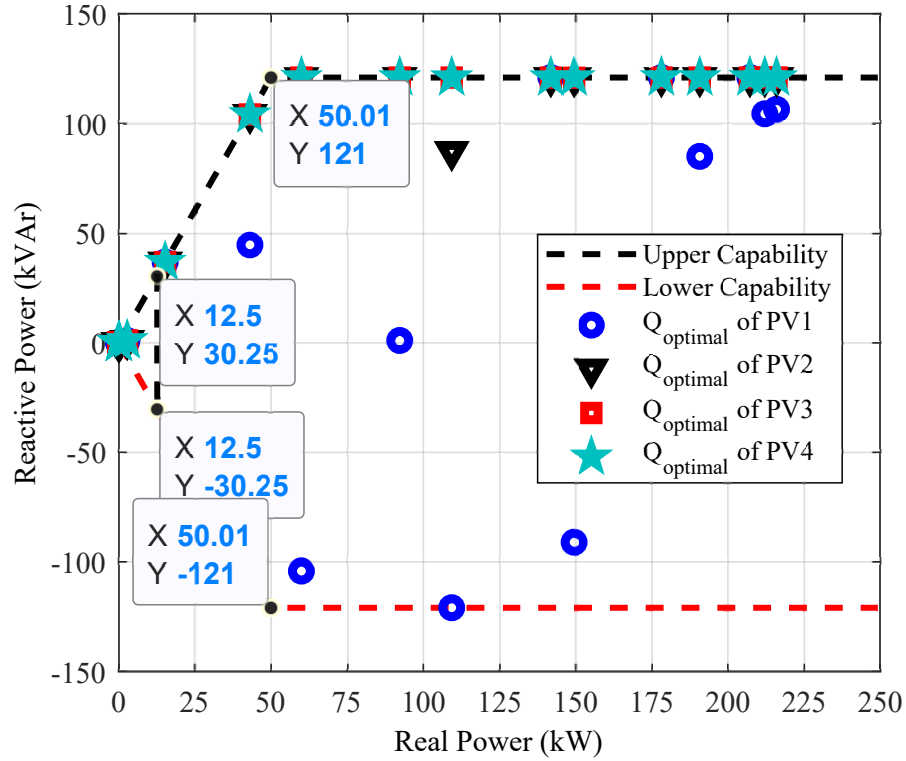
Fig. 5.10. The optimal reactive power dispatch considering limited reactive power capability of smart inverters

Table 5.5. Daily operations of regulators and capacitors

|  |  | Case1 | Case2 | Case3 | Case4 | Case5 |
|---|---|---|---|---|---|---|
|  | Reg1 | 42 | 37 | 31 | 25 | 36 |
|  | Reg2(A) | 29 | 33 | 32 | 22 | 40 |
|  | Reg3(A) | 44 | 33 | 30 | 25 | 48 |
| Regulators | Reg3(C) | 34 | 37 | 29 | 29 | 41 |
|  | Reg4(A) | 45 | 34 | 34 | 28 | 40 |
|  | Reg4(B) | 7 | 14 | 19 | 15 | 46 |
|  | Reg4(C) | 28 | 28 | 42 | 27 | 60 |
|  | Cap83 | 0 | 0 | 2 | 0 | 0 |
|  | Cap88a | 0 | 2 | 0 | 0 | 6 |
| Capacitors | Cap90b | 4 | 2 | 1 | 0 | 6 |
|  | Cap92c | 2 | 0 | 2 | 0 | 2 |
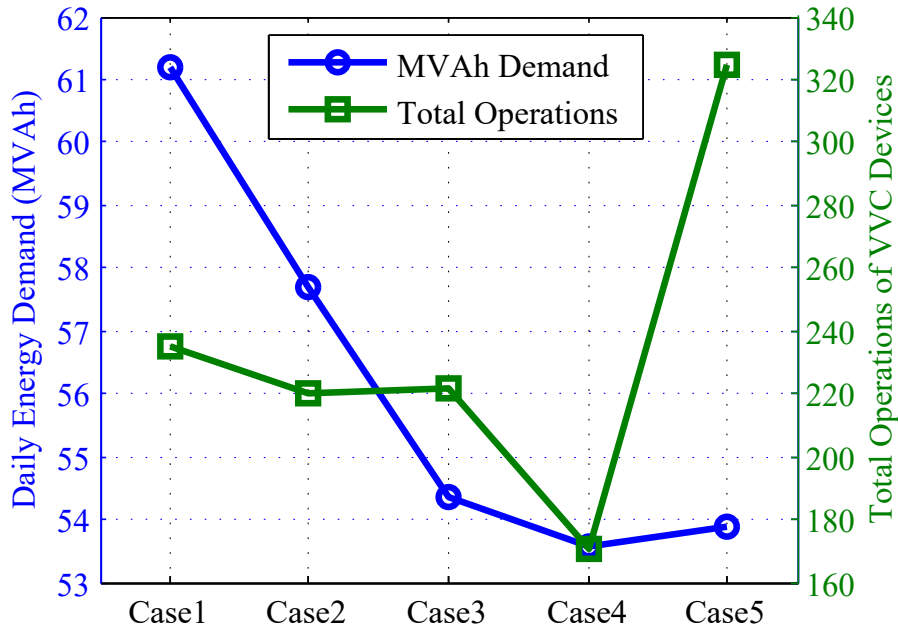
Fig. 5.11. The apparent energy demand of the utility versus total operation of VVC devices of the network

VVC operations.

## 5.6 Summary

In this chapter, the maximization of energy saving in a distribution network has been ensured considering IVVC based on recent IEEE Std. 1547-2018. Here, various cases ranging from VVO performed on a traditional distribution network to an active distribution network have been studied. The concept of smart inverter has also been utilized for estimating energy savings. In order to maximize the energy savings, the usage of optimal operating points for smart inverter (utilizing IVVC) has been proposed. The maximum energy savings have been obtained when operating points of IVVCC are optimally planned by the utility alongside optimal dispatch schedule of VVC devices. The optimal dispatch schedule of inverter's reactive power (kVAr) determined by the utility can be considered as the second most efficient approach from the point of view of overall energy savings. Moreover, loss reduction is maximum in this scheme. The performance of optimal IVVCC has been validated with a set of predefined operating points of IVVCC adopted from IEEE Std. 1547-2018 and limited reactive capability of smart inverters.

Here, the VVO formulation of a future distribution system has been considered as per the DER interconnection guidelines of IEEE Std. 1547-2018. In addition, the limited reactive power capability of a smart inverter has been taken into account while dealing with the reactive power dispatch. Apart from conventional operating strategies of the smart inverter as suggested in IEEE Std. 1547-2018, the determination of optimal IVVCC has also been taken into account while achieving the VVO objectives.

The switching operations of VVC devices are greatly affected with the studied case. These operations are minimum when VVO is performed considering optimal IVVCC of smart inverters. On the other side, maximum switching operations have been recorded for the case when optimal dispatch schedule of reactive power output of smart inverters has been considered.

# CHAPTER 6

# CONCLUSION AND FUTURE SCOPE OF WORK

Volt/VAr Optimization (VVO) attempt to manage network-wide voltage (Volt) levels and reactive power (VAr) flows to accomplish an efficient distribution system operation. VVO helps Distribution Network Operators (DNOs) to reduce energy losses, peak power demand, energy consumption, etc. In VVO, the DNO determines the best possible coordination of control actions for all voltage regulating devices (OLTC and VR) and reactive power control devices (CBs, smart inverters, etc.) to achieve one or more specified objectives without violating any of the system and operating constraints. The VVO formulation presented in this thesis is an attempt to overcome the issues such as minimizing energy losses, peak demand, and energy consumption considering the impact of load models, Distributed Generations (DGs), load-side harmonics, smart inverters, Distributed Energy Resources (DER) interconnection as per IEEE Std. 1547-2018, and so forth.

## 6.1 Summary of Major Contributions

The impact of load models on the scheduling of Volt/VAr Control (VVC) devices has been studied under VVO system considering constant power, constant current, constant impedance, and mixed load models. These models give a distinctive schedule of VVC devices and, henceforth, voltage profile, losses, energy consumption, power factor, and so forth, are unique. Moreover, it is ascertained that the daily operations of VVC devices are enormously influenced by various types of load and their models. It has been also observed that a solution acquired from a particular load model cannot be applied to the same network having different kinds of the loads. This may produce misleading results, such as higher losses, voltage infringement, line congestion, etc. This may also prompt a wrong estimation of life of switching devices because each device has a fixed number of lifetime operations. Consequently, it is very important to choose suitable load models for legitimate scheduling of VVC devices. It can likewise be presumed the exponential load models with an appropriate selection of exponents (i.e., voltage exponents) accurately emulate the practical loads.

The formulation of VVO framework has been extended for active distribution networks

having distributed Solar Photovoltaic (SPV) and Wind Turbine (WT) generators. Because of the particular voltage reliance of active and reactive powers of loads and losses, minimization of the apparent energy demand of distribution systems is considered rather than minimization of active energy or losses. In addition to this, the harmonics are considered on the load-side (load currents) while keeping up the voltage-reliance of different practical loads.

Nowadays, DNOs have more opportunities to optimize the voltage profile in an active distribution network as compared to traditional passive network. Therefore, more energy saving can be realized when DGs are connected in the traditional distribution network. Significant reductions in substation's apparent energy and network losses (kWh) are obtained in the volt/VAr control case. It is also noticed that a proper CVR can be applied to the overall distribution networks when considering volt/VAr control case. However, the voltage reduction is not so effective in the case of voltage control. With the inclusion of harmonics, the substation apparent energy is slightly increased as compared to without harmonics. However, a considerable increase has been seen in the system (energy) losses.

The taps and switching operations of VVC devices are minimum for the base case when considering traditional passive distribution network. These operations increase considerably when moving towards an optimal solution, i.e., from base case to volt/VAr control case. Therefore, it can also be stated that more energy savings can be obtained if VVC devices are allowed to operate frequently as much as required. Moreover, the life of the regulating mechanism of VVC devices will be reduced because each device is associated with a designed maximum number of life-time operations. Therefore, there is a trade-off between energy savings and the number of switching operations.

In this thesis, the VVO formulation of a future distribution system has been proposed as per the DER interconnection guidelines of IEEE Std. 1547-2018. In this, maximization of energy savings of a distribution network (associated with distributed SPV system with smart inverters) has been ensured considering intelligent volt/VAr control (IVVC) based on recent IEEE Std. 1547-2018. Here, various VVO cases ranging from traditional distribution network to an active distribution network have been studied. The concept of smart inverter has also been utilized for estimating the energy savings.

In order to maximize the energy savings, the usage of optimal operating points for smart

116

inverter (utilizing IVVC) has been proposed. The maximum energy savings have been obtained when operating points of the IVVC characteristics (IVVCC) are optimally planned by the distribution utility alongside optimal dispatch schedule of VVC devices. The optimal dispatch schedules of inverters' reactive power (kVAr) determined by the utility can be considered as the second most efficient approach from the point of view of overall energy savings. Moreover, loss reduction is maximum in this scheme.

The performance of optimal IVVCC has been validated with a set of predefined operating points of IVVCC adopted from IEEE Std. 1547-2018. In addition, the limited reactive power capability of smart inverters has been taken into account while dealing with the reactive power dispatch. Apart from conventional operating strategies of the smart inverter as suggested in IEEE Std. 1547-2018, the determination of optimal IVVC characteristics has also been taken into account while achieving the VVO objectives.

## 6.2 Future Scope of Work

In this thesis, VVC devices include OLTC, VRs and CBs. Apart from these devices, smart inverter based SPV systems have additionally been utilized as reactive power compensation devices. However, in the current scenario of smart grid technologies, many advancements in technologies such as plug-in-hybrid electric vehicles, energy storage, system reconfiguration, demand response, and so forth have been left to think about the performance and its impact on VVC devices and smart inverters under VVO framework. Therefore, future work to investigate the effect of these technologies on the performance of VVO. Future work will incorporate following aspect:

1. The network topology may play a significant role while accomplishing VVO objectives. Therefore, the DNO needed optimal settings of VVC devices in the reconfigured system as well. Thus, the impact of system reconfiguration on the scheduling of VVC devices need to be studied as a future aspect and VVO can be carried out with the reconfigured network.

2. The DNO change the taps of OLTC of substation transformer, taps of VRs, and switch status of CBs as often as possible, for maintaining the voltage and VAr flow in the distribution network. This results in the reduction of life of such devices or prompts

117

higher upkeep cost. However, the actual operational cost for these devices has not been considered in VVO formulation. Therefore, in future work, these costs will likewise be considered in the optimization will be carried out to limit them.

3. In a smart grid scenario, energy storage devices (electric vehicles, batteries, domestic/commercial inverters, etc.) may be the potential candidates for peak load relief. The future scope of this work is to consider the effect of energy storage devices on VVO formulations for the purpose of peak load reduction and an overall reduction in energy consumption.

4. Demand Response is also one of the main objectives of the smart grid. In the presence of demand-response, there will be a considerable change in loading patterns throughout the day. Henceforth, there is a requirement for time-varying load modeling and demand response to be considered while achieving the VVO objectives.

5. The peak shaving is essential for grid stability. The VVO can also reduce the peak demand of a distribution network. Thus, the consideration of peak shaving in the VVO objective will also help the DNO to achieve more savings.

# BIBLIOGRAPHY

[1] *Executive Summary Power Sector*, Government Of India Ministry of Power Central Electricity Authority New Delhi, Feb. 2019. [Online]. Available: http://cea.nic.in/reports/monthly/executivesummary/2019/exe_summary-02.pdf

[2] "India gdp per capita [1958 - 2019] [data & charts]," https://www.ceicdata.com/en/indicator/india/gdp-per-capita, (Accessed on 04/12/2019).

[3] "Power Sector at a Glance All India — Government of India — Ministry of Power," https://powermin.nic.in/en/content/power-sector-glance-all-india, (Accessed on 04/11/2019).

[4] *Executive Summary Power Sector*, Government Of India Ministry of Power Central Electricity Authority New Delhi, Jul. 2013. [Online]. Available: http://cea.nic.in/reports/monthly/executivesummary/2013/exe_summary-07.pdf

[5] *Energy Statistics 2018*, Ministry of Statistics and Programme Implementation Government of India New Delhi, Mar. 2018, (Accessed on 04/11/2019). [Online]. Available: http://mospi.nic.in/sites/default/files/publication_reports/Energy_Statistics_2018.pdf

[6] "Electric power transmission and distribution losses (% of output) — data," https://data.worldbank.org/indicator/EG.ELC.LOSS.ZS, (Accessed on 04/11/2019).

[7] "Smart Grid Technologies," in *Smart Grids Infrastructure, Technology, and Solutions*, S. Borlase, Ed., ch. 3, pp. 61–496. Taylor and Francis Group: CRC Press, 2012.

[8] K. Schneider and T. Weaver, "A Method for Evaluating Volt-VAR Optimization Field Demonstrations," *IEEE Transactions on Smart Grid*, vol. 5, no. 4, pp. 1696–1703, Jul. 2014.

[9] V. Dabic, C. Siew, J. Peralta, and D. Acebedo, "BC Hydro's experience on Voltage VAR Optimization in distribution system," in *Transmission and Distribution Conference and Exposition, 2010 IEEE PES*, pp. 1–7, Apr. 2010.

[10] V. Dabic and D. Atanackovic, "Voltage VAR optimization real time closed loop deployment - BC Hydro challenges and opportunities," in *Power Energy Society General Meeting, 2015 IEEE*, pp. 1–5, Jul. 2015.

[11] S. Chanda, F. Shariatzadeh, a. Srivastava, E. Lee, W. Stone, and J. Ham, "Implementation of non-intrusive energy saving estimation for Volt/VAr control of smart distribution system," *Electric Power Systems Research*, vol. 120, pp. 39–46, 2015.

[12] I. Roytelman, B. Wee, R. Lugtu, T. Kulas, and T. Brossart, "Pilot project to estimate the centralized volt/VAr control effectiveness," *IEEE Trans. Power Syst.*, vol. 13, no. 3, pp. 864–869, Aug. 1998.

[13] R.-H. Liang, Y.-K. Chen, and Y.-T. Chen, "Volt/var control in a distribution system by a fuzzy optimization approach," *International Journal of Electrical Power & Energy Systems*, vol. 33, no. 2, pp. 278–287, 2011.

[14] "Bibliography on load models for power flow and dynamic performance simulation," *IEEE Transactions on Power Systems*, vol. 10, no. 1, pp. 523–538, Feb. 1995.

[15] A. Bokhari, A. Raza, M. Diaz-Aguiló, F. De Leon, D. Czarkowski, R. E. Uosef, and D. Wang, "Combined effect of cvr and dg penetration in the voltage profile of low-voltage secondary distribution networks," *IEEE Transactions on Power Delivery*, vol. 31, no. 1, pp. 286–293, 2016.

[16] A. Ulinuha, M. A. S. Masoum, and S. M. Islam, "Optimal Scheduling of LTC and Shunt Capacitors in Large Distorted Distribution Systems Using Evolutionary-Based Algorithms," *IEEE Transactions on Power Delivery*, vol. 23, no. 1, pp. 434–441, Jan. 2008.

[17] A. Ulinuha, M. Masoum, and S. Islam, "Hybrid genetic-fuzzy algorithm for volt/var/total harmonic distortion control of distribution systems with high penetration of non-linear loads," *IET Generation, Transmission & Distribution*, vol. 5, no. 4, p. 425, Apr. 2011.

[18] S. Jashfar and S. Esmaeili, "Volt/var/THD control in distribution networks considering reactive power capability of solar energy conversion," *International Journal of Electrical Power and Energy Systems*, vol. 60, pp. 221–233, 2014.

[19] S. Jashfar, M. M. Hosseini-Biyouki, and S. Esmaeili, "A Stochastic Programming to Volt/VAR/Total Harmonic Distortion Control in Distribution Networks Including Wind Turbines," *Electric Power Components and Systems*, no. 7, pp. 733–746, 2015.

[20] "IEEE Standard for Interconnecting Distributed Resources with Electric Power Systems - Amendment 1," *IEEE Std 1547a-2014 (Amendment to IEEE Std 1547-2003)*, pp. 1–16, May. 2014.

[21] "IEEE Standard for Interconnection and Interoperability of Distributed Energy Resources with Associated Electric Power Systems Interfaces," *IEEE Std 1547-2018 (Revision of IEEE Std 1547-2003)*, pp. 1–138, Apr. 2018.

[22] J. Smith, "Modeling High-Penetration PV for Distribution Interconnection Studies," *Electric Power Research Institute*, pp. 1–1, May. 2017.

[23] D. T. Rizy, J. S. Lawler, J. B. Patton, and W. R. Nelson, "Measuring and analyzing the impact of voltage and capacitor control with high speed data acquisition [distribution system]," *IEEE Transactions on Power Delivery*, vol. 4, no. 1, pp. 704–714, Jan. 1989.

[24] D. Singh, R. K. Misra, and D. Singh, "Effect of load models in distributed generation planning," *IEEE Transactions on Power Systems*, vol. 22, no. 4, pp. 2204–2212, Nov. 2007.

[25] D. Singh, D. Singh, and K. S. Verma, "Multiobjective optimization for dg planning with load models," *IEEE Transactions on Power Systems*, vol. 24, no. 1, pp. 427–436, Feb. 2009.

[26] K. Qian, C. Zhou, M. Allan, and Y. Yuan, "Effect of load models on assessment of energy losses in distributed generation planning," *International Journal of Electrical Power & Energy Systems*, vol. 33, no. 6, pp. 1243 – 1250, 2011.

[27] D. Singh and R. K. Misra, "Multi-objective feeder reconfiguration in different tariff structures," *IET Generation, Transmission Distribution*, vol. 4, no. 8, pp. 974–988, Aug. 2010.

[28] M. Manbachi, M. Nasri, B. Shahabi, H. Farhangi, A. Palizban, S. Arzanpour, M. Moallem, and D. Lee, "Real-Time Adaptive VVO/CVR Topology Using Multi-Agent System and IEC 61850-Based Communication Protocol," *IEEE Transactions on Sustainable Energy*, vol. 5, no. 2, pp. 587–597, Apr. 2014.

[29] M. Manbachi, H. Farhangi, A. Palizban, and S. Arzanpour, "Smart grid adaptive energy conservation and optimization engine utilizing Particle Swarm Optimization and Fuzzification," *Applied Energy*, vol. 174, pp. 69–79, 2016.

[30] F.-C. Lu and Y. Hsu, "Reactive power/voltage control in a distribution substation using dynamic programming," *IEE Proceedings - Generation, Transmission and Distribution*, vol. 142, no. 6, pp. 639–645, Nov. 1995.

[31] A. Borghetti, "Using mixed integer programming for the volt/var optimization in distribution feeders," *Electric Power Systems Research*, vol. 98, pp. 39–50, 2013.

[32] A. Borghetti, F. Napolitano, and C. A. Nucci, "Volt/var optimization of unbalanced distribution feeders via mixed integer linear programming," *International Journal of Electrical Power & Energy Systems*, vol. 72, pp. 40–47, 2015.

[33] H. Ahmadi, J. Marti, and H. Dommel, "A Framework for Volt-VAR Optimization in Distribution Systems," *IEEE Transactions on Smart Grid,*, vol. 6, no. 3, pp. 1473–1483, May. 2015.

[34] B. Milosevic and M. Begovic, "Capacitor placement for conservative voltage reduction on distribution feeders," *IEEE Transactions on Power Delivery*, vol. 19, no. 3, pp. 1360–1367, Jul. 2004.

[35] A. Padilha-Feltrin, D. Quijano Rodezno, and J. Sanches Mantovani, "Volt-VAR Multiobjective Optimization to Peak-Load Relief and Energy Efficiency in Distribution Networks," *IEEE Transactions on Power Delivery*, vol. 30, no. 2, pp. 618–626, Apr. 2015.

[36] A. R. Malekpour and T. Niknam, "A probabilistic multi-objective daily Volt/Var control at distribution networks including renewable energy sources," *Energy*, vol. 36, no. 5, pp. 3477–3488, 2011.

[37] A. R. Malekpour, S. Tabatabaei, and T. Niknam, "Probabilistic approach to multi-objective Volt/Var control of distribution system considering hybrid fuel cell and wind energy sources using Improved Shuffled Frog Leaping Algorithm," *Renewable Energy*, vol. 39, no. 1, pp. 228–240, 2012.

[38] T. Niknam, "A new HBMO algorithm for multiobjective daily Volt/Var control in distribution systems considering Distributed Generators," *Applied Energy*, vol. 88, no. 3, pp. 778–788, 2011.

[39] T. Niknam, M. Zare, and J. Aghaei, "Scenario-based multiobjective volt/var control in distribution networks including renewable energy sources," *IEEE Transactions on Power Delivery*, vol. 27, no. 4, pp. 2004–2019, Oct. 2012.

[40] M. Zare, T. Niknam, R. Azizipanah-Abarghooee, and B. Amiri, "Multi-objective probabilistic reactive power and voltage control with wind site correlations," *Energy*, vol. 66, pp. 810–822, 2014.

[41] F. Sayadi, S. Esmaeili, and F. Keynia, "Two-layer volt/var/total harmonic distortion control in distribution network based on PVs output and load forecast errors," *IET Generation, Transmission Distribution*, vol. 11, no. 8, pp. 2130–2137, 2017.

[42] A. Anwar, A. N. Mahmood, J. Taheri, Z. Tari, and A. Y. Zomaya, "HPC-Based Intelligent Volt/VAr Control of Unbalanced Distribution Smart Grid in the Presence of Noise," *IEEE Transactions on Smart Grid*, vol. 8, no. 3, pp. 1446–1459, May. 2017.

[43] R. Anilkumar, G. Devriese, and A. K. Srivastava, "Voltage and Reactive Power Control to Maximize the Energy Savings in Power Distribution System With Wind Energy," *IEEE Transactions on Industry Applications*, vol. 54, no. 1, pp. 656–664, Jan. 2018.

[44] S. Huang and V. Dinavahi, "GPU-based parallel real-time volt/var optimisation for distribution network considering distributed generators," *IET Generation, Transmission Distribution*, vol. 12, no. 20, pp. 4472–4481, 2018.

[45] S. Satsangi and G. B. Kumbhar, "Integrated Volt-VAr Optimization with Distributed Energy Sources to Minimize Substation Energy in Distribution System," *Electric Power Components and Systems*, DOI 10.1080/15325008.2018.1511004, pp. 1–1, 2018.

[46] L. Gutierrez-Lagos and L. F. Ochoa, "OPF-based CVR Operation in PV-Rich MV-LV Distribution Networks," *IEEE Transactions on Power Systems*, DOI 10.1109/TP-WRS.2019.2894795, pp. 1–1, 2019.

[47] R. R. Jha, A. Dubey, C. Liu, and K. P. Schneider, "Bi-Level Volt-VAR Optimization to Coordinate Smart Inverters with Voltage Control Devices," *IEEE Transactions on Power Systems*, DOI 10.1109/TPWRS.2018.2890613, pp. 1–1, 2019.

[48] M. Chamana and B. H. Chowdhury, "Optimal Voltage Regulation of Distribution Networks With Cascaded Voltage Regulators in the Presence of High PV Penetration," *IEEE Transactions on Sustainable Energy*, vol. 9, no. 3, pp. 1427–1436, Jul. 2018.

[49] F. Ding and M. Baggu, "Coordinated Use of Smart Inverters with Legacy Voltage Regulating Devices in Distribution Systems with High Distributed PV Penetration Increase CVR Energy Savings," *IEEE Transactions on Smart Grid*, DOI 10.1109/TSG.2018.2857410, pp. 1–1, 2018.

[50] R. A. Jabr, "Robust Volt/VAr Control with Photovoltaics," *IEEE Transactions on Power Systems*, DOI 10.1109/TPWRS.2018.2890767, pp. 1–1, 2019.

[51] M. Mukherjee, S. Poudel, A. Dubey, and A. Bose, "Distributed generator sizing for joint optimization of resilience and voltage regulation," in *2018 North American Power Symposium (NAPS)*, pp. 1–6. IEEE, 2018.

[52] M. Daliparthi, M. Jakub-Wood, A. Bose, and A. Srivastava, "Analysis of the volt/var control scheme for smart distribution feeders," in *2012 North American Power Symposium (NAPS)*, pp. 1–6. IEEE, 2012.

[53] M. Ibrahim and M. Salama, "Smart distribution system volt/VAR control using distributed intelligence and wireless communication," *IET Generation, Transmission & Distribution*, vol. 9, no. 4, pp. 307–318, 2015.

[54] T. Niknam, A. Ranjbar, and A. Shirani, "Impact of distributed generation on volt/var control in distribution networks," in *Power Tech Conference Proceedings, 2003 IEEE Bologna*, vol. 3, pp. 7–pp. IEEE, 2003.

[55] M. E. Baran and I. M. El-Markabi, "A multiagent-based dispatching scheme for distributed generators for voltage support on distribution feeders," *IEEE Transactions on Power Systems*, vol. 22, no. 1, pp. 52–59, 2007.

[56] T. Niknam, "A new approach based on ant colony optimization for daily Volt/Var control in distribution networks considering distributed generators," *Energy Conversion and Management*, vol. 49, no. 12, pp. 3417–3424, 2008.

[57] X. Zhang, A. J. Flueck, and C. P. Nguyen, "Agent-based distributed volt/var control with distributed power flow solver in smart grid," *IEEE Transactions on Smart Grid*, vol. 7, no. 2, pp. 600–607, Mar. 2016.

[58] M. Manbachi, H. Farhangi, A. Palizban, and S. Arzanpour, " A novel Volt-VAR Optimization engine for smart distribution networks utilizing Vehicle to Grid dispatch," *International Journal of Electrical Power and Energy Systems*, vol. 74, pp. 238–251, 2016.

[59] Y. Liu, P. Zhang, and X. Qiu, "Optimal volt/var control in distribution systems," *International Journal of Electrical Power and Energy Systems*, vol. 24, no. 4, pp. 271–276, 2002.

[60] F. Viawan and D. Karlsson, "Combined Local and Remote Voltage and Reactive Power Control in the Presence of Induction Machine Distributed Generation," *IEEE Transactions on Power Systems*, vol. 22, no. 4, pp. 2003 –2012, Nov. 2007.

[61] L. Mokgonyana, J. Zhang, L. Zhang, and X. Xia, "Coordinated two-stage volt/var management in distribution networks," *Electric Power Systems Research*, vol. 141, pp. 157–164, 2016.

[62] J. E. Mendoza, D. A. Morales, R. A. Lopez, E. A. Lopez, J.-C. Vannier, and C. A. Coello Coello, "Multiobjective Location of Automatic Voltage Regulators in a Radial Distribution Network Using a Micro Genetic Algorithm," *IEEE Transactions on Power Systems*, vol. 22, no. 1, pp. 404–412, Feb. 2007.

[63] Y. Y. Hong and Y. F. Luo, "Optimal VAR control considering wind Farms using probabilistic load-flow and gray-based genetic algorithms," *IEEE Transactions on Power Delivery*, vol. 24, no. 3, pp. 1441–1449, Jul. 2009.

[64] S. Auchariyamet and S. Sirisumrannukul, "Volt/VAr control in distribution systems by fuzzy multiobjective and particle swarm," in *6th International Conference on Electrical Engineering/Electronics, Computer, Telecommunications and Information Technology(ECTI-CON) 2009.*, vol. 01, pp. 234–237, May. 2009.

[65] S. Auchariyamet and S. Sirisumrannukul, "Optimal daily coordination of volt/VAr control devices in distribution systems with distributed generators," in *45th International Universities Power Engineering Conference (UPEC), 2010*, pp. 1–6, Aug. 2010.

[66] J. Grainger and S. Civanlar, "Volt/Var Control on Distribution Systems with Lateral Branches Using Shunt Capacitors and Voltage Regulators Part I: The Overall Problem," *IEEE Trans. Power App. Syst.*, vol. PAS-104, DOI 10.1109/TPAS.1985.318842, no. 11, pp. 3278–3283, Nov. 1985.

[67] S. Civanlar and J. Grainger, "Volt/Var Control on Distribution Systems with Lateral Branches Using Shunt Capacitors and Voltage Regulators Part II: The Solution Method," *IEEE Trans. Power App. Syst.*, vol. PAS-104, DOI 10.1109/TPAS.1985.318843, no. 11, pp. 3284–3290, Nov. 1985.

[68] S. Civanlar and J. Grainger, "Volt/Var Control on Distribution Systems with Lateral Branches Using Shunt Capacitors and Voltage Regulators Part III: The Numerical Results," *IEEE Trans. Power App. Syst.*, vol. PAS-104, DOI 10.1109/TPAS.1985.318844, no. 11, pp. 3291–3297, Nov. 1985.

[69] G. Ramakrishna and N. Rao, "Adaptive neuro-fuzzy inference system for volt/var control in distribution systems," *Electric Power Systems Research*, vol. 49, no. 2, pp. 87–97, 1999.

[70] Z. Hu, X. Wang, H. Chen, and G. Taylor, "Volt/var control in distribution systems using a time-interval based approach," *Generation, Transmission and Distribution, IEE Proceedings-*, vol. 150, no. 5, pp. 548–554, Sep. 2003.

[71] T. Senjyu, Y. Miyazato, a. Yona, N. Urasaki, and T. Funabashi, "Optimal Distribution Voltage Control and Coordination With Distributed Generation," *IEEE Transactions on Power Delivery*, vol. 23, no. 2, pp. 1236–1242, Apr. 2008.

[72] Z. Wang, J. Wang, B. Chen, M. Begovic, and Y. He, "MPC-Based Voltage/Var Optimization for Distribution Circuits With Distributed Generators and Exponential Load Models," *IEEE Transactions on Smart Grid*, vol. 5, no. 5, pp. 2412–2420, Sep. 2014.

[73] Y. Mohamed Shuaib, M. Surya Kalavathi, and C. Christober Asir Rajan, "Optimal capacitor placement in radial distribution system using Gravitational Search Algorithm," *International Journal of Electrical Power and Energy Systems*, vol. 64, pp. 384–397, 2015.

[74] M. Manbachi, A. Sadu, H. Farhangi, A. Monti, A. Palizban, F. Ponci, and S. Arzanpour, "Real-time co-simulation platform for smart grid volt-var optimization using iec

61850," *IEEE Transactions on Industrial Informatics*, vol. 12, no. 4, pp. 1392–1402, Aug. 2016.

[75] M. Manbachi, A. Sadu, H. Farhangi, A. Monti, A. Palizban, F. Ponci, and S. Arzanpour, "Impact of EV penetration on Volt-VAR Optimization of distribution networks using real-time co-simulation monitoring platform," *Applied Energy*, pp. 28–39, 2016.

[76] M. Liu, C. Canizares, and W. Huang, "Reactive Power and Voltage Control in Distribution Systems With Limited Switching Operations," *IEEE Transactions on Power Systems*, vol. 24, no. 2, pp. 889–899, May. 2009.

[77] B. A. De Souza and A. M. F. De Almeida, "Multiobjective optimization and fuzzy logic applied to planning of the volt/var problem in distributions systems," *IEEE Transactions on Power Systems*, vol. 25, no. 3, pp. 1274–1281, Aug. 2010.

[78] J. F. Franco, M. J. Rider, M. Lavorato, and R. Romero, "A mixed-integer LP model for the optimal allocation of voltage regulators and capacitors in radial distribution systems," *International Journal of Electrical Power and Energy Systems*, vol. 48, no. 1, pp. 123–130, 2013.

[79] M. Zare and T. Niknam, "A new multi-objective for environmental and economic management of Volt/Var Control considering renewable energy resources," *Energy*, vol. 55, pp. 236–252, 2013.

[80] A. Mohapatra, P. Bijwe, and B. Panigrahi, "An Efficient Hybrid Approach for Volt/Var Control in Distribution Systems," *IEEE Transactions on Power Delivery*, vol. 29, no. 4, pp. 1780–1788, Aug. 2014.

[81] M. Resener, S. Haffner, L. A. Pereira, and P. M. Pardalos, "Mixed-integer LP model for volt / var control and energy losses minimization in distribution systems," *Electric Power Systems Research*, vol. 140, pp. 895–905, 2016.

[82] R. Baldick and F. F. Wu, "Efficient integer optimization algorithms for optimal coordination of capacitors and regulators," *IEEE Transactions on Power Systems*, no. 3, pp. 805–812, Aug. 1990.

[83] T. Niknam, B. B. Firouzi, and A. Ostadi, "A new fuzzy adaptive particle swarm optimization for daily Volt/Var control in distribution networks considering distributed generators," *Applied Energy*, vol. 87, no. 6, pp. 1919–1928, 2010.

[84] D. F. Pires, A. Martins, and C. Antunes, "A multiobjective model for VAR planning in radial distribution networks based on tabu search," *IEEE Transactions on Power Systems*, vol. 20, no. 2, pp. 1089–1094, May. 2005.

[85] Y. P. Agalgaonkar, B. C. Pal, and R. a. Jabr, "Distribution voltage control considering the impact of PV generation on tap changers and autonomous regulators," *IEEE Transactions on Power Systems*, vol. 29, no. 1, pp. 182–192, Jan. 2014.

[86] E. Atmaca, "An ordinal optimization based method for power distribution system control," *Electric Power Systems Research*, vol. 78, no. 4, pp. 694–702, 2008.

[87] R. A. Jabr and I. Dzafic, "Sensitivity-based discrete coordinate-descent for volt/var control in distribution networks," *IEEE Transactions on Power Systems*, vol. 31, no. 6, pp. 4670–4678, Nov. 2016.

[88] Feng-Chang Lu and Yuan-Yih Hsu, "Fuzzy dynamic programming approach to reactive power/voltage control in a distribution substation," *IEEE Transactions on Power Systems*, vol. 12, no. 2, pp. 681–688, May. 1997.

[89] Y.-Y. Hsu and F.-C. Lu, "A combined artificial neural network-fuzzy dynamic programming approach to reactive power/voltage control in a distribution substation," *IEEE Transactions on Power Systems*, vol. 13, no. 4, pp. 1265–1271, Nov. 1998.

[90] C. K. Cheng and R. H. Liang, "Dispatch of Main Transformer ULTC and Capacitors in a Distribution System," *IEEE Transaction on Power Delivery*, vol. 16, no. 4, pp. 625–630, Oct. 2001.

[91] R.-h. Liang and Y.-s. Wang, "Fuzzy-based reactive power and voltage control in a distribution system," *IEEE Transactions on Power Delivery*, vol. 18, no. 2, pp. 610–618, Apr. 2003.

[92] P.-I. Hwang, M.-G. Jeong, S.-I. Moon, and I.-K. Song, "Volt/Var optimization of the Korean smart distribution management system," in *22nd International Conference and Exhibition on Electricity Distribution (CIRED 2013)*, pp. 1–4, Jun. 2013.

[93] A. Dwyer, R. Nielsen, J. Stangl, and N. Markushevich, "Load to voltage dependency tests at B.C. Hydro," *IEEE Trans. Power Syst.*, vol. 10, no. 2, pp. 709–715, May. 1995.

[94] *American National Statndard for Electrical Power Systems and Equipment Voltage Ratings(60Hz)*, American National Standard Institute, C84.1-2006, Dec. 2006.

[95] B. Shah, A. Bose, and A. Srivastava, "Load modeling and voltage optimization using smart meter infrastructure," in *Innovative Smart Grid Technologies (ISGT), 2013 IEEE PES*, pp. 1–6, Feb. 2013.

[96] K. Schneider, F. Tuffner, and R. Singh, "Evaluation of Conservation Voltage Reduction (CVR) on a National Level," U.S. Department of Energy, Pacific Northwest National Laboratory, Tech. Rep. PNNL-19596, Jul. 2010.

[97] A. Bokhari, A. Alkan, R. Dogan, M. Diaz-Aguilo, F. de Leon, D. Czarkowski, Z. Zabar, L. Birenbaum, A. Noel, and R. Uosef, "Experimental Determination of the ZIP Coefficients for Modern Residential, Commercial, and Industrial Loads," *IEEE Transactions on Power Delivery*, vol. 29, no. 3, pp. 1372–1381, Jun. 2014.

[98] S. Deshmukh, B. Natarajan, and A. Pahwa, "Voltage/VAR control in distribution networks via reactive power injection through distributed generators," *IEEE Transactions on Smart Grid*, vol. 3, DOI 10.1109/TSG.2012.2196528, no. 3, pp. 1226–1234, Sep. 2012.

[99] I. Roytelman, B. Wee, and R. Lugtu, "Volt/var control algorithm for modern distribution management system," *IEEE Trans. Power Syst.*, vol. 10, no. 3, pp. 1454–1460, Aug. 1995.

[100] E. Hossain, R. Perez, A. Nasiri, and S. Padmanaban, "A comprehensive review on constant power loads compensation techniques," *IEEE access*, vol. 6, pp. 33 285–33 305, 2018.

[101] S. Rahimi, S. Massucco, F. Silvestro, M. Hesamzadeh, and Y. Tohidi, "Applying full milp model to volt-var optimization problem for mv distribution networks," in *Innovative Smart Grid Technologies Conference Europe (ISGT-Europe), 2014 IEEE PES*, pp. 1–5, Oct. 2014.

[102] D. Das, "Reactive power compensation for radial distribution networks using genetic algorithm," *International Journal of Electrical Power & Energy Systems*, vol. 24, no. 7, pp. 573–581, 2002.

[103] R. Ranjan and D. Das, "Voltage stability analysis of radial distribution networks," *Electric Power Components and Systems*, vol. 31, no. 5, pp. 501–511, 2003.

[104] A. T. Sarić and M. S. Ćalović, "Integrated GA-Fuzzy Multi-Objective Model for Centralized Volt/Var Control in Distribution Systems," *Electric Power Components and Systems*, vol. 33, no. 9, pp. 1039–1055, 2005.

[105] M. Alonso, H. Amarís, and M. Chindris, "A multiobjective Var/Volt management system in smartgrids," *Energy Procedia*, vol. 14, no. 2011, pp. 1490–1495, 2012.

[106] S. Moradian, S. Jadid, and O. Homaee, " Optimal allocation of capacitors with stand-alone VAr control systems in radial distribution networks," *International Transactions on Electrical Energy Systems*, vol. 25, pp. 1333–1348, 2015.

[107] R.-H. Liang, Y.-K. Chen, and Y.-T. Chen, "Volt/Var control in a distribution system by a fuzzy optimization approach," *International Journal of Electrical Power & Energy Systems*, no. 2, pp. 278–287, 2011.

[108] B. Das and P. K. Verma, "Artificial neural network-based optimal capacitor switching in a distribution system," *Electric Power Systems Research*, vol. 60, no. 2, pp. 55–62, 2001.

[109] D. Singh and R. K. Misra, "Load type impact on distribution system reconfiguration," *International Journal of Electrical Power  Energy Systems*, vol. 42, no. 1, pp. 583 – 592, 2012.

[110] G. Gutirrez-Alcaraz, "Two-stage heuristic methodology for optimal reconfiguration and volt/var control in the operation of electrical distribution systems," *IET Generation, Transmission  Distribution*, vol. 11, pp. 3946–3954(8), Nov. 2017.

[111] A. Mohapatra, P. Bijwe, and B. Panigrahi, "An opf sensitivity based approach for handling discrete variables," in *2014 IEEE PES General Meeting— Conference & Exposition*, pp. 1–5.    IEEE, 2014.

[112] A. T. Sarić and R. M. Ćirić, "Multi-objective integration of real-time functions in distribution management system," *International Journal of Electrical Power and Energy Systems*, vol. 25, no. 3, pp. 247–256, 2003.

[113] B. Singh and S. Singh, "Wind power interconnection into the power system: A review of grid code requirements," *The Electricity Journal*, vol. 22, no. 5, pp. 54–63, 2009.

[114] S. Deshmukh, B. Natarajan, and A. Pahwa, "State estimation and voltage/var control in distribution network with intermittent measurements," *IEEE Transactions on Smart Grid*, vol. 5, no. 1, pp. 200–209, 2013.

[115] T. Frantz, T. Gentile, S. Ihara, N. Simons, and M. Waldron, "Load Behavior Observed in LILCO and RG E Systems," *IEEE Transactions on Power Apparatus and Systems*, vol. PAS-103, no. 4, pp. 819–831, Apr. 1984.

[116] S. Satsangi and G. B. Kumbhar, "Analysis of substation energy using conservation voltage reduction in distribution system," in *2016 International Conference on Electrical Power and Energy Systems (ICEPES)*, pp. 188–193, Dec. 2016.

[117] S. Satsangi and G. B. Kumbhar, "Effect of load models on energy loss reduction using volt-var optimization," in *2016 National Power Systems Conference (NPSC)*, pp. 1–6, Dec. 2016.

[118] B. Singh and S. Singh, "Reactive capability limitations of doubly-fed induction generators," *Electric Power Components and Systems*, vol. 37, no. 4, pp. 427–440, 2009.

[119] D. Ranamuka, A. Agalgaonkar, and K. Muttaqi, "Innovative volt/var control philosophy for future distribution systems embedded with voltage-regulating devices and distributed renewable energy resources," *IEEE Systems Journal*, 2018.

[120] D. Ranamuka, A. Agalgaonkar, and K. Muttaqi, "Conservation voltage reduction and var management considering urban distribution system operation with solar-pv," *International Journal of Electrical Power & Energy Systems*, vol. 105, pp. 856–866, 2019.

[121] F. Ding, A. Nagarajan, S. Chakraborty, A. Nguyen, S. Walinga, M. Mccarty, F. Ding, A. Nagarajan, and S. Chakraborty, "Photovoltaic Impact Assessment of Smart Inverter Volt-VAR Control on Distribution System Conservation Voltage Reduction and Power Quality," *Technical Report NREL/TP-5D00-67296*, pp. 1–1, Dec. 2016.

[122] W. H. Kersting, *Distribution System Modeling and Analysis*, CRC Press, Boca Raton, Florida, 2002.

[123] *American National Standard for Electric Power Systems and Equipment-Voltage Ratings (60 Hertz).* National Electrical Manufacturers Association ANSI C84.1-2016, 2016.

[124] *Line and Cable Data - PES Test Feeder*, (Accessed on 02/18/2018). [Online]. Available: http://sites.ieee.org/pes-testfeeders/resources/

[125] *IEEE-123 Bus Feeder - PES Test Feeder*, (Accessed on 02/18/2018). [Online]. Available: http://sites.ieee.org/pes-testfeeders/resources/

[126] A. Garg, J. Maheshwari, and J. Upadhyay, *Load Research for Residential and Commercial Establishments in Gujrat*, 2010.

[127] *Day Ahead Demand - (SLDC), Gujarat*, SLDC Gujarat. [Online]. Available: http://www.sldcguj.com/Operation/Dayaheaddemand.asp

[128] R. C. Dugan and T. E. McDermott, "An open source platform for collaborating on smart grid research," in *2011 IEEE Power and Energy Society General Meeting*, pp. 1–7. IEEE, 2011.

[129] A. Ali, S. Padmanaban, B. Twala, and T. Marwala, "Electric power grids distribution generation system for optimal location and sizing case study investigation by various optimization algorithms," *Energies*, vol. 10, no. 7, p. 960, 2017.

[130] K. V. Ramana Reddy, N. Ramesh Babu, and P. Sanjeevikumar, "A review on grid codes and reactive power management in power grids with wecs," in *Advances in Smart Grid and Renewable Energy*, S. SenGupta, A. F. Zobaa, K. S. Sherpa, and A. K. Bhoi, Eds., pp. 525–539. Singapore: Springer Singapore, 2018.

[131] F. A. Mohamed and H. N. Koivo, "System modelling and online optimal management of microgrid using mesh adaptive direct search," *International Journal of Electrical Power Energy Systems*, vol. 32, no. 5, pp. 398 – 407, 2010.

[132] "IEEE Recommended Practice for Establishing Liquid-Filled and Dry-Type Power and Distribution Transformer Capability When Supplying Nonsinusoidal Load Currents," *IEEE Std C57.110-2008 (Revision of IEEE Std C57.110-1998)*, pp. 1–52, Aug. 2008.

[133] "IEEE Approved Draft Standard for General Requirements for Liquid-Immersed Distribution, Power, and Regulating Transformers," *IEEE PC57.12.00/D2.3, October 2015 (Revision of IEEE Std C57.12.00-2010)*, pp. 1–71, Jan. 2015.

[134] "IEEE Recommended Practice and Requirements for Harmonic Control in Electric Power Systems," *IEEE Std 519-2014 (Revision of IEEE Std 519-1992)*, pp. 1–29, Jun. 2014.

[135] M. E. Baran and F. F. Wu, "Network reconfiguration in distribution systems for loss reduction and load balancing," *IEEE Transactions on Power Delivery*, vol. 4, no. 2, pp. 1401–1407, Apr. 1989.

[136] "Global renewable generation continues its strong growth," https://www.irena.org/, (Accessed on 01/20/2019).

[137] "IEEE Standard for Interconnecting Distributed Resources with Electric Power Systems," *IEEE Std 1547-2003*, pp. 1–28, 2003.

# APPENDIX A

## DISTRIBUTION NETWORK DATA

This appendix presents more detail of distribution networks that have been used in order to study the various objectives proposed in this thesis.

## A.1 ORIGINAL IEEE-123 NODE TEST SYSTEM

The original system configuration is displayed in Fig.A.1. The line connection alongside length and configuration can be found in Table A.1. The phase-wise rated load and corresponding load model is displayed in Table A.2. The line configuration for overhead lines and underground cables can be seen in Table A.3 and A.4, respectively. There is one substation transformer and one service transformer, data is displayed in Table A.5. The normal position of various switches is provided in Table A.6. There are a total four regulators in the distribution network, data alongside connections and compensator winding specification is given in Table A.7.

Table A.1. Line segment data

| Node A | Node B | Length (ft.) | Config. | Node A | Node B | Length (ft.) | Config. |
|--------|--------|--------------|---------|--------|--------|--------------|---------|
| 1 | 2 | 175 | 10 | 60 | 61 | 550 | 5 |
| 1 | 3 | 250 | 11 | 60 | 62 | 250 | 12 |
| 1 | 7 | 300 | 1 | 62 | 63 | 175 | 12 |
| 3 | 4 | 200 | 11 | 63 | 64 | 350 | 12 |
| 3 | 5 | 325 | 11 | 64 | 65 | 425 | 12 |
| 5 | 6 | 250 | 11 | 65 | 66 | 325 | 12 |
| 7 | 8 | 200 | 1 | 67 | 68 | 200 | 9 |
| 8 | 12 | 225 | 10 | 67 | 72 | 275 | 3 |

*Continued on next page*

| Node A | Node B | Length (ft.) | Config. | Node A | Node B | Length (ft.) | Config. |
|--------|--------|--------------|---------|--------|--------|--------------|---------|
| 8 | 9 | 225 | 9 | 67 | 97 | 250 | 3 |
| 8 | 13 | 300 | 1 | 68 | 69 | 275 | 9 |
| 9 | 14 | 425 | 9 | 69 | 70 | 325 | 9 |
| 13 | 34 | 150 | 11 | 70 | 71 | 275 | 9 |
| 13 | 18 | 825 | 2 | 72 | 73 | 275 | 11 |
| 14 | 11 | 250 | 9 | 72 | 76 | 200 | 3 |
| 14 | 10 | 250 | 9 | 73 | 74 | 350 | 11 |
| 15 | 16 | 375 | 11 | 74 | 75 | 400 | 11 |
| 15 | 17 | 350 | 11 | 76 | 77 | 400 | 6 |
| 18 | 19 | 250 | 9 | 76 | 86 | 700 | 3 |
| 18 | 21 | 300 | 2 | 77 | 78 | 100 | 6 |
| 19 | 20 | 325 | 9 | 78 | 79 | 225 | 6 |
| 21 | 22 | 525 | 10 | 78 | 80 | 475 | 6 |
| 21 | 23 | 250 | 2 | 80 | 81 | 475 | 6 |
| 23 | 24 | 550 | 11 | 81 | 82 | 250 | 6 |
| 23 | 25 | 275 | 2 | 81 | 84 | 675 | 11 |
| 25 | 26 | 350 | 7 | 82 | 83 | 250 | 6 |
| 25 | 28 | 200 | 2 | 84 | 85 | 475 | 11 |
| 26 | 27 | 275 | 7 | 86 | 87 | 450 | 6 |
| 26 | 31 | 225 | 11 | 87 | 88 | 175 | 9 |
| 27 | 33 | 500 | 9 | 87 | 89 | 275 | 6 |
| 28 | 29 | 300 | 2 | 89 | 90 | 225 | 10 |
| 29 | 30 | 350 | 2 | 89 | 91 | 225 | 6 |
| 30 | 250 | 200 | 2 | 91 | 92 | 300 | 11 |
| 31 | 32 | 300 | 11 | 91 | 93 | 225 | 6 |
| 34 | 15 | 100 | 11 | 93 | 94 | 275 | 9 |
| 35 | 36 | 650 | 8 | 93 | 95 | 300 | 6 |

| Node A | Node B | Length (ft.) | Config. | Node A | Node B | Length (ft.) | Config. |
|---|---|---|---|---|---|---|---|
| 35 | 40 | 250 | 1 | 95 | 96 | 200 | 10 |
| 36 | 37 | 300 | 9 | 97 | 98 | 275 | 3 |
| 36 | 38 | 250 | 10 | 98 | 99 | 550 | 3 |
| 38 | 39 | 325 | 10 | 99 | 100 | 300 | 3 |
| 40 | 41 | 325 | 11 | 100 | 450 | 800 | 3 |
| 40 | 42 | 250 | 1 | 101 | 102 | 225 | 11 |
| 42 | 43 | 500 | 10 | 101 | 105 | 275 | 3 |
| 42 | 44 | 200 | 1 | 102 | 103 | 325 | 11 |
| 44 | 45 | 200 | 9 | 103 | 104 | 700 | 11 |
| 44 | 47 | 250 | 1 | 105 | 106 | 225 | 10 |
| 45 | 46 | 300 | 9 | 105 | 108 | 325 | 3 |
| 47 | 48 | 150 | 4 | 106 | 107 | 575 | 10 |
| 47 | 49 | 250 | 4 | 108 | 109 | 450 | 9 |
| 49 | 50 | 250 | 4 | 108 | 300 | 1000 | 3 |
| 50 | 51 | 250 | 4 | 109 | 110 | 300 | 9 |
| 51 | 151 | 500 | 4 | 110 | 111 | 575 | 9 |
| 52 | 53 | 200 | 1 | 110 | 112 | 125 | 9 |
| 53 | 54 | 125 | 1 | 112 | 113 | 525 | 9 |
| 54 | 55 | 275 | 1 | 113 | 114 | 325 | 9 |
| 54 | 57 | 350 | 3 | 135 | 35 | 375 | 4 |
| 55 | 56 | 275 | 1 | 149 | 1 | 400 | 1 |
| 57 | 58 | 250 | 10 | 152 | 52 | 400 | 1 |
| 57 | 60 | 750 | 3 | 160 | 67 | 350 | 6 |
| 58 | 59 | 250 | 10 | 197 | 101 | 250 | 3 |
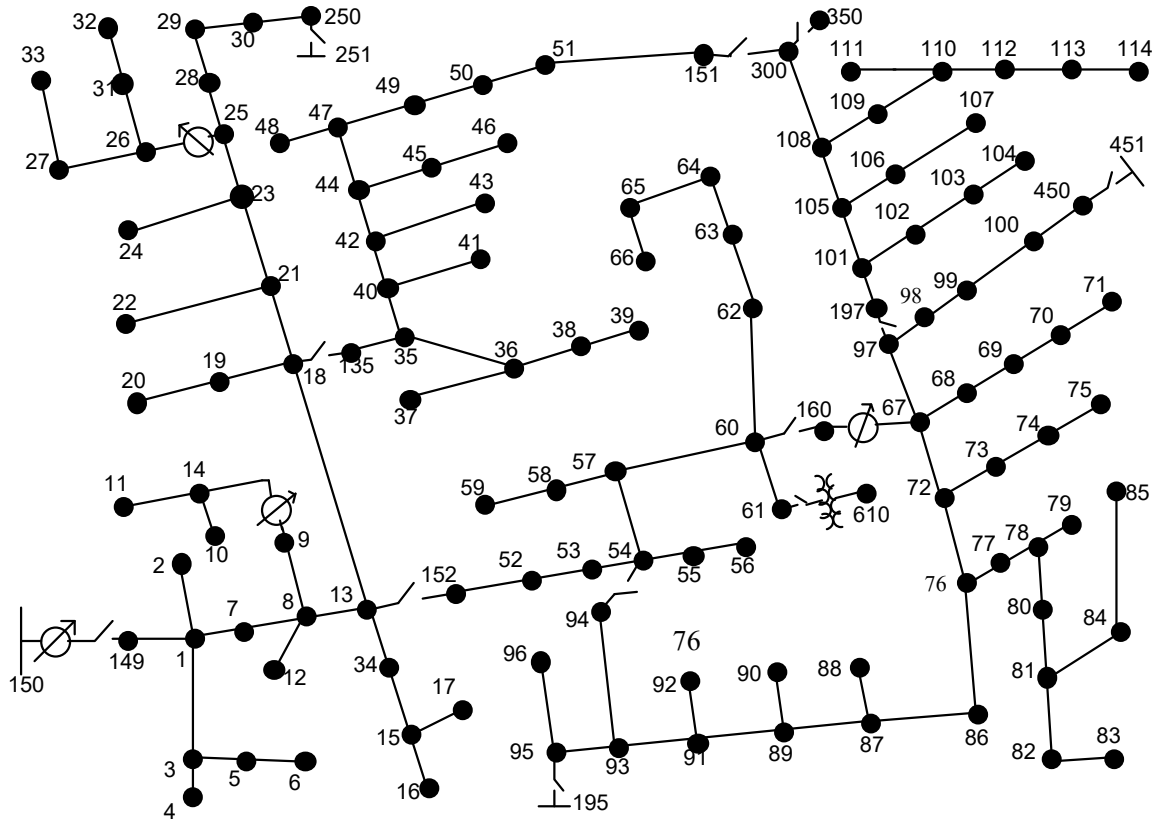
Fig. A.1. Original network topology of IEEE-123 node test feeder

Table A.2. Spot load data

| Node | Load Model | Ph-1 kW | Ph-1 kVAr | Ph-2 kW | Ph-2 kVAr | Ph-3 kW | Ph-4 kVAr |
|------|-----------|---------|-----------|---------|-----------|---------|-----------|
| 1 | Y-PQ | 40 | 20 | 0 | 0 | 0 | 0 |
| 2 | Y-PQ | 0 | 0 | 20 | 10 | 0 | 0 |
| 4 | Y-PR | 0 | 0 | 0 | 0 | 40 | 20 |
| 5 | Y-I | 0 | 0 | 0 | 0 | 20 | 10 |
| 6 | Y-Z | 0 | 0 | 0 | 0 | 40 | 20 |
| 7 | Y-PQ | 20 | 10 | 0 | 0 | 0 | 0 |
| 9 | Y-PQ | 40 | 20 | 0 | 0 | 0 | 0 |
| 10 | Y-I | 20 | 10 | 0 | 0 | 0 | 0 |

*Continued on next page*

Table A.2 – *Continued from previous page*

| Node | Load Model | Ph-1 kW | Ph-1 kVAr | Ph-2 kW | Ph-2 kVAr | Ph-3 kW | Ph-4 kVAr |
|------|-----------|---------|-----------|---------|-----------|---------|-----------|
| 11 | Y-Z | 40 | 20 | 0 | 0 | 0 | 0 |
| 12 | Y-PQ | 0 | 0 | 20 | 10 | 0 | 0 |
| 16 | Y-PQ | 0 | 0 | 0 | 0 | 40 | 20 |
| 17 | Y-PQ | 0 | 0 | 0 | 0 | 20 | 10 |
| 19 | Y-PQ | 40 | 20 | 0 | 0 | 0 | 0 |
| 20 | Y-I | 40 | 20 | 0 | 0 | 0 | 0 |
| 22 | Y-Z | 0 | 0 | 40 | 20 | 0 | 0 |
| 24 | Y-PQ | 0 | 0 | 0 | 0 | 40 | 20 |
| 28 | Y-I | 40 | 20 | 0 | 0 | 0 | 0 |
| 29 | Y-Z | 40 | 20 | 0 | 0 | 0 | 0 |
| 30 | Y-PQ | 0 | 0 | 0 | 0 | 40 | 20 |
| 31 | Y-PQ | 0 | 0 | 0 | 0 | 20 | 10 |
| 32 | Y-PQ | 0 | 0 | 0 | 0 | 20 | 10 |
| 33 | Y-I | 40 | 20 | 0 | 0 | 0 | 0 |
| 34 | Y-Z | 0 | 0 | 0 | 0 | 40 | 20 |
| 35 | D-PQ | 40 | 20 | 0 | 0 | 0 | 0 |
| 37 | Y-Z | 40 | 20 | 0 | 0 | 0 | 0 |
| 38 | Y-I | 0 | 0 | 20 | 10 | 0 | 0 |
| 39 | Y-PQ | 0 | 0 | 20 | 10 | 0 | 0 |
| 41 | Y-PQ | 0 | 0 | 0 | 0 | 20 | 10 |
| 42 | Y-PQ | 20 | 10 | 0 | 0 | 0 | 0 |
| 43 | Y-Z | 0 | 0 | 40 | 20 | 0 | 0 |
| 45 | Y-I | 20 | 10 | 0 | 0 | 0 | 0 |
| 46 | Y-PQ | 20 | 10 | 0 | 0 | 0 | 0 |
| 47 | Y-I | 35 | 25 | 35 | 25 | 35 | 25 |
| 48 | Y-Z | 70 | 50 | 70 | 50 | 70 | 50 |

*Continued on next page*

Table A.2 – *Continued from previous page*

| Node | Load Model | Ph-1 kW | Ph-1 kVAr | Ph-2 kW | Ph-2 kVAr | Ph-3 kW | Ph-4 kVAr |
|------|-----------|---------|-----------|---------|-----------|---------|-----------|
| 49 | Y-PQ | 35 | 25 | 70 | 50 | 35 | 20 |
| 50 | Y-PQ | 0 | 0 | 0 | 0 | 40 | 20 |
| 51 | Y-PQ | 20 | 10 | 0 | 0 | 0 | 0 |
| 52 | Y-PQ | 40 | 20 | 0 | 0 | 0 | 0 |
| 53 | Y-PQ | 40 | 20 | 0 | 0 | 0 | 0 |
| 55 | Y-Z | 20 | 10 | 0 | 0 | 0 | 0 |
| 56 | Y-PQ | 0 | 0 | 20 | 10 | 0 | 0 |
| 58 | Y-I | 0 | 0 | 20 | 10 | 0 | 0 |
| 59 | Y-PQ | 0 | 0 | 20 | 10 | 0 | 0 |
| 60 | Y-PQ | 20 | 10 | 0 | 0 | 0 | 0 |
| 62 | Y-Z | 0 | 0 | 0 | 0 | 40 | 20 |
| 63 | Y-PQ | 40 | 20 | 0 | 0 | 0 | 0 |
| 64 | Y-I | 0 | 0 | 75 | 35 | 0 | 0 |
| 65 | D-Z | 35 | 25 | 35 | 25 | 70 | 50 |
| 66 | Y-PQ | 0 | 0 | 0 | 0 | 75 | 35 |
| 68 | Y-PQ | 20 | 10 | 0 | 0 | 0 | 0 |
| 69 | Y-PQ | 40 | 20 | 0 | 0 | 0 | 0 |
| 70 | Y-PQ | 20 | 10 | 0 | 0 | 0 | 0 |
| 71 | Y-PQ | 40 | 20 | 0 | 0 | 0 | 0 |
| 73 | Y-PQ | 0 | 0 | 0 | 0 | 40 | 20 |
| 74 | Y-Z | 0 | 0 | 0 | 0 | 40 | 20 |
| 75 | Y-PQ | 0 | 0 | 0 | 0 | 40 | 20 |
| 76 | D-I | 105 | 80 | 70 | 50 | 70 | 50 |
| 77 | Y-PQ | 0 | 0 | 40 | 20 | 0 | 0 |
| 79 | Y-Z | 40 | 20 | 0 | 0 | 0 | 0 |
| 80 | Y-PQ | 0 | 0 | 40 | 20 | 0 | 0 |

*Continued on next page*

| Node | Load Model | Ph-1 kW | Ph-1 kVAr | Ph-2 kW | Ph-2 kVAr | Ph-3 kW | Ph-4 kVAr |
|------|------------|---------|-----------|---------|-----------|---------|-----------|
| 82 | Y-PQ | 40 | 20 | 0 | 0 | 0 | 0 |
| 83 | Y-PQ | 0 | 0 | 0 | 0 | 20 | 10 |
| 84 | Y-PQ | 0 | 0 | 0 | 0 | 20 | 10 |
| 85 | Y-PQ | 0 | 0 | 0 | 0 | 40 | 20 |
| 86 | Y-PQ | 0 | 0 | 20 | 10 | 0 | 0 |
| 87 | Y-PQ | 0 | 0 | 40 | 20 | 0 | 0 |
| 88 | Y-PQ | 40 | 20 | 0 | 0 | 0 | 0 |
| 90 | Y-I | 0 | 0 | 40 | 20 | 0 | 0 |
| 92 | Y-PQ | 0 | 0 | 0 | 0 | 40 | 20 |
| 94 | Y-PQ | 40 | 20 | 0 | 0 | 0 | 0 |
| 95 | Y-PQ | 0 | 0 | 20 | 10 | 0 | 0 |
| 96 | Y-PQ | 0 | 0 | 20 | 10 | 0 | 0 |
| 98 | Y-PQ | 40 | 20 | 0 | 0 | 0 | 0 |
| 99 | Y-PQ | 0 | 0 | 40 | 20 | 0 | 0 |
| 100 | Y-Z | 0 | 0 | 0 | 0 | 40 | 20 |
| 102 | Y-PQ | 0 | 0 | 0 | 0 | 20 | 10 |
| 103 | Y-PQ | 0 | 0 | 0 | 0 | 40 | 20 |
| 104 | Y-PQ | 0 | 0 | 0 | 0 | 40 | 20 |
| 106 | Y-PQ | 0 | 0 | 40 | 20 | 0 | 0 |
| 107 | Y-PQ | 0 | 0 | 40 | 20 | 0 | 0 |
| 109 | Y-PQ | 40 | 20 | 0 | 0 | 0 | 0 |
| 111 | Y-PQ | 20 | 10 | 0 | 0 | 0 | 0 |
| 112 | Y-I | 20 | 10 | 0 | 0 | 0 | 0 |
| 113 | Y-Z | 40 | 20 | 0 | 0 | 0 | 0 |
| 114 | Y-PQ | 20 | 10 | 0 | 0 | 0 | 0 |

Table A.3. Overhead line configurations (Config.)

| Config. | Phasing | Phase Cond. ACSR | Neutral Cond. ACSR | Spacing ID |
|---------|---------|------------------|--------------------|------------|
| 1 | A B C N | 336,400 26/7 | 4/0 6/1 | 500 |
| 2 | C A B N | 336,400 26/7 | 4/0 6/1 | 500 |
| 3 | B C A N | 336,400 26/7 | 4/0 6/1 | 500 |
| 4 | C B A N | 336,400 26/7 | 4/0 6/1 | 500 |
| 5 | B A C N | 336,400 26/7 | 4/0 6/1 | 500 |
| 6 | A C B N | 336,400 26/7 | 4/0 6/1 | 500 |
| 7 | A C N | 336,400 26/7 | 4/0 6/1 | 505 |
| 8 | A B N | 336,400 26/7 | 4/0 6/1 | 505 |
| 9 | A N | 1/0 | 1/0 | 510 |
| 10 | B N | 1/0 | 1/0 | 510 |
| 11 | C N | 1/0 | 1/0 | 510 |

Table A.4. Underground cable configurations

| Config. | Phasing | Cable | Spacing ID |
|---------|---------|-------|------------|
| 12 | A B C | 1/0 AA, CN | 515 |

Table A.5. Transformer's data

|  | kVA | kV-high | kV-low | R - % | X - % |
|--|-----|---------|--------|-------|-------|
| Substation | 5,000 | 115 - D | 4.16 Gr-W | 1 | 8 |
| XFM - 1 | 150 | 4.16 - D | .480 - D | 1.27 | 2.72 |

Table A.6. 3-phase switch status

| Node A | Node B | Normal |
| --- | --- | --- |
| 13 | 152 | closed |
| 18 | 135 | closed |
| 60 | 160 | closed |
| 61 | 610 | closed |
| 97 | 197 | closed |
| 150 | 149 | closed |
| 250 | 251 | open |
| 450 | 451 | open |
| 54 | 94 | open |
| 151 | 300 | open |
| 300 | 350 | open |

Table A.7. Regulators data connected at various locations

| ID | Line Segment | Location | Phases | Connection | Monitoring Phase | Bandwidth | PT Ratio | CT Rating (Primary) | Compensator | Settings R | X | Voltage Level |
|----|----|----|----|----|----|----|----|----|----|----|----|----|
| 1 | 150 - 149 | 150 | A-B-C | 3-Ph, Wye | A | 2.0 volts | 20 | 700 Amp | Ph-A | 3 | 7.5 | 120 |
| 2 | 9 - 14 | 9 | A | 1-Ph, L-G | A | 2.0 volts | 20 | 50 Amp | Ph-A | 0.4 | 0.4 | 120 |
| 3 | 25 - 26 | 25 | A-C | 2-Ph, L-G | A-C | 1.0 volt | 20 | 50 Amp | Ph-A | 0.4 | 0.4 | 120 |
|  |  |  |  |  |  |  |  |  | Ph-C | 0.4 | 0.4 | 120 |
| 4 | 160 - 67 | 160 | A-B-C | 3-Ph, LG | A-B-C | 2.0 volts | 20 | 300 Amp | Ph-A | 0.6 | 1.3 | 124 |
|  |  |  |  |  |  |  |  |  | Ph-B | 1.4 | 2.6 | 124 |
|  |  |  |  |  |  |  |  |  | Ph-C | 0.2 | 1.4 | 124 |

## A.2 ORIGINAL IEEE-33 BUS SYSTEM

The line connection alongside line constants (resistance and reactanc) can be found in Table A.8. This is a balanced single phase system without any mesh inside it. The rated load connected at various location can be found in Table A.9.

Table A.8. Branch connections and line constants

| From Node | To Node | Line Constants (in Ohms) | | From Node | To Node | Line Constants (in Ohms) | |
| --- | --- | --- | --- | --- | --- | --- | --- |
| | | R | X | | | R | X |
| 1 | 2 | 0.0922 | 0.0477 | 17 | 18 | 0.732 | 0.574 |
| 2 | 3 | 0.493 | 0.2511 | 2 | 19 | 0.164 | 0.1565 |
| 3 | 4 | 0.366 | 0.1864 | 19 | 20 | 1.5042 | 1.3554 |
| 4 | 5 | 0.3811 | 0.1941 | 20 | 21 | 0.4095 | 0.4784 |
| 5 | 6 | 0.819 | 0.707 | 21 | 22 | 0.7089 | 0.9373 |
| 6 | 7 | 0.1872 | 0.6188 | 3 | 23 | 0.4512 | 0.3083 |
| 7 | 8 | 1.7114 | 1.2351 | 23 | 24 | 0.898 | 0.7091 |
| 8 | 9 | 1.03 | 0.740 | 24 | 25 | 0.896 | 0.7011 |
| 9 | 10 | 1.04 | 0.740 | 6 | 26 | 0.203 | 0.1034 |
| 10 | 11 | 0.1966 | 0.0650 | 26 | 27 | 0.2842 | 0.1447 |
| 11 | 12 | 0.3744 | 0.1238 | 27 | 28 | 1.059 | 0.9337 |
| 12 | 13 | 1.468 | 1.155 | 28 | 29 | 0.8042 | 0.7006 |
| 13 | 14 | 0.5416 | 0.7129 | 29 | 30 | 0.5075 | 0.2585 |
| 14 | 15 | 0.591 | 0.526 | 30 | 31 | 0.9744 | 0.963 |
| 15 | 16 | 0.7463 | 0.545 | 31 | 32 | 0.3105 | 0.3619 |
| 16 | 17 | 1.289 | 1.721 | 32 | 33 | 0.341 | 0.5302 |

Table A.9. Real and reactive power load at different locations

| Node | Loads in kW and kVAr | | Node | Loads in kW and kVAr | |
|---|---|---|---|---|---|
| | P (kW) | Q (kVAr) | | P (kW) | Q (kVAr) |
| 2 | 100 | 60 | 18 | 90 | 40 |
| 3 | 90 | 40 | 19 | 90 | 40 |
| 4 | 120 | 80 | 20 | 90 | 40 |
| 5 | 60 | 30 | 21 | 90 | 40 |
| 6 | 60 | 20 | 22 | 90 | 40 |
| 7 | 200 | 100 | 23 | 90 | 50 |
| 8 | 200 | 100 | 24 | 420 | 200 |
| 9 | 60 | 20 | 25 | 420 | 200 |
| 10 | 60 | 20 | 26 | 60 | 25 |
| 11 | 45 | 30 | 27 | 60 | 25 |
| 12 | 60 | 35 | 28 | 60 | 20 |
| 13 | 60 | 35 | 29 | 120 | 70 |
| 14 | 120 | 80 | 30 | 200 | 600 |
| 15 | 60 | 10 | 31 | 150 | 70 |
| 16 | 60 | 20 | 32 | 210 | 100 |
| 17 | 60 | 20 | 33 | 60 | 40 |

# APPENDIX B

# LIST OF PUBLICATIONS AND AWARD

**PEER-REVIEWED JOURNALS**

1. **Saran Satsangi** and Ganesh Balu Kumbhar, "Effect of Load Models on Scheduling of VVC Devices in a Distribution Network," *IET Generation, Transmission and Distribution*, vol. 12, no. 17, pp. 3993-4001, 2018.

2. **Saran Satsangi** and Ganesh Balu Kumbhar, " Integrated Volt-VAr Optimization with Distributed Energy Sources to Minimize Substation Energy in Distribution System," *Electric Power Components and Systems*, vol. 46, no. 14-15, pp. 1522-1539, 2018.'

3. **Saran Satsangi** and Ganesh Balu Kumbhar, "Maximization of Energy Saving in a Distribution System with Intelligent Volt/VAr Control Based on IEEE Std. 1547-2018", *IEEE Transactions on Power Delivery.* (Manuscript Under Preparation).

**NATIONAL/INTERNATIONAL CONFERENCES**

4. **Saran Satsangi** and Ganesh Balu Kumbhar, "Review on Volt/VAr Optimization and Control in Electric Distribution System," in *2016 IEEE 1st International Conference on Power Electronics, Intelligent Control and Energy Systems (ICPEICES)*, New Delhi, India, pp. 1–6, Jul. 2016.

5. **Saran Satsangi** and Ganesh Balu Kumbhar, "Analysis of Substation Energy using Conservation Voltage Reduction in Distribution System," in *2016 International Conference on Electrical Power and Energy Systems (ICEPES)*, Bhopal, India, pp. 188–193, Dec. 2016.

6. **Saran Satsangi** and Ganesh Balu Kumbhar, "Effect of Load Models on Energy Loss Reduction using Volt-VAr Optimization," in *2016 National Power Systems Conference (NPSC)*, Bhubaneswar, India, pp. 1–6, Dec. 2016.

7. **Saran Satsangi** and Ganesh Balu Kumbhar, "Energy Savings Estimation Considering Volt/VAr Optimization and Distributed Generation," in *2019 IEEE 28th International Symposium on Industrial Electronics (ISIE)*, Vancouver, Canada, pp. 87–92, June 2019.

**AWARD**

**IEEE IES Student and Young Professional Award** for paper titled "Energy Savings Estimation Considering Volt/VAr Optimization and Distributed Generation" in *IEEE 28th International Symposium on Industrial Electronics (ISIE-2019)*, Vancouver, Canada